KATHOLISCHE UNIVERSITÄT EICHSTÄTT-INGOLSTADT

# Methods and solution approaches for resilient supply chain network design: Novel case studies for waterborne disruptions in transportation networks

Daniel Müllerklein

Kumulative Dissertation
zur Erlangung des akademischen Grades
Doctor rerum politicarum (Dr. rer. pol.)

Juni 2025

Tag der mündlichen Prüfung: 2. Oktober 2025
Referent: Prof. Dr. Pirmin Fontaine
Korreferent: Prof. Dr. Thomas Setzer

# Danksagung

Diese Dissertation wäre ohne die Unterstützung und Ermutigung vieler Menschen nicht möglich gewesen, denen ich an dieser Stelle meinen herzlichen Dank aussprechen möchte.

Zuerst möchte ich meinem Doktorvater, Prof. Dr. Pirmin Fontaine, meinen tief empfundenen Dank für die exzellente Betreuung, die mir stets entgegengebrachte Forschungsfreiheit und das Vertrauen in meine Promotion aussprechen. Seine wertvollen Anregungen und seine konstruktive Kritik haben maßgeblich zum Gelingen dieser Arbeit beigetragen. Seine Fachkenntnis und sein Engagement waren zudem eine große Inspirationsquelle für mich. Des Weiteren möchte ich mich bei Prof. Dr. Heinrich Kuhn für wertvolles und konstruktives Feedback im Rahmen zahlreicher Forschungsworkshops bedanken. Mein besonderer Dank gilt auch Prof. Dr. Janosch Ortmann für die hervorragende Zusammenarbeit während einer der Publikationen. Ich danke auch Prof. Dr. Thomas Setzer für die Übernahme des Zweitgutachtens.

Außerdem danke ich Birgit Jürgens, die mich stets bei allen organisatorischen Aufgaben des Universitäts-Dschungels unterstützte und immer ein offenes Ohr für mich hatte. Mein besonderer Dank gilt auch meinen Kollegen und Freunden am Lehrstuhl für die wertvollen Anregungen und Ideen bei gemeinsamen Forschungsworkshops, vor allem aber auch für die tolle Zeit innerhalb und außerhalb der Universitätsgebäude: Dr. Markus Frank, Johannes Gückel, Moritz Hundhammer, Simon Mader, Tobias Potoczki, Dr. Alexander Rave, Dr. Stefan Voigt, und Dr. Sandra Zajac.

Ein weiterer Dank geht an meine Familie, die mich in all den Jahren bedingungslos unterstützt hat. Meinen Eltern, Margret und Werner, möchte ich für ihre stete Ermutigung und ihr Vertrauen in meine Fähigkeiten danken. Ohne ihre Unterstützung wäre diese Arbeit nicht möglich gewesen.

Mein tiefster Dank gilt meiner langjährigen Partnerin, Denise, deren Liebe, Geduld und Verständnis mich während des gesamten Promotionsprozesses begleitet haben. Du warst immer an meiner Seite und hast mich immer motiviert weiter zu machen. Ich freue mich auf viele weitere Jahre mit dir!

Daniel Müllerklein

# Summary

More than 75% of today's global trade volumes are shipped through ocean freight. As such, ocean shipping has played a crucial role in the ever-increasing globalization of worldwide supply chains. Various transportation modes are available for the transshipment of maritime cargo to or from locations inside the country. For specific industries and seaports, inland shipping plays a critical role in the connection to the mainland. These critical waterways can be found worldwide: 60% of all grain exported from the United States is shipped on the Mississippi River through the Port of New Orleans and the Port of South Louisiana (Steinbach and Zhuang 2023). The Panama canal is of even higher importance for global trade through which more than 70% of all products to and from the United States surpass (LaRocco 2023). In Germany, the Rhine River transports 11% of all chemicals used by the German industry and 30% of coal, crude oil, and natural gas (Ademmer et al. 2020). Unfortunately, recent years have also shown how vulnerable worldwide waterways have become to waterborne disruptions. For example, 2018 an exceptionally dry summer resulted in low water levels at the Rhine River that affected and even stopped cargo transport on the river for multiple weeks and months. Ademmer et al. (2020) estimated that a single month of low water level of the Rhine River reduces industrial production in Germany by about 1%. In 2022, the Mississippi River experienced a historic drought. Despite a significant rise of transportation costs up to 400%, Steinbach and Zhuang (2023) estimated that the drought resulted in a 3.9% reduction in agricultural exports and an agricultural trade loss of 563.9mn USD. Similarly, droughts in the Panama Canal have resulted in restrictions on the number and type of vessels that can travel the canal. As a result, low water level surcharges of up to 500 USD per twenty-foot equivalent unit (TEU) have been introduced. Due to climate change, waterborne disruptions might even increase in frequency and impact (van Meijeren and Groen 2010) affecting individual companies, regions, and even global trade flows.

To connect the various stages of these interconnected supply chains, reliable transportation modes are required to ensure efficient operations (Mattsson and Jenelius 2015). This need for reliability and efficiency has motivated practitioners and academia to develop different concepts on increasing their supply chain resilience (SCR) against disruptions that occur along the supply chain (Hosseini et al. 2019a). While many of the key components in increasing SCR have been discovered many years ago, adaptations in practice are still behind. To increase the adaptation in practice, ensuring the overall cost-competitiveness of resilience strategies has been identified as a key enabler (Aldrighetti et al. 2021).

In order to increase SCR while ensuring efficient and cost-competitive operations, a number of decisions on different decision levels need to be taken from the strategic network design to the operational routing of transports just prior to and during a disruption. This thesis and its papers aim to establish a holistic overview on the number of different decisions to be taken while presenting dif-

ferent methodologies to support their implementation. To test the different approaches, all papers present case studies of waterborne disruptions that affect the transportation costs and shipment abilities on the Rhine River regularly, creating an immediate threat to many companies in Germany that rely on the shipment abilities for their inbound and outbound product flows (Ademmer et al. 2020). For this, real disruption data is used and studied to derive realistic managerial insights. First, Paper 1 addresses the problem of the integrated resilient network design covering resilience strategies from strategic to operational level while considering the possibility to predict disruptions in the short-term. Based on the improvement potentials of short-term predictions, Paper 2 provides a decision-support methodology to optimize the operational routing of transports considering all information known to the decision maker at each respective day. The focus of Paper 3 is on understanding the impacts of different product characteristics as well as the consideration of multiple products on the resilient network design. Finally, Paper 4 summarizes the findings in an end-to-end decision framework that guides decision makers through the process of increasing their SCR.

Different decision models and solution methodologies are presented that address the various complex problem settings and develop support tools for decision makers aiming at increasing their SCR. The problems of Papers 1,2, and 3 are formulated as mixed-integer programming models, which could be solved to optimality using available commercial solvers. In addition, Paper 1 outlines a problem-specific Benders decomposition algorithm to particularly solve large problem instances efficiently. Paper 2 uses a combination of optimization and machine learning to identify a cost-optimal operational replenishment strategy. Paper 3 presents enhancements to the standard model formulation to improve the solution time for large instances. Lastly, Paper 4 conceptually summarizes the different findings in an end-to-end framework.

Through the introduced novel problem settings, the methodologies, and the numerical results derived from a new case study, this thesis represents an innovative and relevant contribution to existing literature. In addition, the findings help to gather several managerial insights that are relevant for practitioners and help to create supply chains that are not only efficient but also resilient for a better future. We summarize the four different papers individually in greater detail.

### Paper 1 - Resilient transportation network design with disruption uncertainty and lead times

In October 2018, low water levels on the Rhine River halted transportation for over a month, significantly impacting many companies by forcing production cuts and lowering profit forecasts due to raw material shortages and increased logistics costs. These disruptions are somewhat predictable on the short-term but their exact timing and impact remain uncertain, posing planning challenges for decision-makers. This paper focuses on the key network resilience design decisions from strategic to operational level for an inbound supply chain with suppliers shipping using various transportation modes, all susceptible to disruptions affecting duration, impact, and occurrence. These disruptions lead to transportation surcharges, which vary based on the severity of the disruption, from modest increases to full transportation stops. Particularly, the question is answered how individual lead time differences, the possibility to predict disruptions on the short-term, and potentially limited rerouting capacities impact the overall total expected costs and cost-optimal set of resilience strategies across the different decision levels.

From a methodological perspective, a new two-stage stochastic programming formulation is introduced for solving the multi-period supply chain network design (SCND) problem, accounting for uncertain transportation disruptions affecting transportation costs that can be predicted on the short-term. To solve particularly large problem instances faster, an enhanced Benders decomposition algorithm is developed with a non-traditional split of decision variables.

Through a case study we show that the total expected costs can be improved by up to 50% compared to the alternative of risk-taking without resilience investments and operational re-routing. The possibility to predict disruptions can further reduce the resilience-related costs by 10% though the marginal value-add of additional forecasting days reduces with an increase in the number of prediction days. Further, a re-routing capacity equaling to at least 40% of the daily demand value is needed to ensure that a significant share of the savings through disruption prediction can be achieved.

### Paper 2 - Cost-driven decision tree rules for transportation planning under cost uncertainty

Companies aim to balance risks and cost-efficiency in their supply chains. Recent disruptions have led to efforts in re-designing supply chains for greater resilience, focusing on strategies like increasing inventory and sourcing from multiple suppliers. These adjustments require effective inventory replenishment policies, which is a complex challenge for decision-makers. Traditional methods focus on demand uncertainty, but there is a growing need to consider uncertainties in transportation disruptions, particularly due to climate change affecting inland waterway transport. These disruptions cause unpredictable surcharges and service stops, making it crucial to anticipate transportation costs accurately.

The paper addresses the Stochastic Inventory Routing Problem with Direct Deliveries (SIRPDD), focusing on uncertainties in transportation costs. This problem involves suppliers shipping raw materials directly to a customer, with transportation costs being uncertain and varying based on conditions like water levels. Decision makers must decide on the timing, quantity, and supplier for replenishment under these uncertainties. The key question this paper answers is how these decisions can be determined through a data-driven approach without relying on estimations for stochastic variables, which are difficult to determine. The SIRPDD is first modeled as multi-stage stochastic program that incorporates transportation cost uncertainty at each decision stage, including multiple suppliers, lead time differences, and various transportation quantities. The core methodological contribution is the introduction of the new Cost-driven Decision Tree (CDDT) framework that minimizes the total costs within the validation step of hyperparameter tuning for different replenishment policies. Using the optimal decisions generated with perfect information, a supervised machine learning algorithm is trained and tuned for total costs instead of prediction performance. To efficiently handle the hyperparameter tuning, a genetic algorithm is developed.

Through a case study the cost performance of the CDDT framework is benchmarked against traditional optimization-machine learning approaches and standard replenishment policies as industry benchmark. While traditional learning approaches result in inefficient policies, the paper shows that the CDDT can reduce costs by 20% compared to the (s,Q)-reorder policies, and 18% compared to classical machine learning frameworks.

### Paper 3 - On product characteristics in a two-echelon resilient network design

In order to produce a finished good, companies rely on a number of raw materials that need to be made available in-time for production to avoid shortages or production stops. Once transportation arcs are disrupted, these typically affect a large share of the product portfolio in parallel as multiple products rely on identical transportation modes and routes. Resilient SCND is essential to mitigate these disruptions. Once multiple products are affected, two key questions arise. First, how do different product characteristics affect the optimal resilience strategy mix. Second, does the resilience mix for independent products change once multiple products are considered.

The problem focuses on a two-echelon resilient SCND involving multiple products and transportation modes prone to disruptions. In this setting, multiple suppliers ship raw materials to a production facility via a central warehouse. Disruptions in the inland waterway transport between the warehouse and the production facility cause surcharges that vary based on the disruption's severity on the shipment day. The decision-making process involves selecting resilience strategies, such as near-shoring, capacity investments, backup suppliers, and additional inventory, tailored to different product characteristics. The problem is formulated as two-stage stochastic program to minimize the total expected costs under transportation cost uncertainty, balancing proactive investments and potential surcharges or stockouts for multiple products. To improve the convergence behavior and provide strong initial solutions, lower-bound-lifting and valid inequalities are added to improve the standard model formulation.

The paper presents a case study to examine the influence of product characteristics on the optimal mix of resilience strategies, providing practical insights. Compared to the cost-optimal resilience mix of the independent single-product problems, solving the integrated problem reduces the resilience costs by up to 79%.

### Paper 4 - A seven-step supply chain resilience framework for mitigating waterborne disruptions in transportation network design

Based on the novel problem setting and case studies that have been the focus of Paper 1-3, this paper summarizes the various novel problem characteristics, solution approaches, and managerial findings in an end-to-end decision framework. The various problem specifics of waterborne disruptions affecting the transportation arcs within existing supply chain networks are studied concerning the probability and impacts that typically occur.

The paper presents a decision framework that starts at identifying the right objective of resilient network design from a purely risk-neutral decision maker that optimizes total expected costs to more risk-adverse or even robust approaches. Then, parameters and disruption data needs to be gathered, a step often overlooked in practice. At the core of the framework is the assessment of the potential disruption situation a decision maker faces to identify how decision support tools can provide value to either proactive or reactive decisions considering disruption occurrence.

# Contents

# List of Figures

# List of Tables

# Acronyms

**BC** branch-and-cut

**BD** Benders decomposition

**CART** Classification and Regression Tree

**CDDT** Cost-driven Decision Tree

**DSP** dual subproblem

**IRPDD** Inventory Routing Problem with Direct Deliveries

**LSHP** L-shaped implementation

**MILP** mixed-integer linear program

**ML-DT** decision tree

**ML-LR** logistic regression

**ML-NN** neural network

**MP** master problem

**PI** perfect information

**RA** risk averse

**SC** supply chain

**SCND** supply chain network design

**SCR** supply chain resilience

**SIRPDD** Stochastic Inventory Routing Problem with Direct Deliveries

**SP** subproblem

**TEU** twenty-foot equivalent unit

# Contribution 1 - Resilient transportation network design with disruption uncertainty and lead times

# 1 Resilient transportation network design with disruption uncertainty and lead times

Daniel Müllerklein, Pirmin Fontaine

**Abstract** Cost-efficient and reliable transports are needed to supply products competitively. Thus, particularly in increasingly complex and global supply chains, identifying the optimal transportation mode is a critical decision. Transportation modes, however, are prone to disruptions, such as hurricanes, low water levels, or port shutdowns, resulting in transportation stops and cost increases. To counteract these disruptions, different resilience strategies are studied to increase the capability of a network to withstand, adapt, and recover from disruptions. For a cost-optimal use, it is necessary to determine the optimal mix of strategic, tactical, and operational strategies.

We provide a decision-support model that decides on the optimal mix of resilience strategies, such as multi-sourcing, inventory, or operational re-routing, for a supply chain with transportation disruption uncertainty to minimize total expected costs. The problem is formulated as a two-stage stochastic mixed-integer linear program that explicitly considers lead times. To handle large instances, we propose a Benders decomposition approach enhanced through lower-bound lifting and valid inequalities, branch-and-benders-cut, and a warm-start heuristic. Computational experiments show that large instances can be solved to near-optimality, whereas a commercial solver does not find feasible solutions.

We present a case study for a company's inbound supply chain design with recurring transportation cost uncertainty. Considering disruption and lead time effects, a mix of resilience strategies from strategic to operational level leads to cost improvements of up to 50%. Furthermore, we show that the ability to predict disruptions can further reduce resilience-related costs by 10% if sufficient operational re-routing capacities are available.

---

Published: European Journal of Operational Research
URL: `https://doi.org/10.1016/j.ejor.2024.11.021`

## 1.1 Introduction

In October 2018, low water levels on the Rhine River, one of Europe's most important waterways, forced transportation for more than a month to a standstill. No barge, even if loaded only to a fraction of its original capacity, could travel without the risk of being grounded. As a result, missing raw materials forced several companies, including the chemical company BASF, to cut back production. This shortage and a rise in logistics costs led BASF to lower its yearly profit forecast. Experts estimate that the low water levels caused a 0.4% drop in GDP in Germany (Ademmer et al. 2020). More importantly, this was not the first time water levels limited the transportation capacities along the river. Unlike single-event disruptions, such as the Suez-Canal blockage, they occur regularly, even following seasonal patterns (Jonkeren et al. 2007). In 2015, 2017, and 2021, low water levels led to similar, yet not that extreme, reductions in shipping capacity and increases in transportation costs. Note that such recurring disruptive effects are not only seen in waterway transportation. The hurricane season in North America is another example of recurring yet impact-varying disruptions that regularly result in port shutdowns and damage to transportation infrastructure. While these disruptive events can be predicted somewhat, the exact timing and impact remain uncertain. This uncertainty challenges decision-makers to plan and prepare.

In parallel, margin pressure has pushed companies to design their supply chains increasingly complex, interdependent, and global. Thus, supply chains need reliable transportation to connect the various stages and ensure efficient operations. This need for reliability has motivated practitioners to rethink how to increase their SCR. One of the critical elements in improving SCR is the SCND (Tang 2006). The SCND involves strategic decisions on the number, location, and capacity of own assets as well as the selection of suppliers to serve demand in a timely and efficient manner (Klibi et al. 2010). These strategic decisions are made under uncertainty about the future and require anticipating the consequences on the tactical and operational level (Farahani et al. 2014). Thus, SCND models need to account for the disruption uncertainty on the strategic level, while decisions made play a role in operational transport decisions once a disruption is known.

We study a SCND problem where a central decision-maker at the production facility sources from various suppliers and is in full responsibility of the inbound flows. Transportation modes are prone to uncertain disruptions concerning their duration, impact, and occurrence along the planning horizon. As a result of these disruptions, transportation carriers enforce surcharges on their regular transportation prices that increase the mode-specific transportation costs. In practice, these surcharges occur regularly due to, e.g., low water levels (St. Lawrence River Canada, Rhine River Germany, Panama Canal) accounting for lost shipment capacities within the general contractual obligations. Depending on the disruption impact, surcharges and thus cost increases range from modest surcharges to full transportation stops, i.e., infinitely high costs. In addition, we explicitly consider lead time differences between transportation alternatives. These lead time differences can occur from varying transportation modes or geographical distances between suppliers and the production facility. We aim to evaluate and compare the cost-effectiveness of strategic, tactical, and operational resilience measures.

The following contributions are made. First, we introduce a two-stage stochastic programming formulation to solve the multi-period SCND problem with recurring disruptions that are uncertain concerning their time of occurrence and impact on the mode-specific costs. Furthermore, we integrate strategic, tactical, and operational resilience strategies. Second, we are the first to explicitly consider individual lead times for all transportation modes in a resilient SCND problem to model the lead time-delayed disruption response through the network flow on operational level. Considering individual lead times allows us to quantify the trade-off in choosing a closer supplier at higher disruption-free costs (near-shoring) and their impact on the optimal resilience strategy mix. Third, we show the value of disruption prediction and assess the interdependence with daily operational re-routing capacities. Fourth, we methodologically propose an enhanced Benders decomposition (BD) algorithm with a non-standard split of decision variables to solve the resulting two-stage stochastic problem and compare its performance against a commercial solver and a standard BD implementation (L-shaped). Lastly, we present a case with time-dependent disruption probability shifts that follow seasonal patterns to study differences in the cost-optimal resilience mix to a numerical study with equal probabilities of disruption occurrence throughout the planning horizon.

This paper is structured as follows. Section 1.2 presents an overview of related literature. Section 1.3 details the research problem. Section 1.4 introduces the two-stage stochastic program. Next, we propose a solution procedure based on BD, including its enhancements in Section 1.5. Section 1.6 outlines numerical results, and a case study is discussed in Section 1.7. Finally, Section 1.8 concludes by summarizing findings and proposing future research areas.

## 1.2 Literature review

Section 1.2.1 discusses literature on general levers that aim at increasing the SCR. Then, in Section 1.2.2, work on resilient supply chain network design for the SCND problem under uncertainty is reviewed. Section 1.2.3 summarizes literature on resilient transportation systems while Section 1.2.4 reviews work on BD with a focus on two-stage stochastic programs. Finally, Section 1.2.5 summarizes research gaps.

### 1.2.1 Increasing supply chain resilience with consideration of lead times

Various authors defined SCR, including crucial design characteristics and capabilities in the past. We refer to Hosseini et al. (2019a) for a detailed overview. Designing resilient supply chains involves uncertainty regarding both the impact and the occurrence of disruptions. Due to this uncertainty, supply chains require a detailed understanding of hidden interactions across different decision levels. In order to increase SCR, firms can adjust their network design as well as their tactical and operational decisions (Govindan et al. 2017). Various SCR drivers have been identified and discussed in analytical models, such as supplier segregation, multiple sourcing strategy, inventory positioning, multiple transportation channels, backup suppliers, re-routing, and product substitution (Hosseini et al. 2019a). Even though most studies highlight the benefits of multiple sourcing and backup suppliers, the explicit role of lead time is still not well understood as immediate effects of disruptions and SCR strategies are common assumptions (Aldrighetti et al. 2023).

To date, the effects of lead time under uncertainty have mostly been discussed in related inventory control literature. De Treville et al. (2014) presented a case study with managers of three companies that underestimated the benefits of short lead times under uncertainty. Boute and Van Mieghem (2015) study single and dual inventory control policies and compare local and global sourcing alternatives based on the inclusion of capacity cost and flexibility in addition to sourcing costs and lead times. In further understanding the effects of fast but expensive suppliers, Sun and Van Mieghem (2019) determine a capped dual index policy for the dual replenishment decision. Gijsbrechts et al. (2022) extend this view by considering fast, thus local, supply that is less flexible and more expensive and identify that local suppliers need to improve their volume flexibility to compete with cheaper offshore supply. Boute et al. (2022) show that local SpeedFactories can be valuable even when purchasing costs from near-shored suppliers are higher than the offshore costs due to significant inventory savings. However, the attractiveness of the near-shoring option is strongly influenced by the demand uncertainty studied. While we assume known demands, we focus on the influence of lead time effects through near-shored suppliers given the influence of supply uncertainty that affect the transportation from global suppliers.

### 1.2.2 Supply chain network design under uncertainty

Quantitative decision models that decide on the cost-optimal mix of resilience strategies for the SCND under disruption risks have become increasingly relevant. We refer to Snyder et al. (2016) and Aldrighetti et al. (2021) for recent overviews. Overall, SCND problems under disruption uncertainty have developed from primary facility locations to more integrated decision problems. Qi et al. (2010) solved the facility location problem under disruption uncertainty and compared an integrated against a sequential supply chain design to achieve considerable cost benefits considering disruption uncertainty at the strategic design phase. In contrast, Mete and Zabinsky (2010) proposed a two-stage stochastic programming formulation to account for both the strategic and tactical design policies while considering operational re-routing decisions to solve the storage and distribution problem of medical supplies in disaster management. While they focus on the special case of earthquake disaster mitigation, we extend their work on an integration of strategic to operational resilience strategies for transportation uncertainty to wider disruption scenarios. Nooraie and Parast (2016) were the first to propose an end-to-end decision model for supply chain design from suppliers to customers under disruption uncertainty considering multiple time periods. Khalili et al. (2017) extended previous two-stage stochastic programming formulations by integrating production and distribution planning problems under disruption risk, considering both proactive and reactive resilience strategies. Similarly, Azad et al. (2016) used a network optimization model to study the cost-effectiveness of installing alternative links in railroad networks under random disruption scenarios. With an overall focus shift from outbound to inbound logistic network models, Namdar et al. (2018) analyzed the benefits of a multiple sourcing strategy under disruption risks of inbound suppliers. Snoeck et al. (2019) combined strategic mitigation with operational decisions by incorporating the inbound supply chain planning with production planning and setup for the chemical industry and proposing a solution scheme based on linear approximation. As an extension of previous supplier selection problems, Hosseini et al. (2019b) incorporated decisions on additional manufacturing capacities and geographical separation of suppliers, considering regional disruption scenarios. Azad and Hassini (2019) developed an optimization model with partial failure of facilities and multi-mitigation strategies and proposed an enhanced BD to solve the problem. We build on their contribution of explicitly considering partial disruption of facilities with uncertain recovery duration by considering disruptions that are uncertain concerning their timing, length, and impact with seasonal patterns across the planning horizon. Alikhani et al. (2023) used a multi-methodological approach to select the best resilience strategies for varying supply chain disruptions. Specifically, they quantified the synergistic effects of the best-fit of candidate strategies on different disruption characteristics, such as cyberattacks and natural disasters. Based on this idea, we study the general differences on cost-optimal resilience strategies between low-impact but high-probability against high-probability but low-impact disruption events. They considered facility fortification, direct shipping, inventory increase, facility dispersation, multiple set covering, and cybersecurity in a single product flow and single time period environment. Aldrighetti et al. (2023) studied a resilient SCND in a multi-echelon, multi-period, and single-product setting with equal disruption probabilities for all locations. Through numerical and a case study focusing on the COVID-19 pandemic, they identified a good trade-off between resilience and investment costs with minimal investments focusing on agile and reconfigurable supply chains. Particularly, backup suppliers outside the main supply chain footprint are most efficient for disruptions on the supply side, while re-routing of material flows was a key SCR strategy for disruptions at own facilities. However, they assumed all disruption and recovery events with immediate impacts, ignoring the potential impact of lead times. In a similar multi-period setting, we study the impacts of disruption probability shifts across the planning horizon on the optimal mix of resilience strategies. Besides, in comparison to assuming immediate impacts of particularly re-routing decisions, we explicitly consider lead times to account more realistically for the impacts of strategic decisions on the operational level, such as near-shoring.

### 1.2.3 Resilient transportation systems

Transportation systems are part of the critical infrastructure to provide essential commodities and services. Similar to supply chains, they have become more and more complex and interdependent, making them prone to disruptions and increasing the time to recover. As a result, research on resilient transportation systems is becoming increasingly popular (Mattsson and Jenelius 2015).

Miller-Hooks et al. (2012) determined the optimal set of mitigation and recovery actions to achieve service constraints of a transportation system given a budget through a two-stage stochastic program for a rail-based container network. Omer et al. (2012) study the resilience of maritime transportation networks and the impacts of disruptions on port capacities by identifying three different resilience metrics. To increase the overall system understanding, Chen et al. (2017) study the port-hinterland container transportation network under disruption uncertainty. Motivated by the diverging operator interests, Chen et al. (2018) investigate the strategic resilience investments in a port-hinterland container transportation network. Due to its vulnerability and importance to the economy of China, Wang and Yuen (2022) conducted a simulation study on the Yangtze

Estuary Deepwater Channel to develop a resilience assessment indicator tested for different accident scenarios. While the focus of port-hinterland networks has been on the effects of disruptions on port infrastructure and their capacity, we discuss a new case example in which disruptions affect the transportation links between the nodes, e.g., through water-level driven effects.

### 1.2.4 Benders decomposition for two-stage network design

As first proposed by Benders (1962), BD is a commonly used exact algorithm for problems with complicated and continuous variables in which, when fixing the complicated variables, an easier subproblem remains. Due to the popularity of two-stage stochastic programs in SCND under uncertainty (Govindan et al. 2017), we focus on the application and recent improvements of the BD algorithm in two-stage stochastic programs and recommend the detailed overview of Rahmaniani et al. (2017).

The L-shaped method, as introduced by Van Slyke and Wets (1969), is a BD algorithm applied to two-stage stochastic programs in which the problem is decomposed into a master problem (MP) that includes the first-stage decisions and a subproblem (SP) that contains the second-stage decision variables. In contrast, we compare the performance of this split against alternatives in which first-stage flow decisions are decomposed in the SP. Based on this idea, Birge and Louveaux (1988) introduced the multicut algorithm for two-stage stochastic programs in which a single cut is generated for each scenario from the subproblem. Still, a straightforward application of the BD algorithm might result in time-consuming iterations, poor feasibility, and zigzagging behavior. Thus, work has focused on exploring ways to improve the (problem-specific) performance of the BD algorithm. We classify these strategies that are relevant for this work into three different categories and discuss their benefits for the specific problem at hand..

The first category contains strategies that aim to improve and strengthen the cut-generation process itself. Particularly, we focus on improving the cut-generation process by adding problem-specific valid inequalities to complement or replace adding feasibility and optimality cuts. Cordeau et al. (2006) have shown that introducing problem-specific valid inequalities can significantly improve the algorithm's performance. While valid inequalities aim at strengthening the feasible solution space of the MP, Adulyasak et al. (2015) have shown that lower-bound lifting inequalities can significantly improve the performance of the BD algorithm for a two-stage production routing problem under demand uncertainty. Similarly, we derive lower-bound lifting inequalities for our problem setting. In addition, they included pareto-optimal cuts based on Papadakos (2008) and scenario group cuts in which, in contrast to Birge and Louveaux (1988), cuts are only generated for groups of scenarios.

The second category groups methods that are based on the idea of generating cuts without solving the master or subproblem to optimality each time. For example, Easwaran and Üster (2009) incorporated a tabu search in the BD algorithm to provide initial strong upper bounds and, thus, initial good Benders cuts for a capacitated closed-loop network design. Similarly, Pishvaee et al. (2014) used valid inequalities and a local branching strategy that does not solve the master problem to optimality at each iteration for a sustainable network design problem under uncertainty.

The third category includes strategies that adjust the decomposition strategy considering the separation of information and decisions into master and subproblem for two-stage problems itself. Crainic et al. (2021) introduced the idea of partial BD to include information from the SP into the MP and showed its benefits for a general class of two-stage stochastic multi-commodity network design problems. Recently, Rahmaniani et al. (2024) explored parallelization strategies in which multiple SPs are solved in parallel on different processors and implemented the algorithm in a branch-and-cut (BC) framework for a two-stage multi-commodity capacitated fixed-charge network design problem with stochastic demands.

### 1.2.5 Discussion of research opportunities

To date, there needs to be more research combining strategic, tactical, and operational resilience strategies to understand their interdependence and cost-competitiveness (Govindan et al. 2017). Only Mete and Zabinsky (2010) considered this combination for transportation uncertainty; however, for the specific case of immediate earthquake disaster mitigation. While multi-period models have been introduced, time-dependent changes of the disruption probabilities to adequately consider the dynamic nature of supply chain vulnerability still need to be addressed (Aldrighetti et al. 2021, Hosseini and Khaled 2019). In addition, most models focus on low-probability / high-impact events that are impossible to predict. With few exceptions, such as the time-to-recover model (Simchi-Levi et al. 2015), common literature focuses on equal disruption probabilities and assumes immediate effects of disruptions and SCR strategies. However, this ignores both the effects of lead times on operational decisions and the potential benefits of short-term disruption prediction. As a result, research on disruption uncertainty remains on expert estimates or assumes known distributions that do not contribute towards an improved understanding of the proposed SCR strategies' cost-competitiveness (Aldrighetti et al. 2021).

## 1.3 Problem setting

Section 1.3.1 introduces the process and network structure of the SCND problem. We discuss the effect of disruptions on parameters in Section1.3.2. Finally, the resilience strategies are introduced in Section 1.3.3.

### 1.3.1 Network and process description

We consider a SCND problem with a single product in a discrete-time horizon, where the transportation network consists of multiple suppliers *(as sources)*, multiple transportation modes *(as arcs)*, and a single production facility *(as sink)*. Each supplier can deliver in unlimited quantities and in each time period. To deliver, however, a supplier needs to be qualified in the initial stage of the decision problem. Such a qualification comes at an investment cost as it includes negotiations, development of contracts or receiving and testing of product samples. Different transportation modes are available for each supplier to deliver raw materials to the production facility. However, only a single transportation mode might be available depending on the supplier. These transportation modes differ in transportation lead times, costs, and disruption proneness. The production

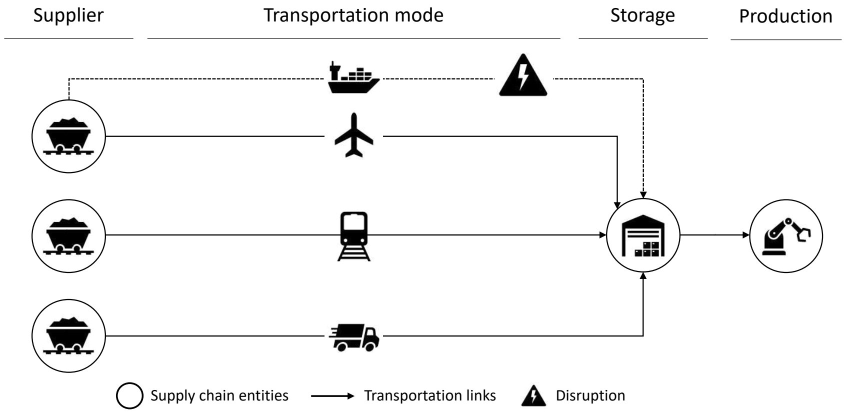


Figure 1.1: Overview of SCND structure considered.

facility holds inventory to fulfill its production demands. At the beginning of each period, transport shipments arrive that were ordered lead time periods earlier. The inventory capacity is limited and storage results in inventory holding costs linear to the inventory quantity stored. Then, production demands are fulfilled. These demands at the sink are defined through a deterministic production schedule for each time period along the planning horizon. Such deterministic schedules, e.g., are common for capital-intensive process industries such as chemicals that often rely on a continuous production process (Silver et al. 1998). An unfulfilled production demand, thus if no inventory is available, forces a production stop that results in shortage costs. Inventory holding costs are charged to the inventory level at the end of the period and transportation costs to the period of ordering. The simplified structure is shown in Figure 1.1.

### 1.3.2 Transportation disruptions

We define a transportation disruption as an unfortunate event causing a transportation cost increase to a single or multiple transportation modes along the planning horizon with varying duration and impact. Disruption events occur independently from each other. Merely the probability of occurrence and its impact depends on the transportation mode. These cost increases are a result of surcharges that transportation carriers enforce as reaction to disruptions to balance the lost capacities with the demands. Given these surcharge on top of the regular transportation costs, a transport is always available. Depending on the disruption impact and mode, these surcharges range from modest increases to full production stops, i.e., an unlimited increase in transportation costs. To account for full transportation stops, we bound the surcharges with the shortage costs. After the disruption event, its effects terminate immediately and transportation costs decrease to their disruption-free values.

Limited time prior to a disruption, its duration and impact on the transportation costs becomes known to the central decision-maker. We define this time as the *information window*. This information window is determined through the ability of a decision-maker to predict a disruption prior to its occurrence. On a longer horizon, however, the occurrence and impact of a disruption remain uncertain. For example, this applies to hurricanes where the route and intensity of the storm is known days before a landfall or strikes that are announced in advance. Figure 1.2 visualizes an example of a single disruption during the planning horizon. In the example, the transportation disruption lasts from $t = 50$ to $t = 70$. With $t^{info} = 5$, the disruption becomes known in $t = 45$ regarding its duration (20 days) and impact. Concerning the model formulation in Section 1.4, this translates to $T_s = \{45; 70\}$. In practice, the possibility of predicting disruptions strongly depends on the specific situation. We highlight the relevance of the information window as part of our case study in Section 1.7.2.2.

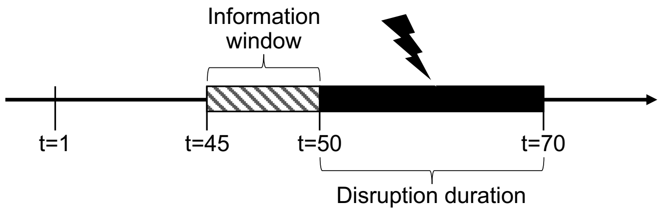


Figure 1.2: Time window on information certainty of the transportation disruption impact.

### 1.3.3 Resilience strategies

A central decision-maker at the production facility sources from various suppliers and is in full responsibility of the inbound flows. The goal is to minimize the expected costs through an optimal mix of SCR strategies. Thus, we minimize the trade-off between the costs of paying a cost premium for strategic and tactical resilience capacities when no disruption occurs and the uncertain cost increase from a disruption given the potential limited re-routing abilities on the operational level. We consider the following strategic, tactical, and operational SCR strategies in a two-stage stochastic decision problem.

***Multi-sourcing*** *(strategic, first-stage).* Qualification of multiple suppliers. This includes both multi-sourcing, i.e., purchasing from two or more suppliers in parallel, and the investment in a backup supplier.

***Near-shoring*** *(strategic, first-stage).* Qualification of a supplier that offers a transportation mode with a shorter lead-time (Chang and Lin 2019) or less prone to disruptions at a cost-premium.

***Inventory capacity adjustment*** *(strategic, first-stage).* Investment decision in additional inventory capacity increases the flexibility of decisions on the tactical and operational level.

***Inventory*** *(tactical, first-stage).* Decision to increase inventory through tactical transportation plan.

***Re-routing*** *(operational, second-stage).* Decision to re-route quantities from the tactical transportation plan due to a disruption. Besides the differences in mode-specific transportation costs, re-routing comes at a cancellation cost for the originally planned transportation quantities on the tactical level.

In contrast, the decision-maker can decide for risk-taking and against any SCR strategy but execute the same transportation plan across all scenarios.

## 1.4 Model formulation

Sets, decision variables and parameters are introduced in Sections 1.4.1-1.4.3 before we introduce the two-stage stochastic programming formulation in Section 1.4.4.

### 1.4.1 Sets

A set of suppliers $I$ delivers a product using a set of transport modes $\mathcal{M}$ to the production facility over a time horizon $\mathcal{T}$. To account for the stochastic nature of the decision problem, we introduce a set of disruption scenarios $\mathcal{S}$ and model the decision problem as two-stage stochastic program. For each disruption scenario, we introduce $\mathcal{T}_s \subset \mathcal{T}$ as disruptive time periods including a potential information window (see Section 1.3.2) where operational re-routing is allowed.

### 1.4.2 Parameters

Scenarios occur with probability $\pi_s$, with $0 \leq \pi_s \leq 1$ and $\sum_{s \in S} \pi_s = 1$. Each scenario $s$ represents a specific disruption situation as they can occur along the planning horizon. Thus, the transportation costs $c^M_{mts}$ reflect the scenario-specific ($s$) transportation costs for each time period ($t$) as an outcome of the transportation mode-specific ($m$) base costs and disruption-driven cost increases.

Per time period and product units stored, inventory holding costs $c^H$ occur. Each unfulfilled unit of demand $d_t$ results in shortage costs $c^N$. The total sum of all demands across the planning horizon is $d^A$. The operational re-routing of transportation quantities requires cancellation costs $c^P_i$ specific to supplier $i$. To qualify a supplier $i$, qualification costs $f^I_i$ are needed that depend on the specific supplier. The initial inventory capacity to store inventory on hand is $Y$. Through an investment decision this capacity can be increased by multiples of $Y^+$ at costs $f^Y$ per multiple. In the starting period, an initial inventory of $j_0$ is available. Transportation lead times $l_m$ are considered that depend on the transportation time via mode $m$.

### 1.4.3 Decision variables

The model decides between different SCR strategies (see Section 1.3.3) to minimize the total expected costs in a two-stage stochastic program. Thus, the interlink between the strategic and tactical decisions (first-stage) and the operational decisions (second-stage) are considered.

The first-stage decisions determine the network structure. The binary decision $z_i$ determines if supplier $i$ is qualified ($= 1$) or not ($= 0$). The initial inventory capacity can be extended through an integer investment decision $w$ in multiples of additional inventory capacity. Lastly, a tactical transportation plan $x_{imt}$ determines transportation quantities across scenarios. On the second-stage, this transportation plan can be adapted whenever disruptions occur in scenario $s$. This operational re-routing consists of additional shipments $\hat{x}_{imts}$ or quantity reductions $\check{x}_{imts}$ from the original plan.

Additional decision variables are needed to formulate the SCND problem. Variables $x_{imts}$ reflect the final transportation quantities from supplier $i$ via transport mode $m$ in scenario $s$ based on the tactical plan $x_{imt}$ (first-stage) and the operational re-routing decisions (second-stage) ($\check{x}_{imts}$,

$\hat{x}_{imts}$). In addition, we introduce the on-hand inventory $y_{ts}$ in period $t$ and scenario $s$. Instead of negative inventories, shortages $p_{ts}$ occur.

## 1.4.4 Model formulation

### 1.4.4.1 Objective function

$$\textit{minimize} \quad \overbrace{f^Y \cdot w + \sum_{i\in\mathcal{I}} f_i^I \cdot z_i}^{\text{first-stage}} + \sum_{s\in\mathcal{S}} \pi_s \cdot \underbrace{\Bigg( \sum_{i\in\mathcal{I},m\in\mathcal{M},t\in\mathcal{T}} c_{mts}^M \cdot x_{imts} + \sum_{t\in\mathcal{T}} c^H \cdot y_{ts} + \sum_{t\in\mathcal{T}} c^N \cdot p_{ts} + \sum_{i\in\mathcal{I},m\in\mathcal{M},t\in\mathcal{T}_s} c_i^P \cdot \check{x}_{imts} \Bigg)}_{\text{second-stage}} \tag{1.1}$$

The objective function (1.1) minimizes the total expected costs across scenarios by considering first-stage and second-stage decisions. Investment costs, on the first-stage, occur depending on the decision to invest in multiples ($w$) of inventory capacity ($Y^+$) and supplier qualification ($z_i$). On the second-stage, we consider transportation costs based on the quantities shipped ($x_{imts}$), inventory holding costs driven by inventory on hand ($y_{ts}$), shortage costs ($p_{ts}$), and cancellation costs for transportation plan changes ($\check{x}_{imts}$). Note that disruptions affect the transportation mode-specific costs ($c_{mts}^M$) in scenario $s$.

### 1.4.4.2 Constraints

$$\sum_{i\in\mathcal{I},m\in\mathcal{M},t\in\mathcal{T}} x_{imt} = d^A \tag{1.2}$$

Across the planning horizon, quantities that equal the total demand ($d^A$) must be assigned to the tactical transportation plan on the first-stage decision, ensured by constraints (1.2).

$$\sum_{m\in\mathcal{M}} x_{imts} \leq d^A \cdot z_i \qquad \forall i \in \mathcal{I}, t \in \mathcal{T}, s \in \mathcal{S} \tag{1.3}$$

$$y_{ts} \leq Y + Y^+ \cdot w \qquad \forall t \in \mathcal{T}, s \in \mathcal{S} \tag{1.4}$$

A supplier can only deliver once qualified ($z_i$), ensured by constraints (1.3). Constraints (1.4) limit the inventory on hand to the respective capacity, which is the sum of the initial available capacity $Y$ and the integer multiples $w$ of additional inventory capacity $Y^+$ invested for.

$$y_{ts} = y_{(t-1)s} + p_{ts} - d_t + \sum_{i\in\mathcal{I},m\in\mathcal{M}} x_{im(t-l_m)s} \qquad \forall t \in \mathcal{T} \setminus \{1\} | t > l_m, s \in \mathcal{S} \tag{1.5}$$

$$y_{1s} = j_0 - d_1 \qquad \forall s \in \mathcal{S} \tag{1.6}$$

Constraints (1.5) describe the inventory balance between two consecutive periods $t$ and $t-1$. The inventory on hand for each period $t$ consists of the sum of the final inventory of the previous period $t-1$, incoming units ($x_{im(t-l_m)s}$) ordered lead time ($l_m$) periods earlier and demands ($d_t$). The starting inventory for the initial period $t$ is defined in constraints (1.6). If the demands $d_t$ exceed the available inventory, shortages ($p_{ts}$) occur, leading to lost sales,which are penalized in the objective function (1.1).

$$x_{imts} = x_{imt} + \hat{x}_{imts} - \check{x}_{imts} \qquad \forall m \in \mathcal{M}, i \in \mathcal{I}, t \in \mathcal{T}_s, s \in \mathcal{S} \tag{1.7}$$

$$x_{imts} = x_{imt} \qquad \forall i \in \mathcal{I}, m \in \mathcal{M}, t \in \mathcal{T} \setminus \{\mathcal{T}_s\}, s \in \mathcal{S} \tag{1.8}$$

$$\check{x}_{imts} \leq x_{imt} \qquad \forall i \in \mathcal{I}, m \in \mathcal{M}, t \in \mathcal{T}_s, s \in \mathcal{S} \tag{1.9}$$

$$\sum_{i \in \mathcal{I}, m \in \mathcal{M}, t \in \mathcal{T}_s} \hat{x}_{imts} - \check{x}_{imts} = 0 \qquad \forall s \in \mathcal{S} \tag{1.10}$$

Constraints (1.7) ensure that actual transported quantities for each scenario $s$ equal the tactical transport plan ($x_{imt}$) while taking operational re-routing options during a disruption ($t \in \mathcal{T}_s$) into account. This approach is motivated by Lanza et al. (2021), who propose a similar decomposition strategy of tactical and operational decisions for scheduled service networks. The re-routing consists of transport cancellations ($\check{x}_{imts}$) from the tactical plan and short-term orders from alternative suppliers or transportation modes ($\hat{x}_{imts}$). Without disruptions and outside of the information window, the actual transportation quantities $x_{imts}$ equal the tactical transportation plan $x_{imt}$ as defined in constraints (1.8). Constraints (1.9) limit the cancellation quantity to the quantities of the tactical transport plan from supplier $i$ via transport mode $m$ and in time period $t$. On the operational level, constraints (1.10) ensure that operational cancellations and additional order quantities are balanced.

$$w \in \mathbb{Z} \tag{1.11}$$

$$z_i \in \{0, 1\} \qquad \forall i \in \mathcal{I} \tag{1.12}$$

$$y_{ts}, p_{ts} \geq 0 \qquad \forall t \in \mathcal{T}, s \in \mathcal{S} \tag{1.13}$$

$$x_{imts}, x_{imt} \geq 0 \qquad \forall i \in \mathcal{I}, m \in \mathcal{M}, t \in \mathcal{T}, s \in \mathcal{S} \tag{1.14}$$

$$\hat{x}_{imts}, \check{x}_{imts} \geq 0 \qquad \forall i \in \mathcal{I}, m \in \mathcal{M}, t \in \mathcal{T}_s, s \in \mathcal{S} \tag{1.15}$$

The non-negativity and variable definition constraints are summarized in (1.11)-(1.15).

## 1.5 Benders decomposition

In our two-stage stochastic program for the SCND problem, the first-stage decisions consist of a set of binary and integer investment decisions and a continuous variable $x_{imt}$. By fixing all first-stage decisions, a network flow problem results as subproblem, which can be decomposed by scenario and is easy to solve. However, our numerical tests showed that this significantly increases the complexity of the MP, and keeping $x_{imt}$ (as first-stage decision) in the SP, with the drawback of not decomposing the SP by scenario, outperforms the L-shaped method. We show the performance of both formulations in Section 1.6.2. Algorithm 1 outlines the proposed BD algorithm with $x_{imt}$ in the SP. After initialization and warm start, the MP (see Section 1.5.2) is solved to obtain the supplier qualification decision ($\bar{z}_i$), the investment decision in inventory multiples ($\bar{w}$), as well as the master objective, which equals the current lower bound (LB). Using the fixed decision outputs of the MP ($\bar{z}_i$, $\bar{w}$), the dual subproblem (DSP) (see Section 1.5.1) is solved, and we check whether the current upper bound (UB) is better than the known UB. Using the dual variables, an optimality cut is added to the MP in each iteration $l$ of the cutting plane procedure as the dual is always feasible (see Section 1.5.1). This procedure repeats until the tolerance $TOL$ is met.

**Algorithm 1** Benders decomposition algorithm.

```
Initialize l ← 1, TOL, UB ← +∞, LB ← −∞
Conduct warm start to obtain starting solution
Solve master problem to obtain w̄^l and z̄_i^l
LB ← Master objective
while UB − LB ≥ TOL do
    Solve dual subproblem with w̄^l and z̄_i^l
    UB ←min[UB, (Master objective) + (Dual subproblem objective)]
    Add a new optimality cut to master problem
    l ← l + 1
    Solve master problem to obtain w̄^l and z̄_i^l
    LB ← Master objective
end while
```

Particularly due to the many time periods and thus decision variables, the BD algorithm as outlined in Algorithm 1 does, even for small instances, not converge in an acceptable time limit. Thus, we solve the two-stage stochastic SCND problem by deriving enhancements from ideas previously investigated in literature. These are lower-bound lifting and valid inequalities (Section 1.5.3.1), branch-and-benders-cut (Section 1.5.3.2), and warm-start (Section 1.5.3.3).

### 1.5.1 Subproblem

Upon fixing the first-stage decisions to $\bar{w}$ and $\bar{z}_i$, we obtain a continuous linear program that is much easier to solve but not separable by scenario $s$ due to $x_{imt}$. Due to the presence of decision variables $p_{ts}$, the SP is always feasible since negative inventory levels can be avoided if at least one supplier is qualified (see Section 1.5.3.1). The total expected costs $v(\bar{w}, \bar{z}_i)$ of the second-stage can be calculated as weighted sum across all scenarios $s$ with their probability of occurrence $\pi_s$. In addition, since all cost parameters in (1.16) are finite and subject to constraints (1.5) - (1.6), any feasible solution of the SP must be bounded. As a result, the dual of the SP is feasible and bounded as well. Thus, we solve the following SP:

$$v(\bar{w}, \bar{z}_i) := min \sum_{s \in S} \pi_s \cdot ( \sum_{i \in \mathcal{I}, m \in \mathcal{M}, t \in \mathcal{T}} c^M_{mts} \cdot x_{imts} + \sum_{t \in \mathcal{T}} c^H \cdot y_{ts} + \sum_{t \in \mathcal{T}} c^N \cdot p_{ts} + \sum_{i \in \mathcal{I}, m \in \mathcal{M}, t \in \mathcal{T}_s} c^P_i \cdot \check{x}_{imts}) \tag{1.16}$$

*subject to:*

$$\sum_{i \in \mathcal{I}, m \in \mathcal{M}, t \in \mathcal{T}} x_{imt} = d^A \tag{1.17}$$

$$x_{imts} \leq d^A \cdot \bar{z}_i \qquad \forall i \in I, m \in M, t \in T, s \in \mathcal{S} \tag{1.18}$$

$$y_{ts} \leq Y + Y^+ \cdot \bar{w} \qquad \forall t \in \mathcal{T}, s \in \mathcal{S} \tag{1.19}$$

(1.5)-(1.10), (1.13)-(1.15).

To derive the Benders cuts, we define the DSP. In the DSP, the variable $\alpha$ is the dual variable of constraint (1.17), which ensures that the tactical transportation plan matches the total demand. The variables $\beta_{imts}$ are the dual variables of the transportation limitation to suppliers qualified (1.18), $\gamma_{ts}$ are the duals of the inventory capacity constraint (1.19), $\delta_{ts}$ are the dual variables of the inventory balance constraints (1.5) and (1.6), $\varepsilon_{imts}$ are the dual variables of re-routing constraints (1.7)-(1.8), and $\zeta_{imts}$ are the dual variables of constraints (1.9) limiting cancellations, and $\theta_s$ the dual variables of the operational re-routing balance constraints (1.10). The DSP can be stated as follows:

$$\begin{aligned} v(\bar{w}, \bar{z}_i) = max \qquad & d^A \cdot \alpha + \sum_{i \in \mathcal{I}, m \in \mathcal{M}, t \in \mathcal{T}, s \in \mathcal{S}} \bar{z}_i \cdot d^A \cdot \beta_{imts} \\ + \sum_{t \in \mathcal{T}, s \in \mathcal{S}} (Y + Y^+ \cdot \bar{w}) \cdot \gamma_{ts} & + \sum_{s \in \mathcal{S}} (j_0 - d_1) \cdot \delta_{1s} + \sum_{s \in \mathcal{S}} \sum_{t=2}^{\mathcal{T}} d_t \cdot \delta_{ts} \end{aligned} \tag{1.20}$$

*subject to:*

$$\beta_{imts} + \delta_{(t+L_m)s} + \varepsilon_{imts} \leq \pi_s \cdot c^M_{mts} \qquad \forall i \in \mathcal{I}, m \in \mathcal{M}, t \in \mathcal{T} \setminus \{1\}, s \in \mathcal{S} \tag{1.21}$$

$$\beta_{imts} - \delta_{ts} + \varepsilon_{imts} \leq \pi_s \cdot c^M_{mts} \qquad \forall i \in \mathcal{I}, m \in \mathcal{M}, t = 1, s \in \mathcal{S} \tag{1.22}$$

$$\gamma_{ts} + \delta_{(t+1)s} \leq \pi_s \cdot c^H \qquad \forall t \in \mathcal{T} \setminus \{n\}, s \in \mathcal{S} \tag{1.23}$$

$$\gamma_{ts} + \delta_{ts} \leq \pi_s \cdot c^H \qquad \forall t = 1, s \in \mathcal{S} \tag{1.24}$$

$$\delta_{ts} \leq \pi_s \cdot c^N \qquad \forall t \in \mathcal{T} \setminus \{1\}, s \in \mathcal{S} \tag{1.25}$$

$$\varepsilon_{imts} + \zeta_{imts} - \theta_s \leq \pi_s \cdot c^P_i \qquad \forall i \in \mathcal{I}, m \in \mathcal{M}, t \in \mathcal{T}_s, s \in \mathcal{S} \tag{1.26}$$

$$\alpha \leq 0, \beta_{imts} \leq 0, \delta_s \leq 0, \zeta_{imts} \leq 0, \gamma_{ts}, \varepsilon_{imts}, \theta_s \in \mathbb{R}, \qquad \forall i \in \mathcal{I}, m \in \mathcal{M}, t \in \mathcal{T}, s \in \mathcal{S} \tag{1.27}$$

### 1.5.2 Master problem

The MP is a relaxation of the two-stage stochastic problem defined in Section 1.4 that only considers the binary and integer first-stage decisions $w$ and $z_i$. At each iteration $l$ of the BD algorithm, an optimality cut (1.29) needs to be added to the MP from the DSP($\bar{w}$, $\bar{z}_i$). We formulate the master problem as follows:

$$min \qquad f \cdot w + \sum_{i \in \mathcal{I}} f_i \cdot z_i + \psi \tag{1.28}$$

*subject to:*

$$\begin{aligned} d^A \cdot \bar{\alpha}^l + \sum_{i \in \mathcal{I}, m \in \mathcal{M}, t \in \mathcal{T}, s \in \mathcal{S}} d^A \cdot \bar{\beta}^l_{imts} \cdot z_i + \sum_{t \in \mathcal{T}, s \in \mathcal{S}} (Y + Y^+ \cdot w) \cdot \bar{\gamma}^l_{ts} \\ + \sum_{s \in \mathcal{S}} (j_0 - d_1) \cdot \bar{\delta}^l_{1s} + \sum_{s \in \mathcal{S}} \sum_{t=2}^{T} d_t \cdot \bar{\delta}^l_{ts} \leq \psi \qquad \forall l = 1, 2, 3, ... \end{aligned} \tag{1.29}$$

$$w \in \mathbb{Z}, \psi \geq 0, z_i \in \{0, 1\} \qquad \forall i \in \mathcal{I} \tag{1.30}$$

### 1.5.3 Algorithmic enhancements

#### 1.5.3.1 Lower-bound lifting and valid inequalities

In BD, specifically in this problem setting, the optimality gap, which is the delta between upper and lower bound divided by the upper bound, may be large in initial iterations due to the poor quality of the LB. To address this issue, Adulyasak et al. (2015) proposed using initial cuts, called lower-bound lifting inequalities, for a production routing problem. Following this idea, we derive problem-specific lower-bound-lifting cuts for the MP by focusing on the flow costs, i.e., transportation and inventory costs. These constraints are added to the MP formulation of Section 1.5.2. We observe that, depending on the suppliers qualified in the master problem, the total flow costs can not be lower than the transportation costs in the disruption-free state $\hat{c}^M_{im}$ of the most cost-efficient transportation mode from a supplier qualified. We define the additional auxiliary decision variable $\tilde{x}_{im} \geq 0$ to define the lower-bound lifting inequalities:

$$\sum_{i \in \mathcal{I}} z_i \geq 1 \tag{1.31}$$

$$\sum_{i \in \mathcal{I}, m \in \mathcal{M}} \tilde{x}_{im} = d^A \tag{1.32}$$

$$\tilde{x}_{im} \leq d^A \cdot z_i \qquad \forall i \in \mathcal{I}, m \in \mathcal{M} \tag{1.33}$$

$$\sum_{i\in\mathcal{I},m\in\mathcal{M}} \hat{c}^{M}_{im} \cdot \tilde{x}_{im} + c^{H} \cdot \tilde{J}_0 \ \leq \psi \tag{1.34}$$

$$\tilde{x}_{im} \geq 0 \qquad \forall i \in \mathcal{I}, m \in \mathcal{M} \tag{1.35}$$

Constraint (1.31) ensures that at least one supplier is qualified. Constraint (1.32) ensures that the total demand is transported via one of the available transportation modes from qualified suppliers ($z_i = 1$) as defined in constraints (1.33). Based on this, constraint (1.34) provides a lower bound for the transportation costs, which account for the largest part of the total flow cost, and the initial inventory holding cost based on the pre-defined average starting inventory $\tilde{J}_0$ until its full consumption without any transports. Through these inequalities, we ensure a higher LB in the initial iterations and a faster convergence as suppliers with transportation modes that would already be higher in terms of disruption-free transportation costs are neglected.

#### 1.5.3.2 Branch-and-benders-cut

Instead of solving the updated MP at each iteration, we solve the Benders reformulation in a BC framework, often referred to as branch-and-benders-cut. To avoid a large number of optimal cuts added within a single tree, these cuts are added to the master problem only when an incumbent solution is found. This technique has yielded promising results in recent research (e.g., Codato and Fischetti 2006, Crainic et al. 2021).

#### 1.5.3.3 Warm start

We obtain a starting solution by solving the deterministic, disruption-free transportation problem and obtaining its objective value $Z^{Det}$. To further strengthen the model formulation, we add the deterministic solution as a lower bound for the master problem for the initial iterations.

$$Z^{Det} \leq \psi \tag{1.36}$$

## 1.6 Numerical study

We performed numerical tests on eight problem instances of different sizes. Section 1.6.1 outlines the numerical setup. We evaluate the effectiveness of our proposed BD solution method in Section 1.6.2. Numerical results and sensitivities are shown in Section 1.6.3.

### 1.6.1 Numerical setup

The algorithm is implemented in Python 3.8 using Gurobi 10.0.3. A desktop PC with an AMD Ryzen 9 5950X 16-Core processor with 3.4 GHz and 128 GB of RAM is used for model execution. All computational results are reported in seconds. We generate eight different problem sets as summarized in Table 1.1. Each problem set is generated in six problem sizes with the number of suppliers $|I|$ ranging from 2 to 32, suppliers $|M|$ ranging from 2 to 64, 100 scenarios $|S|$, and a

| Problem instance | Modes per supplier | Δ Mode costs | Disruptions | |
|---|---|---|---|---|
| | | | Probability | Impact |
| P1 | 1 | Low | Low | High |
| P2 | 1 | High | Low | High |
| P3 | 1 | Low | High | Low |
| P4 | 1 | High | High | Low |
| P5 | 2 | Low | Low | High |
| P6 | 2 | High | Low | High |
| P7 | 2 | Low | High | Low |
| P8 | 2 | High | High | Low |

Table 1.1: Overview of problem sets.

planning horizon of 365 days. While the number of scenarios significantly drives computational complexity in two-stage network design (Alikhani et al. 2023), we obtain first-stage decisions with only minor differences in inventory capacity investments with 100 scenarios. Of the 24 problem set-size combinations that were solved to optimality for all test instances, only 10 show a difference between the maximum and minimum inventory capacity investment observed while the overall mean of this delta is 0.61, thus less than a single incremental integer investment capacity. Especially for commodities, even for single product cases, many suppliers are available to source products from various distribution facilities worldwide. Demands are constant and deterministic. We distinguish between problem sets with ($P1 - P4$) and without ($P5 - P8$) a backup transportation mode per supplier. For the main transportation mode, we assume a linear dependence between disruption free costs $\hat{c}_{im}^M$ and lead time $l_m$ as shown in equation (1.37):

$$\hat{c}_{im}^M = -l_m \cdot a + b \tag{1.37}$$

Specifically, we distinguish a low ($a = 0.0025, b = 0.215$) and a high ($a = 0.005, b = 0.30$) delta on mode costs. All problem instances have the same disruption-free costs for the supplier with the longest lead time, and, thus, are comparable. For this supplier with the longest lead time, transportation costs in the disruption-free state account for 13% of the product value in comparison to 20% of inventory holding costs, which represents a typical ratio in the process industry. Thus, the difference is in the higher disruption-free costs of suppliers with a shorter lead time (high Δ on mode costs). Transportation lead times range from 3 to 34 time periods (days). Each additional supplier is considered to have a lower lead time on the main transportation mode but higher transportation costs. For all backup transportation modes $m$, the transportation costs are set to $\hat{c}_{im}^M = 0.3$ with a lead time of $l_m = 14$.

Disruption events within and across scenarios occur independently of each other. Scenarios occur with equal probability. In each scenario, each transport mode can either face no disruption, a single or two disruptions. We differentiate low-probability but high-impact and a high-probability but low-impact disruption situation. All disruption probabilities and impacts are motivated by the case example of recurring disruptions at the Rhine River. We consider a low-probability situation of 16% probability of a single and 4% of two disruptions during the planning horizon. In this situation, disruption impacts range from a 200% transportation cost increase to a full transportation stop, modeled through a Big-M increase of transportation cost. This represents a situation in which severe disruptions occur every five years with severe impacts. In the case of a high-probability but low-impact, a single disruption occurs with a probability of 75% and two disruptions with a probability of 20%. Their impacts range from a 40%-80% cost increase, representing a nearly annual recurring disruption that affects the cost-competitiveness of suppliers but not the general ability to deliver goods. Each disruption occurs randomly during the planning horizon with a uniformly distributed disruption length between 20 and 40 days. To account for the disruption uncertainty, we generate three instances for each problem set in each problem size, thus solving 144 instances in total.

### 1.6.2 Algorithm performance

We benchmark our BD against the branch-and-bound algorithm of Gurobi (GB) and the classical L-shaped implementation (LSHP) with all first-stage decisions in the MP, enhanced with partial BD (Rahmaniani et al. 2017, Crainic et al. 2021) and lower-bound-lifting constraints. The algorithms are terminated after 3,600 seconds if no optimal solution is found prior. Table 1.2 summarizes the average results by problem size and across problem sets with a backup transportation mode ($P5 - P8$). For each problem size, the number of instances solved to optimality is reported. In addition, we report whether or not a feasible solution was found. While GB can prove optimal solutions faster for small problem sizes, the BD algorithm starts to outperform GB, starting with a problem size of 8 suppliers and 16 transportation modes. Particularly for large instances, where GB cannot find feasible solutions within the time limit, the BD can still identify solutions with low average optimality gaps of 1.27%. Additionally, three instances can still be solved to optimality. Further, the enhanced LSHP leads to sub-optimal results. When keeping $x_{imt}$ in the MP, a facility location problem structure with flows remains. This is known to converge slowly. While the SP is solved faster, an enormous number of cuts are needed to prove optimality, which we can avoid through the alternative split of decision variables in our BD.

| | | Average optimality gap | | | Average CPU | | | Feasability | | | Optimality | | |
|---|---|---|---|---|---|---|---|---|---|---|---|---|---|
| $\|I\|$ | $\|M\|$ | BD | LSHP | GB | BD | LSHP | GB | BD | LSHP | GB | BD | LSHP | GB |
| 2 | 4 | 0.00% | 0.81% | 0.00% | 306 | 3600 | 221 | 12/12 | 12/12 | 12/12 | 12/12 | 0/12 | 12/12 |
| 4 | 8 | 0.00% | 1.62% | 0.00% | 1053 | 3600 | 1000 | 12/12 | 12/12 | 12/12 | 12/12 | 0/12 | 12/12 |
| 8 | 16 | 0.04% | 2.97% | 0.71% | 2031 | 3600 | 2356 | 12/12 | 12/12 | 12/12 | 9/12 | 0/12 | 8/12 |
| 16 | 32 | 0.25% | 2.63% | 2.44% | 3257 | 3600 | 3600 | 12/12 | 12/12 | 5/12 | 3/12 | 0/12 | 0/12 |
| 32 | 64 | 1.27% | 3.49% | - | 3412 | 3600 | - | 12/12 | 12/12 | 0/12 | 3/12 | 0/12 | 0/12 |

Table 1.2: Comparison of proposed BD algorithm against Gurobi and LSHP.

To understand the behaviors of the different BD algorithms and their improvements, Figure 1.3 visualizes the convergence curves for our proposed BD algorithm, our proposed algorithm without problem-specific valid inequalities and lower-bound-lifting constraints (BD-NoLBL), and the LSHP when solving $P5$ with an instance size of 8 suppliers and 16 transportation modes. Starting with the classical LSHP, one can see that because of the lower-bound-lifting constraints, the lower bound approaches the optimal solution relatively fast after 300 seconds of computation time. In addition, a strong incumbent solution is found even slightly faster than for our BD algorithm. However, no further improved incumbent solution is found, resulting in a remaining gap after the algorithm is terminated after one hour. Next, we analyze the behavior of our proposed BD without the problem-specific valid inequalities and lower-bound-lifting constraint. It takes the longest for this algorithm to find a strong first incumbent solution (after 2,100 seconds). This incumbent solution is even better than the LSHP incumbent solution after 3,600 seconds. However, without the lower-bound-lifting-constraints, we still see no significant improvement of the lower bound after one hour of computation time, and thus a remaining large optimality gap. After continuing the algorithm, finally, a slight improvement of the lower bound can be observed. Our BD, in comparison, finds the strongest incumbent solution with a very low gap to optimality because of the lower-bound-lifting constraints. After 600 seconds, optimality of the incumbent solution is proven and the algorithm terminates.

These analyses have demonstrated the added value of both the problem-specific lower-bound-lifting constraints and the choice of the tactical transportation decision variable $x_{imt}$ in the sub-problem as non-standard split of decision variables in two-stage stochastic programs.

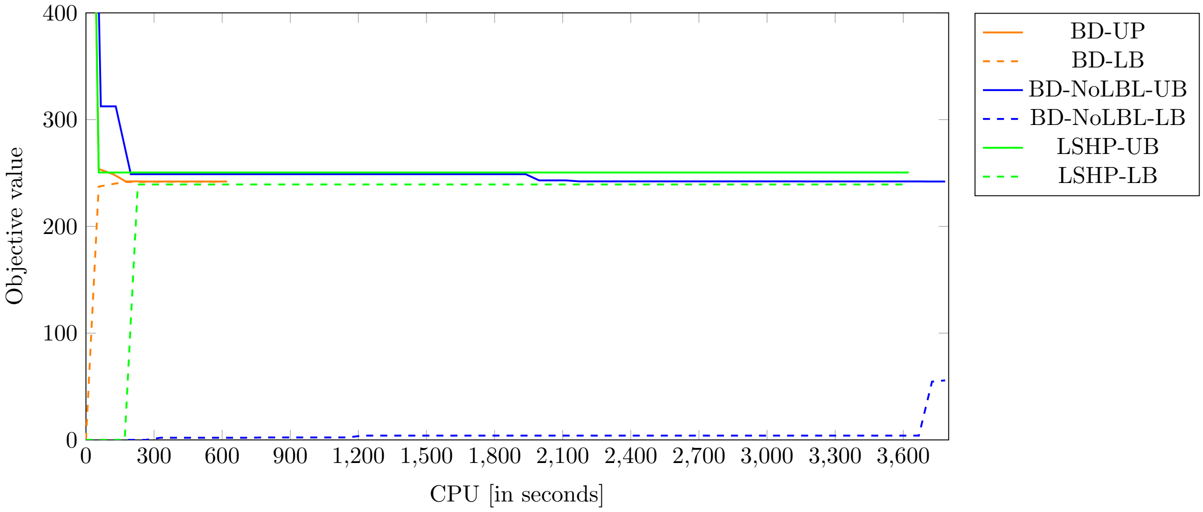


Figure 1.3: Convergence behavior of upper and lower bound.

### 1.6.3 Sensitivity analysis

We discuss the benefits of considering multiple SCR strategies in a joint decision framework. Specifically, we study the impact of backup transportation modes (Section 1.6.3.1), the influence of disruption characteristics (Section 1.6.3.2), and the benefits of near-shoring (Section 1.6.3.3) on optimal decisions and costs by analyzing the differences between the problem sets $P1 - P8$. We split the total objective value in a theoretical minimum cost ($MinC$) obtained by excluding disruptions from each instance and define the resilience cost ($ResC$) as the delta between the total expected costs and $MinC$. In addition, we discuss the impact of lead time aspects for a single supplier with different backup transportation mode cost settings in Section 1.6.3.4. Finally, Section 1.6.3.5 summarizes the insights from the sensitivity analysis.

#### 1.6.3.1 Value of a backup transportation mode

Depending on the specific problem set, there might only be a single transportation mode that is available to ship products from the supplier to the production location. Thus, we are interested in understanding the impact of the availability of a backup transportation mode per supplier (P5-P8) against sets without this availability (P1-P4). Table 1.3 summarizes the average results. The availability of a backup transportation mode has significant effects in the single-supplier case, decreasing $ResC$ by 32% on average. Compared to sets with multiple suppliers, the improvement reduces to 2%. Interestingly, the availability of a backup transportation mode increases the tendency for inventory investments $w$, as additional capacities might be required to grasp the savings from operational re-routing fully. Overall, we see a significant drop in the cost-competitiveness of inventory investments once multiple suppliers are available.

| | Single-supplier case | | | Multi-supplier case | | |
|---|---|---|---|---|---|---|
| Problem | ResC | $\lvert z \rvert$ | $\lvert w \rvert$ | $ResC$ | $\lvert z \rvert$ | $\lvert w \rvert$ |
| Without backup transportation mode | 13.13 | 1.00 | 4.42 | 3.87 | 2.00 | 0.31 |
| With backup transportation mode | 8.98 | 1.00 | 5.08 | 3.80 | 2.00 | 0.44 |

Table 1.3: Average optimal strategic resilience decisions across problem instances.

#### 1.6.3.2 Influence of disruption characteristics

Research in SCR literature has focused mostly on low-probability high-impact events. Table 1.4 presents the average results for the single and multi-supplier case when faced with different disruption characteristics. Interestingly, we see a shift in the importance of inventory investments. For low-probability but high-impact disruptions, significant investments of 6.58 additional inventory capacity units for the single-supplier case are needed, while they are reduced to nearly no investments when multiple suppliers are available. For high-probability disruptions, investments remain at least of some significance. While the resilience costs $ResC$ are not directly comparable between the two disruption probability characteristics, we see that the costs of the low-probability but high-impact disruptions can be more efficiently reduced through using multiple suppliers.

| | Single-supplier case | | | Multi-supplier case | | |
|---|---|---|---|---|---|---|
| | ResC | $\lvert z \rvert$ | $\lvert w \rvert$ | ResC | $\lvert z \rvert$ | $\lvert w \rvert$ |
| low-probability / high-impact | 9.80 | 1.00 | 6.58 | 2.62 | 2.00 | 0.08 |
| high-probability / low-impact | 12.31 | 1.00 | 2.92 | 5.01 | 2.00 | 0.69 |

Table 1.4: Average optimal strategic resilience decisions and costs for different probability characteristics.

#### 1.6.3.3 Cost-competitiveness of near-shoring

Lastly, we study the effects of near-shoring, thus sourcing from closer suppliers at higher transportation prices. We solve problem sets $P5 - P8$ with 16 suppliers and set lead times from 4 to 34 days without changing the disruption-free transportation costs $\hat{c}_{im}^{M}$. Thus, transportation costs of the fastest supplier are 30% higher than the slowest for the low delta on mode cost sets (60% for Δ Mode: High). By only allowing suppliers with high lead times, we obtain the optimal costs and decisions without near-shoring. Table 1.5 summarizes the results by the delta on mode costs and the disruption characteristics. For our high delta on mode costs, near-shoring is not a cost-competitive strategy as no closer supplier is considered in any of the instances. This changes for the low delta scenario. While near-shoring can reduce the *ResC* slightly for the low-probability and high-impact disruption situation (2.63%), these costs can be reduced by 23.93% for a high disruption probability.

| | low-probability / high-impact | | | | | | high-probability / low-impact | | | | | |
|---|---|---|---|---|---|---|---|---|---|---|---|---|
| | Δ Mode costs: Low | | | Δ Mode costs: High | | | Δ Mode costs: Low | | | Δ Mode costs: High | | |
| | ResC | $\|z\|$ | $\|w\|$ | ResC | $\|z\|$ | $\|w\|$ | ResC | $\|z\|$ | $\|w\|$ | ResC | $\|z\|$ | $\|w\|$ |
| No near-shoring | 2.63 | 2.00 | 0.00 | 2.72 | 2.00 | 0.00 | 4.85 | 2.00 | 0.67 | 5.09 | 1.67 | 2.67 |
| W. near-shoring | 2.56 | 2.00 | 0.00 | 2.72 | 2.00 | 0.00 | 3.91 | 2.00 | 0.33 | 5.09 | 1.67 | 2.67 |

Table 1.5: The effect of near-shoring on average resilience costs with different disruption characteristics.

#### 1.6.3.4 Influence of time for the backup transportation mode

We discuss the impact of lead time aspects for the backup transportation mode on the optimal total resilience costs. So far, we have assumed a backup transportation mode with a fixed lead time of 14 days and a 130% cost increase compared to the lowest-cost sourcing option in the disruption-free state. While we have analyzed the impact of multiple suppliers with shorter lead-times at higher costs, we want to understand the interdependence between the backup transportation mode costs and lead times in a single supplier setting. Figure 1.4 summarizes the results for three different costs of the backup transportation mode $\hat{c}_{im}^{M}$, a lead time from 4 to 34 days, and a main transportation mode with a lead time of 14 days that is prone to disruptions with costs of 0.13 in the disruption-free state.

Three main insights are drawn. First, as past orders triggered lead time periods prior to a disruption can not be canceled, there is limited value in lead times of a backup transportation modes that are shorter than the incumbent main transportation mode lead time. In contrast, we even observe negligible resilience cost increases due to inventory effects in operational re-routing. However, secondly, if backup transportation mode lead times increase above 14 days, the overall resilience costs increase dramatically by up to 186% in the case of $\hat{c}_{im}^{M} = 0.15$. Lastly, this potential increase strongly depends on the cost delta between the main transportation mode and the backup transportation mode. While this 186% increases reduces to 19% for $\hat{c}_{im}^{M} = 0.3$, even these high backup transportation mode costs still can lower the resilience costs.

#### 1.6.3.5 General insights on cost-competitiveness of resilience strategies

We summarize the findings of the numerical study based on the test instances P1-P8, which cover a variety of potential situations decision-makers will face in practice.

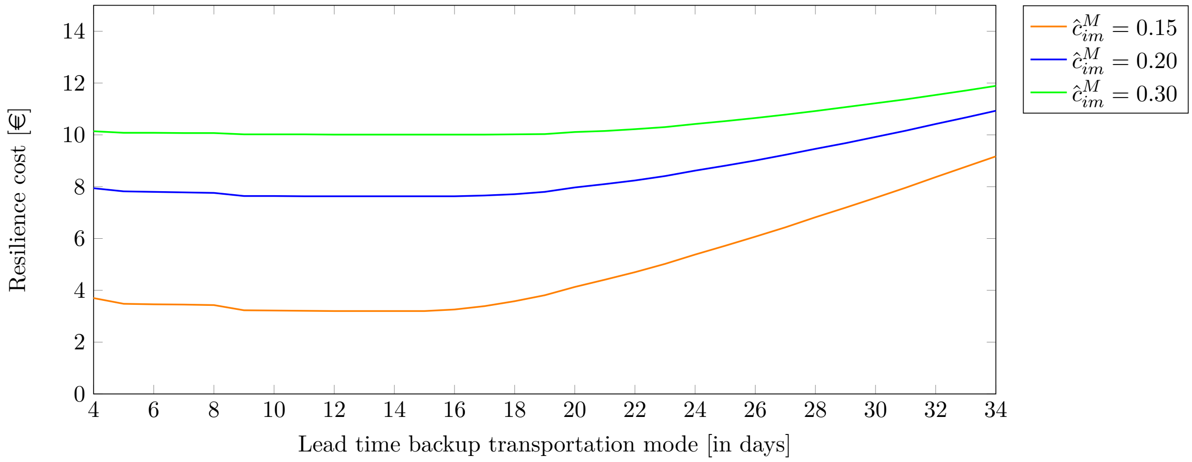


Figure 1.4: Relationship between backup transportation mode costs and lead time.

- Especially in sourcing situations where only a single supplier is available (e.g., highly specialized products to be sourced), there is a high need to understand the possibilities of backup transportation modes in case the main transportation mode is disrupted. Even if these backup transportation modes require significant cost increases (e.g., more than 100%), they can still be valuable as long as they represent an improvement compared to the maximum disruption surcharges. The same accounts for sourcing situations in which multiple suppliers are generally available but sourcing is limited to a specific region in which multiple suppliers share the same transportation mode (e.g., ports, sea routes, inland waterways, etc.).

- Disruption probabilities and impacts have a direct effect on the cost-competitiveness of resilience strategies. Interestingly, there is an inter-dependence between the various measures and the characteristics of low-probability / high-impact and high-probability / low-impact disruption scenarios. While in cases where only one supplier is available, optimal inventory investments in the cost-optimal state are higher, this characteristic changes in the multi-supplier case.

- Near-shoring can be an efficient resilience strategy for disruptions that occur often enough and in situations where the lead times of the main transportation mode prone to disruptions can be significantly reduced. While in the low-probability but high-impact disruption scenario both high and low $\Delta$ mode costs are significantly lower for the fastest supplier (60% and 120%), the resilience costs can only be reduced on a modest level. At the same time, significant savings can be achieved through near-shoring for the high-probability / low-impact case.

## 1.7 Case study

A case study, motivated by a real-life example, assesses the cost-competitiveness of resilience strategies based on actual disruption data. Section 1.7.1 introduces the case in detail, while Section 1.7.2 presents numerical results. Finally, managerial insights are drawn in Section 1.7.3.

### 1.7.1 Case introduction

This case is based on a real-life example from a chemical company located on the border of the Rhine River, Germany. Typical for the region, more than 40% of the inbound supply is transported through inland shipping via the Rhine River and transportation accounts for up to 10% of sourcing costs. Within our analysis, we focus on one exemplary product whose transport costs account for 10% of the sourcing costs, normalized at a value of 1. Inventory holding consist of capital, handling, storage, and depreciation costs. We assume annual inventory holding costs of 20% of the product value ($c^H = 0.2$). In the chemical industry, material shortage costs typically exceed the sum of finished good lost margins and customer penalty costs as complex production systems need to be shut down and re-started. After a restart, it can take hours to days to produce again a quality sufficient for customer requirements. Thus, we assume shortage costs that equal product value ($c^N = 1$).

Without disruptions, sourcing from Asia via ocean transport followed by inland shipping is the most cost-efficient transportation mode ($m = 1$). This mode has the longest lead time of $l_1 = 21$ and, without disruptions, the lowest transportation costs of $\hat{c}_{11}^M = 0.1$ per unit transported. However, this mode is prone to recurring disruptions due to water level changes that lead to surcharges depending on daily water levels as part of long-term contractual agreements between the transportation carriers and the case company. We focus on three transportation alternatives to highlight the influences of lead time and cost differences. All are assumed to be free of disruptions. The product can be air shipped ($m = 2$), however at very high transportation costs $\hat{c}_{22}^M = 0.5$ but in short lead time ($l_2 = 7$) by the main supplier ($i = 1$). Two additional near-shore suppliers ($i = 2; i = 3$) are available to deliver the products. From the closest supplier, products can be transported via truck ($m = 3$) in very short lead time ($l_3 = 3$) at a modest price increase $\hat{c}_{23}^M = 0.14$. Even at lower costs $\hat{c}_{34}^M = 0.12$, but with higher lead times ($l_4 = 14$), rail shipments ($m = 4$) from eastern Europe are possible.

Concerning the disruption uncertainty of the cheapest transportation mode, Figure 1.5 shows the water level fluctuations on the river Rhine for the last eight years. As can be seen, transportation stops due to low water levels occurred in 2015, 2017, 2018, 2020, and 2022, while high tides caused transportation stops in 2018 and 2021. In addition, occurrences where low water levels force vessels to carry reduced capacities and thus result in surcharges occur regularly. In addition, Figure 1.5 shows seasonal patterns as well. For example, high tides happen exclusively in winter while low water levels are typically seen in late summer or autumn.

Transportation surcharges for low and high water levels are significant, as highlighted in Table 1.6. Overall, the contractual surcharges range from a 78% to a 261% cost increase compared to water levels between 150 and 460cm, while on water levels less than 80cm and higher than 640cm, no transportation is possible. The orange line in Figure 1.5 highlights water level thresholds for cost increases and the red line indicates transportation stops. To ensure that we cover the uncertainty of the problem entirely, we construct additional scenarios beyond the eight years of history and surcharges available (Contargo 2023) by combining all quarters of each year randomly. As a result, we obtain 92 additional scenarios where each scenario occurs with a possibility of $\pi_s = \frac{1}{100}$.

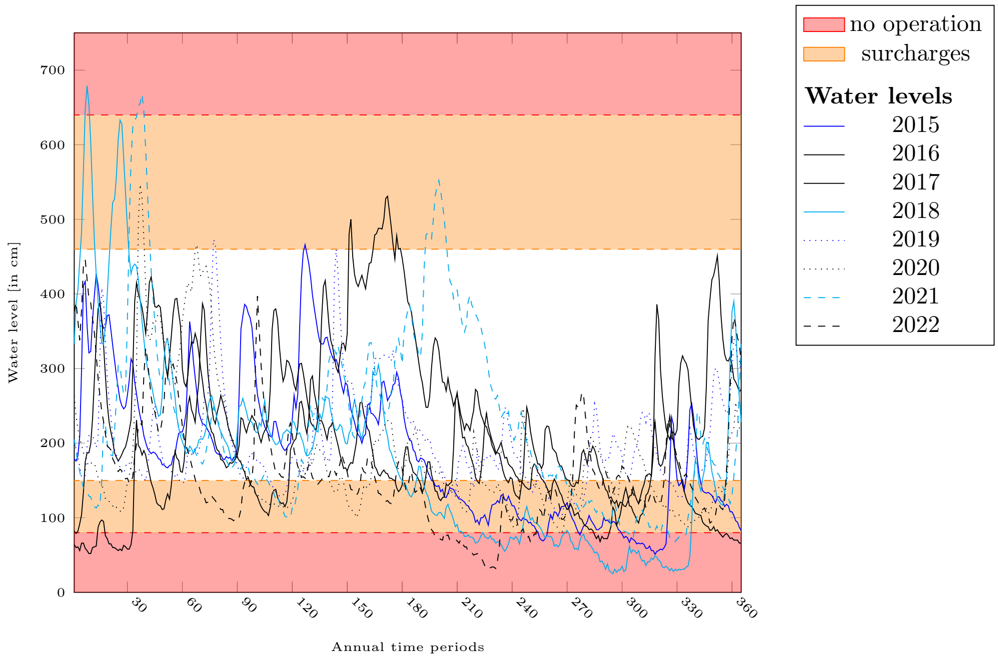


Figure 1.5: Historical water levels at shipment critical point for Rhine River as main transportation mode ($m = 1$).

| Water level [cm] | < 80 | < 90 | < 100 | < 110 | < 130 | < 150 | < 460 | < 640 | >= 640 |
|---|---|---|---|---|---|---|---|---|---|
| Costs [EUR] | - | 415 | 340 | 295 | 250 | 205 | 115 | 205 | - |

Table 1.6: Transportation costs per container transported depending on water level.

### 1.7.2 Numerical results

#### 1.7.2.1 Cost-optimal decision with uncertainty

Figure 1.6 summarizes the cost-effectiveness from risk-taking to the full integrated decision model. Each delta (light blue bars) describes the cost-impact for the decision maker to consider the resilience strategies mentioned starting from the risk-taking strategy. The tactical bar describes the total expected costs when only allowing second-stage decisions. As a result, the following conclusions can be drawn. First, decision-makers need to invest in resilience as risk-taking results in the highest total expected costs of 386 (123% cost increase compared to the disruption-free costs). Second, there is a clear need for a joint consideration of resilience strategies. For example, allowing operational re-routing as well as a tactical inventory decision without any strategic measures improves the expected costs by 30% while the incorporation of all resilience strategies improves the total expected costs by 50%. In addition, the interdependence of the resilience strategies is highlighted as the incorporation of multi-sourcing increases the optimal inventory investment by 33% additional capacity. Lastly, still, the total expected costs across the eight years are 10% higher than the disruption-free ideal state. This shows that all strategies can only limit the disruption-driven cost increase. However, significant cost savings can be achieved compared to risk-taking.

Besides the optimal resilience strategies chosen, we are further interested in the potential effects of seasonality. Figure 1.7 shows the average inventory across all scenarios and for the planning horizon

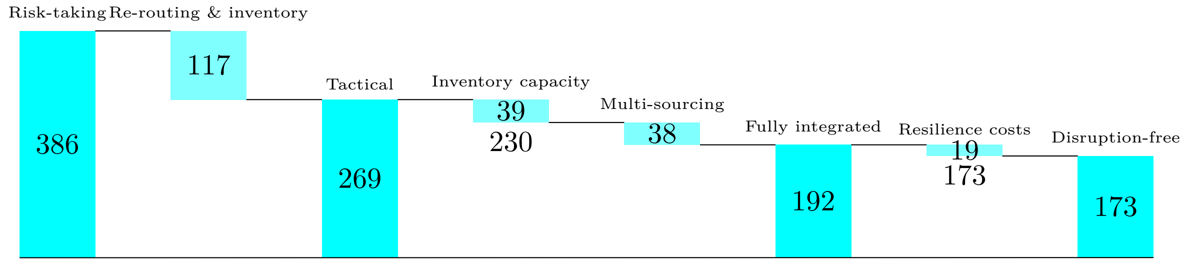


Figure 1.6: Impact of resilience strategies on total expected cost.

of one year. As can be seen, the average inventory level varies throughout. Peak inventories can be seen in January ($t = 0 - 10$), May ($t = 120 - 130$, and August ($t = 230 - 240$) while no inventory is held in parts of April ($t = 90 - 120$) and July ($t = 180 - 200$). These peaks follow seasonal water level fluctuations. Time periods with no disruptions are either used to avoid inventory carrying, as in April, or increase inventory to peaks just prior times of increased disruption uncertainty, as in August for September. Thus, the tactical inventory decision is clearly influenced by seasonal characteristics. As a result, this emphasizes the need to evaluate potential disruption probability shifts during the planning horizon.

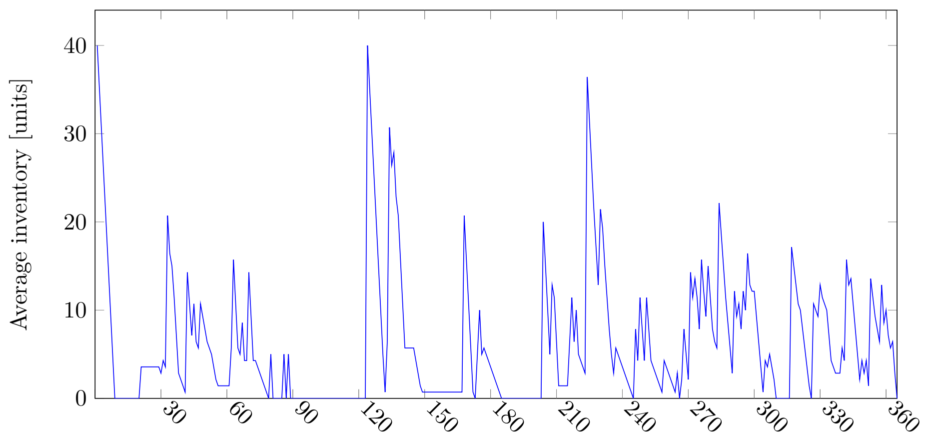


Figure 1.7: Optimal average inventory for all scenarios across the planning horizon.

#### 1.7.2.2 Benefit of information window increase through disruption prediction

As defined in Section 1.3.2, the information window describes the time a disruption is known to the decision-maker in its length and impact prior to the actual occurrence. To this end, all results are obtained taking no information window into account, i.e., assuming a disruption is not known in advance. However, significant efforts have been made to forecast disruptions, such as the water levels on the river Rhine in Germany (e.g., Bazartseren et al. 2003, Toonen 2015). Thus, we want to understand the impact of the ability to predict disruptions while varying the lead times of the alternative transportation modes.

We increase the information window from 0 to 21 days, representing a maximum ability to predict disruptions of three weeks. Further, we analyze three different situations for the backup transportation modes. First option I with very short lead times ($l_3 = 1, l_4 = 7$), second option II with modest lead times ($l_3 = 7, l_4 = 14$), and third option III with long lead times ($l_3 = 14, l_4 = 21$). In practice, this represents three situations with varying geographical distances and available transportation modes of the backup suppliers. Figure 1.8 highlights the results and their effects on the total resilience costs in %. The highest costs are observed for the last option with a time window of 0 days (set to 100% resilience costs). In comparison, without the ability to predict the disruption, shorter lead times already lower the resilience costs by more than 17%. In addition, knowing disruptions up to three weeks in advance can reduce resilience costs by up to 10%. Thus, the combination of shorter lead times and the ability to predict disruptions can reduce resilience costs by 27%. Generally, the resilience costs decrease with the information window, while the degree of reduction depends on the specific lead times. Overall, backup transportation modes' lead time significantly impacts the resilience costs. Thus, considering a backup transport alternative with shorter lead times but higher transportation costs could be more cost-competitive.

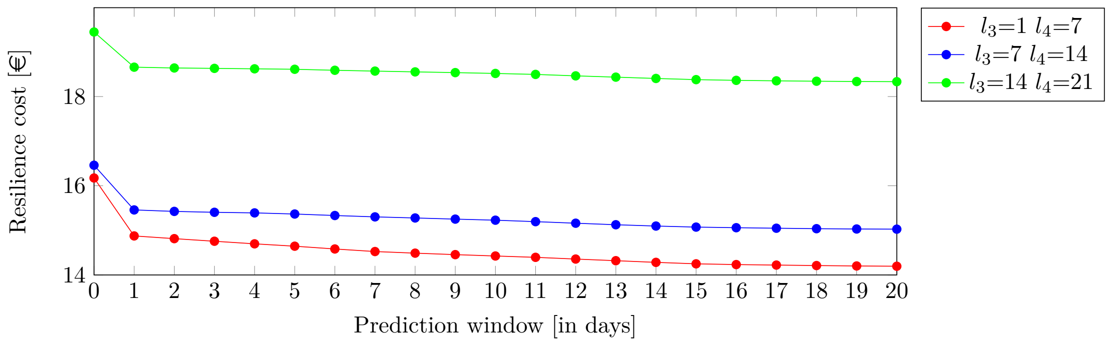


Figure 1.8: Effect of disruption prediction on various lead-times of backup transportation modes.

#### 1.7.2.3 Limited operational re-routing capacities

So far, we have assumed unlimited operational re-routing capacities. However, alternative suppliers or transportation modes might only offer limited capacities on the operational level depending on the disruption characteristics or the product to be sourced. Thus, we conduct a sensitivity analysis by limiting the second-stage additional order quantities $\hat{x}_{imts}$ to a maximum of daily demand $R_{im}$ by adding constraints (1.38) to the model formulation. We increase $R_{im}$ from 0% to 180% in steps of 20%. In addition, we vary the information window from 0 to 3 days.

$$\hat{x}_{imts} \leq R_{im} \qquad \forall i \in \mathcal{I}, m \in \mathcal{M}, t \in \mathcal{T}_s, s \in \mathcal{S} \tag{1.38}$$

Table 1.7 summarizes the results. All information windows result in the identical total expected costs for a re-routing capacity of 0%. Using this as a baseline, we show the resilience cost improvements in %. The highest reductions can already be achieved if only a share of the daily demand can be operationally re-routed from alternative suppliers or through alternative transportation modes. In the case example, a re-routing capacity of 40% of the daily demand volume already achieves more than half of the full potential with unlimited re-routing. This effect can be explained through additional inventory requirements to benefit from unlimited re-routing capacities fully. Whereas no inventory investment $w$ is required for the low capacities, starting from 80%, the benefits of re-routing require an inventory investment of $w = 1$, and in case of unlimited re-routing capacities, an investment of $w = 2$. The effects on the information window become increasingly relevant the higher the overall operational re-routing capacity. Whereas an information window of 1 day has only a minor cost effect for capacities $\leq 60\%$, the resilience costs are reduced by more than 10% for the unlimited capacities case (see Section 7.2.2.).

| Information | Maximum capacities for daily operational re-routing [% of daily demand] | | | | | | | | | |
|---|---|---|---|---|---|---|---|---|---|---|
| window [days] | 0 | 20 | 40 | 60 | 80 | 100 | 120 | 140 | 160 | 180 | $\infty$ |
| 0 | - | 9% | 13% | 16% | 18% | 20% | 20% | 20% | 20% | 20% | 21% |
| 1 | - | 9% | 14% | 17% | 20% | 21% | 22% | 22% | 22% | 23% | 24% |
| 2 | - | 10% | 15% | 18% | 21% | 22% | 23% | 23% | 23% | 24% | 24% |
| 3 | - | 10% | 15% | 19% | 21% | 23% | 23% | 24% | 24% | 24% | 25% |

Table 1.7: Potential of re-routing capacities on resilience cost reduction based on scenario without re-routing.

### 1.7.3 Managerial insights

To summarize, the following insights are drawn:

- For high-probability but low-impact disruption situations, near-shoring can significantly reduce resilience costs even when transportation costs are 30% higher in the disruption-free state.
- Disruption probability characteristics influence the cost-competitiveness of inventory as SCR strategy. For equal probabilities, as in our numerical study, inventory investments are mainly competitive when backup transportation modes or alternative suppliers are unavailable. In the case, however, the seasonal disruption characteristics result in time-dependent inventory build-ups along the planning horizon. Inventory build-ups can be efficient in time periods with low disruption probability prior to time periods with an increased disruption probability. In comparison, equal disruption probabilities would demand high inventory levels throughout the planning horizon, which lowers the cost-competitiveness of inventory as SCR strategy.
- The possibility to predict disruptions in the short-term, i.e., days in advance, can significantly lower resilience costs. Most notably, the biggest reductions can already be achieved if a disruption is known a day earlier, as operational re-routing can be triggered. To benefit from this potential, sufficient operational re-routing capacities must be available. Similar to the prediction ability, the largest share of improvement potential is already achieved if at least 60% of the daily demand can be re-routed on the operational level. In addition, investing a premium in near-shore backup suppliers, i.e., at higher transportation rates but lower lead times, can be cost-competitive, particularly with the ability to predict disruptions.

## 1.8 Conclusion

We have addressed disruption uncertainty in the integrated transportation problem from the strategic to operational level within a two-stage decision process. To solve large problem instances efficiently, we have proposed a BD algorithm enhanced through valid and lower-bound-lifting inequalities, branch-and-benders-cut, and a warm-start heuristic. The computational results show that the BD algorithm finds strong solutions for large problem instances, or even optimal ones, where commercial solvers do not find feasible solutions. Through numerical studies and a case from the chemical industry, we have shown that disruption probability characteristics influence the choice of optimal resilience strategies on strategic and tactical levels as well as costs. Near-shoring, even at higher disruption-free costs, can help to significantly lower costs when disruptions occur regularly. If sufficient daily operational re-routing capacities are available, predicting disruptions at least a day in advance can significantly lower resilience costs.

Although we have highlighted the benefits of our models and solution approach, our study is not without limitations. We studied a single-product SCND problem with a single echelon and demand destination. Thus, the proposed model can set the stage for future models that consider lead times for transporting multiple products with multiple inventory storage points under disruption uncertainty to understand the effects of various product characteristics on the optimal SCR strategy mix. Further, it would be interesting to analyse the impact of resilience strategy mixes for other industries with different cost structures. Another interesting research direction would be incorporating data-driven techniques to more adequately account for the stochastic nature of the problem at hand.

## Acknowledgments

We thank the Federal Institute of Hydrology (BfG) for providing the historical data that supported the analysis. In addition, the authors would like to thank the anonymous reviewers and the editor for their valuable recommendations, which have significantly improved our paper.

# Contribution 2 - Cost-driven decision tree rules for transportation planning under cost uncertainty

# 2 Cost-driven decision tree rules for transportation planning under cost uncertainty

Daniel Müllerklein, Pirmin Fontaine, Janosch Ortmann

**Abstract** The problem of determining optimal inventory replenishment decisions balances the costs of excess inventory with shortage risks and transportation costs. While demand uncertainty has been the focus of stochastic inventory modeling, the effects of transportation cost uncertainty are poorly understood. In practice, however, transportation modes are prone to disruptions that result in stops and cost increases. While historical disruption data is available, it is difficult for practitioners to understand how transportation mode decisions and their timings must be adjusted. To overcome this gap, we combine mathematical optimization with machine learning to predict cost-optimal replenishment orders using only historical data. The problem is modeled as SIRPDD that minimizes total expected costs. With perfect information, optimal decisions are generated as labels for the supervised learning using features from inventory control and disruption-related information. Specifically, we propose a new CDDT framework that optimizes the costs of applying the resulting replenishment policy within hyperparameter tuning instead of the prediction score of the individual decisions. To handle the resulting computational complexity, we develop a genetic algorithm. We present a case study for the SIRPDD with transportation cost uncertainty based on a chemical company at the border of the river Rhine. Relevant features include the inventory position, historical water level, their trends, and predictions. While traditional learning approaches result in inefficient policies concerning transportation mode decisions and timings, we show that our CDDT can reduce costs by 20% compared to the (s,Q)-reorder policy, which represents the industry standard, and 18% compared to classical machine learning frameworks. For academics, our CDDT framework provides a new methodology to derive data-driven decision under uncertainty. For practitioners, we show how simple decision rules can be derived for replenishment decisions under cost uncertainty

---

URL (working paper): `https://www.gerad.ca/fr/papers/G-2024-04`

## 2.1 Introduction

Companies worldwide seek a balance between risks and cost-efficiency in their supply chains. Due to the various disruptions in recent years, many companies are undertaking efforts to re-design their supply chains to increase resilience. Following this objective, increasing inventory and sourcing from multiple suppliers are two key levers (Hosseini et al. 2019a). In order to achieve significant savings, transportation and inventory management issues need to be considered jointly (Berman and Wang 2006). In practice, this requires adjusting the policies that set rules for inventory replenishment. Due to their ease of implementation, these policies are industry standard. Determining a cost-optimal inventory replenishment policy, however, that defines when to order, how many units, from which supplier, through which transportation mode, is a challenging problem for decision makers. Historically, extensive efforts have been made to identify the optimal replenishment policy under uncertainty, mainly focusing on demand uncertainty with known stochastic distributions.

However, uncertainties concerning recurring transportation disruptions driven by man-made (*e.g.*, strikes) or natural disruptions (*e.g.*, hurricanes) affect transportation costs and thus the inventory replenishment decisions on a regular level (Chen et al. 2012). Due to the increase in extreme weather events, particularly global inland waterway transport disruptions gained growing attention as low- and high-water-level situations affect the shipment carrier's transport capacities and abilities. This specifically means that, based on the actual water level at the day of a potential shipment, they enforce contractual surcharges on top of their standard prices or even stop their service completely. For example, in 2018, the low water levels at the river Rhine forced a stop of all transportation through the river for 132 days, resulting in production stops due to material shortages for many companies. In 2023, container carriers, including Maersk and Hapag-Lloyd, implemented a low water surcharge between 100-150 USD per TEU, a container equivalent, on all cargo transported through the St. Lawrence River in Canada. In addition, low water levels on the Panama Canal forced vessels to lighten their loads. As a result, Hapag Lloyd announced a 500 USD surcharge per TEU on all cargo between Asia and the US East Coast shipped through the canal. Due to climate change, many experts expect an increased frequency of these high and low water events on major waterways in the future (Koetse and Rietveld 2009). While these surcharges are of high economic importance, the disruptions that drive the future surcharges are uncertain and difficult to predict in advance.

As a result, a decision maker needs to anticipate the relevant transportation costs in delivery time periods in the future as surcharges are determined upon the water level during transport and not upon order. The longer the lead time between ordering and the arrival at the critical transportation mode, the higher the corresponding uncertainty. In addition, practitioners that face uncertain costs are less interested in the single optimal solution but in decision rules that can help determine an inventory replenishment policy that performs near-optimal under uncertainty. They need to understand which attributes of the problem drive the replenishment decision and how such rules can be extracted from historical data to transfer findings to existing control systems. While an increasing amount of data becomes available, there is still a lack of understanding on how to apply these data-driven inventory management approaches in both practice and academia. In the past, these problems were solved in a two-step framework by estimating random variables and then incorporating these estimations into policy building. Estimating these random variables, however, is a challenging problem itself.

Motivated by the uncertain transportation costs that decision makers can face due to surcharges in waterway transport, we model the problem as SIRPDD (Coelho et al. 2014). This special case of inventory routing takes direct deliveries into account, which is highly relevant in cases where storage capacities and demands of customers are large relative to vehicle capacity, and thus it is cost-beneficial to deliver full-truck loads (Gallego and Simchi-Levi 1990). Delivering full-truck loads is particularly relevant where inventory holding costs are low compared to transport costs. Both holds true for the process industry, which majorly uses inland shipping. We particularly extend the standard problem setting by stochastic transportation costs on arcs connecting the suppliers with the customer location. Thus, at the time of the replenishment decision, the total procurement cost as the sum of transportation and unit costs are uncertain.

While the introduced multi-stage stochastic programming formulation could be solved in theory, it is clear that obtaining the scenario tree in a data-driven way as well as solving the problem is extremely challenging. Instead, we want to predict future decisions that perform cost-optimal in a data-driven way through a combination of mathematical optimization with machine learning. Thus, we propose a new CDDT framework for the inventory replenishment problem with multiple suppliers and transportation cost uncertainty to decide when to source, which quantity, from which supplier. This approach builds on the idea that a replenishment policy can be learned from historical cost-optimal decisions without estimating stochastic distributions. Within our CDDT, we first create labels by solving the Inventory Routing Problem with Direct Deliveries (IRPDD) assuming perfect information. Then, for each order size and each supplier, we train a supervised machine learning algorithm on the labels. In contrast to state-of-the-art machine learning-optimization frameworks that optimize for classifiers' individual prediction performance, we optimize hyperparameters to directly minimize the costs of applying the resulting replenishment policy. This evaluation is critical as otherwise, inter-dependencies between the individual classifiers are neglected. To overcome the rise in computational complexity, we develop a genetic algorithm with the total costs of applying the predicted replenishment orders as fitness function.

Our main contributions are as follows:

1. We introduce a multi-stage stochastic program for a new type of the SIRPDD with transportation cost uncertainty at every decision stage. The replenishment problem considers multiple suppliers, lead time differences between suppliers, and different transportation quantities.

2. We propose our new CDDT framework that directly minimizes the total costs, as defined in the objective function of the SIRPDD, within the validation step of hyperparameter tuning. Instead of approximating a surrogate loss function, we directly evaluate the predictions for interdependent decisions by setting all decisions to the predictions values of the SIRPDD within the validation step of hyperparameter tuning. We show the value of our new framework for data-driven interdependent replenishment decisions under uncertainty with multiple suppliers, different order quantities, and lead time differences.

3. To handle the rise in computational complexity through deriving the loss function directly from the optimization problem compared to traditional hyperparameter tuning approaches, we develop a genetic algorithm that incorporates the objective of the SIRPDD as fitness function.

4. We present a case study and compare our CDDT against state-of-the-art optimization-and-machine learning frameworks and replenishment policies from the literature. Particularly, we show that traditional hyperparameter tuning that maximizes prediction performance leads to inefficient and unstable policies.

5. Via the case study, we derive managerial insights on the data-driven inventory replenishment with multiple suppliers and cost uncertainty, leveraging public databases for waterway transport disruption uncertainty. Through our CDDT, well-performing and interpretable policies can be directly extracted without assumptions on any its structural components.

This paper is structured as follows. Relevant literature is discussed in Section 2.2, and the problem is formalized in Section 2.3. Section 2.4 presents the SIRPDD with transportation cost uncertainty. The CDDT framework is outlined in Section 2.5. The results of a case motivated by a real-life example are discussed in Section 2.6. Section 2.7 summarizes and concludes.

## 2.2 Literature review

Section 2.2.1 reviews literature in inventory management under supply uncertainty with a focus on replenishment policies for multiple suppliers. We then shift to data-driven approaches in inventory management in Section 2.2.2. Lastly, Section 2.2.3 reviews the use of machine learning in supply chain resilience as a related field, and Section 2.2.4 summarizes research opportunities.

### 2.2.1 Inventory management under supply uncertainty and multiple suppliers

Inventory management aims to optimize the holding of stocks along the supply chain to minimize costs while fulfilling customer demand. Over time, a variety of standard problems have been formalized for which mathematically developed decision rules exist that determine when to order, from which supplier, and which quantity. We refer to Silver (1981) for an overview. Despite the early focus on stochastic problem settings (Karlin 1960), in which models on stochastic demand outweigh those on deterministic demand (Williams and Tokar 2008), analyzing situations with stochastic supply was not of major attention until the early 2000s (Güllü et al. 1999). In inventory routing, supply uncertainty even gained attention only recently (Alvarez et al. 2021). We summarize the literature concerning supply uncertainty based on its uncertainty characteristics, namely, lead time, yield, and cost uncertainty. In addition, we distinguish between single and multiple supplier settings as multi-sourcing is a lever for supply-side disruption uncertainty. We recommend the recent overview of Svoboda et al. (2021) on inventory replenishment models with multiple suppliers and Coelho et al. (2014) on inventory routing.

*Lead time* uncertainty analyzes situations in which the replenishment of inventory from a supplier deviates from the contractually agreed time. While the area of lead time uncertainty has been discussed early on in respective literature (Whybark and Williams 1976, Schmitt 1984), it is still of relevance today. For example, Chopra et al. (2004) analyze the impact of lead time uncertainty on necessary safety stocks for different service level requirements. Kouvelis and Li (2008) analyze imperfect information on lead times from a primary supplier where a flexible backup supplier can be used as emergency response.

The uncertainty of the *yield* is relevant in problem settings where only a limited number of suppliers is available, and suppliers face a disruption risk or production systems produce a random yield. Thus, inventory can help to reduce the dependency risk on these suppliers. To combine demand uncertainty with the uncertainty of delivery quantity received, Bollapragada and Rao (2006) proposed a heuristic to solve the capacitated inventory system with both demand and supply uncertainty. Iakovou et al. (2010) captured the trade-off between inventory holding and disruption risks at the supplier capacities in a single period stochastic inventory decision-making model extending the classic newsvendor analysis. Similarly, Saghafian and Oyen (2012) analyzed the value of flexible backup suppliers under disruption risks using a newsvendor analysis with recourse. For multiple supplier cases with equal lead times, Chen et al. (2012) propose optimal replenishment decisions in a closed form, studying the problem of a regular supplier that faces disruption uncertainty and a reliable backup supplier at a price premium. They further highlight the need to consider different lead times for suppliers, however, requiring multiple dimensional state spaces to model the system dynamics. Hu and Kostamis (2014) studied multiple-sourcing strategies when some suppliers face risks of complete supply disruptions. Using an approximate model, they showed that the total order quantity and its allocation between a reliable and an unreliable supplier are independent decisions when the unreliable supplier faces a risk of a complete or near-complete supply disruption. Berling and Sonntag (2022) studied a production-inventory system with random demand, random yield, and rework and proposed a new solution procedure to find the optimal base-stock policy for this specific problem setting. Hasturk et al. (2024) introduced and solved the stochastic, cyclic, inventory routing problem with supply uncertainty. They propose a generic solution approach that leverages the idea of parameterized cost functions to anticipate dynamic purchasing decisions.

Lastly, *procurement as well as transportation cost* uncertainty is highly relevant in the areas of commodities and fluctuating spot prices in which inventory plays a significant role in risk hedging. One of the first to analyze the impact of fluctuating costs for a single item and multi-period model was Kalymon (1971), assuming a known Markovian stochastic process for the description of future costs. More recently, Xiao et al. (2015) analyze a periodic review joint pricing and inventory control model facing both stochastic demand and fluctuating procurement costs in a dual-sourcing strategy. As one of the rare data-driven approaches, Xiong et al. (2022) used a robust optimization approach for the periodic-review dual sourcing inventory replenishment management in the presence of purchase price and demand uncertainty. The data-driven results lead to some deviating findings from traditional approaches assuming complete distributional information. However, only a robust rolling-horizon model was used due to limited historical data.

### 2.2.2 Data-driven inventory replenishment

Historical data is available in many companies to develop distribution-free inventory control approaches. Still, most literature (see Section 2.2.1) relies on distributional assumptions, weakening the accuracy of models at the expense of simplicity (Svoboda et al. 2021). To increase their accuracy in practical applications, data-driven uncertainty modeling is gaining increasing attention. We recommend the overview of Mišić and Perakis (2020) on data-driven approaches in inventory management and summarize relevant works in the following. Priore et al. (2019) use machine learning to choose between four different replenishment policies for a single product in a three-echelon supply chain assuming periodic-review inventory policies and achieve an accuracy above 80% in the prediction of the ideal replenishment rule for the specific supply chain scenario simulated. Ban and Rudin (2019) investigated the data-driven newsvendor problem in which feature information is related to future demand and proposed different solution procedures based on singe-step machine learning algorithms. Bravo and Shaposhnik (2020) proposed a learning framework with the idea of deriving optimal policies for optimization problems that can be modeled as dynamic programming problem. They test their approach on the single-item, finite-horizon periodic-review model and show that the optimal thresholds of a base-stock policy can be learned from linear functions in a two-step process. Neghab et al. (2022) propose an algorithm based on integrating optimization, neural networks, and hidden Markov models for the single-period newsvendor problem with demand that depends on observable features rather than a known demand distribution. Gijsbrechts et al. (2022) showed that deep reinforcement learning can solve classic, intractable inventory problems, such as lost sales, dual-sourcing, and multi-echelon problems. Beyond the need to extend their findings to other real-world environments, they highlight the need for inventory researchers to generate structural policy insights beyond black box approaches. Bertsimas et al. (2023) proposed a new approach for adressing multi-stage stochastic problems with unknown distributions where uncertainty is correlated across time by solving a robust optimization problem and providing asymptotic optimality guarantees. They conduct numerical experiments with two single product, single supplier, and stochastic inventory settings where the optimal replenishment quantity is to be determined at each given decision stage. Recently, Qi et al. (2023) proposed a data-driven end-to-end framework for the multi-period decision on inventory replenishment quantities under uncertain demand and lead times using deep-learning. In contrast to this work, they assume a single supplier, fixed replenishment cycles, and conduct the hyperparameter tuning within the validation with the objective of minimizing the difference between predicted and cost-optimal replenishment quantities.

### 2.2.3 Increasing supply chain resilience with machine learning

While traditional supply chain risk management strategies cannot deal with supply chain disruptions as unexpected events (Pettit et al. 2010), recent focus has shifted towards the usage of big data and advanced analytics for risk prediction and the selection of resilience strategies (Baryannis et al. 2019b, Ivanov et al. 2019). Kosasih and Brintrup (2021) use graph neural networks to detect potential links within a supply chain to increase supply chain visibility to counteract disruptions that occur within the network. Following the objective of increasing transparency, Baryannis et al.

(2019a) test different machine learning techniques for risk prediction in combination with expert estimates. Similarly, Brintrup et al. (2020) use a three phase machine learning approach to predict supply-side disruptions at the suppliers with an accuracy of 80%. They highlight the need of incorporating external data sources to increase prediction accuracy and discuss the challenge of class imbalance for disruption-related predictions. Besides, various approaches emerged as a result of the COVID-19 pandemic. For example, Nikolopoulos et al. (2021) use deep-learning models based on google trends and simulating governmental decisions to predict supply chain disruptions while Bassiouni et al. (2023) applied several deep-learning approaches to predict shipment risks that link manufacturers and customers under potential COVID-19 imposed restrictions. Overall, related literature has focused on the ability of disruption predictions with initial success, however, this ability has not been incorporated in corresponding decision models and support systems.

### 2.2.4 Summary of research opportunities

Operations management research, in general, but particularly research in inventory management usually simplifies their models by assuming distributions for uncertain parameters thereby weakening the accuracy of models (Chen et al. 2023). As a result, there is still a need for data-driven approaches in inventory management (Svoboda et al. 2021). There is especially a need for such approaches that can provide explainable and interpretable results for the acceptance of decision makers (Mišić and Perakis 2020). Ideally, these approaches even result in specialized policies that perform near-optimal for the specific problem setting at hand (Gijsbrechts et al. 2022). Furthermore, there is an ongoing need for inventory replenishment models with supply uncertainty. Specifically, the area of cost uncertainty has mainly been covered through newsvendor approaches that reduce the dimensionality of the replenishment problem to a pure decision on quantity; neglecting the need to decide on when to order from which supplier in a multiperiod setting where past decisions influence the future replenishments. Lastly, while an increasing amount of information on supply uncertainty may become available to decision-makers, its value on decision-making may vary significantly (Mehrotra and Schmidt 2021). Thus, decision-makers ideally require frameworks that can evaluate and assess the value of information while incorporating them directly into decision support.

## 2.3 Problem setting

A single product is distributed with direct deliveries from multiple suppliers to a single customer location with unlimited transportation capacity over a finite horizon of discrete time periods. Over the time periods, each direct delivery is done through a specific transportation mode that differs by supplier in terms of transportation costs and delivery times. The single customer location can store inventory to satisfy its demands, whereas unlimited supply capacity is available from suppliers within the delivery time. The customer has a known inventory storage capacity. At the beginning of each period, deliveries from suppliers arrive that were ordered at delivery time periods in the past. Then, a customer's demand is fulfilled, which is known and constant as determined by a production plan. This is a valid assumption for many inbound processes in many industries and particularly the case of chemical production which we consider. In case the demand exceeds the available inventory, shortages occur. After the fulfillment of customer demand, replenishment orders are placed. Lastly, at the end of each time period an inventory quantity remains that forms the starting inventory of the next time period. Inventory holding and shortage costs are charged at the end of the period, while transportation costs are determined at the time period of arrival. Figure 2.1 visualizes the overall problem. Here, in time period $t$ the decision maker has two suppliers as options to place an order that will either arrive in $t+3$ or $t+5$. Due to the potential occurrence of disruptions, the corresponding costs of both options are still uncertain in $t$ and will only become known upon arrival, thus in $t+3$ and $t+5$.

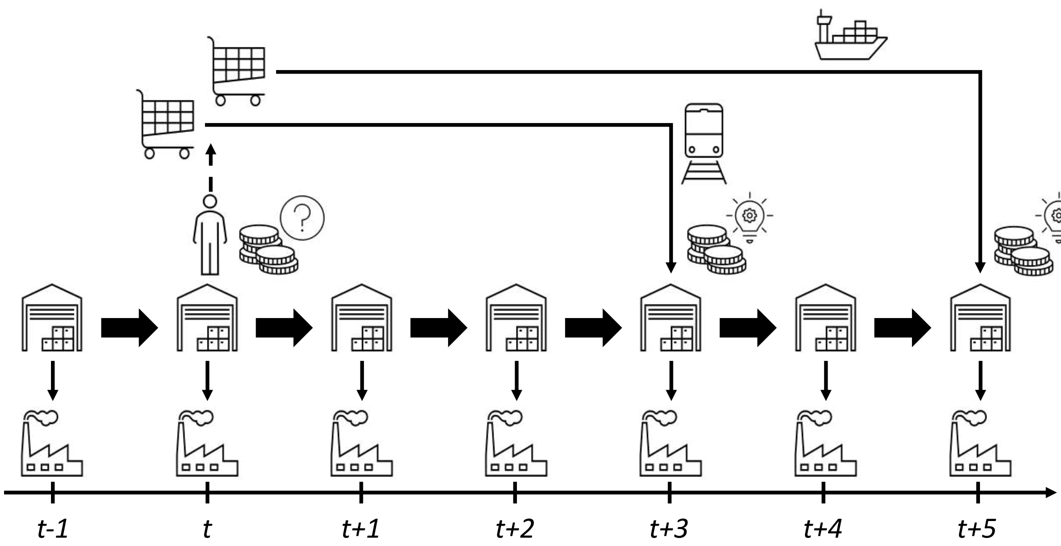


Figure 2.1: Inventory replenishment problem under transportation cost uncertainty.

In our setting, these disruptions are uncertain concerning their impact on transportation cost increases, duration, and time of occurrence during the planning horizon. Hence, the decision maker needs to anticipate the relevant transportation costs in delivery time periods in the future since the surcharge is not defined when the reorder is placed but when the replenishment is executed. This need to anticipate future cost developments depends on the specific supplier lead time offered. The longer the supplier lead time, the more time periods in the future costs need to be anticipated. No probability distribution for the future occurrence of disruptions is known; however, historical information is available.

Thus, a central decision maker manages inventory at the customer location and decides on the supplier to replenish from, how much to replenish, and when to replenish, given that a replenishment order can be made at each of the time periods. In the environment of direct deliveries, the replenishment quantity is a multiple of full-truck load equivalents. The overall objective is to minimize the total expected costs as sum of inventory holding, transportation, and shortage costs. Specifically, we minimize the trade-off between the costs of paying a cost premium to replenish for an alternative supplier or building inventory when no disruption occurs and the uncertain cost increase from a replenishment that is affected by a disruption.

## 2.4 Model development

In this section, we present a mathematical formulation for the SIRPDD. We first describe a deterministic model formulation in Section 2.4.1, and discuss the stochastic programming extensions for the transportation cost uncertainty in Section 2.4.2.

### 2.4.1 A deterministic formulation for the IRPDD

A set of suppliers $\mathcal{I}$ delivers a single product to the production facility over a discrete time horizon $\mathcal{T}$. Suppliers deliver in specific order sizes $o \in \mathcal{O}$ that define the replenishment quantities $q_{io}$, which are multiples of full-truck load equivalents. Each supplier uses a specific transportation mode that requires a delivery time $l_i$ at a transportation cost. These transportation costs $c^{tp}_{io(t+l_i)}$ occur upon arrival $(t + l_i)$, thus $l_i$ periods after a replenishment order was placed in order time period $t$ and include the supplier-specific product price for the order size $o$. The customer holds inventory to satisfy the demands $d_t$. The overall inventory stored is limited by the inventory capacity $\hat{Y}$ with the starting inventory being $Y_0$. Besides transportation costs, the total costs consist of inventory holding costs $c^{ih}$ per product unit that is stored in each time period and a penalty costs of $c^{sh}$ per product unit that is not fulfilled.

The binary decision variable $x_{iot}$ decides in which time period $t$ to order from which supplier $i$ and in which order size $o$ to minimize the total costs. In addition, two auxiliary decision variables are taken into account that depend on the choice and timing of orders. First, $y_t$ is continuous and describes the inventory level at the customer location in time period $t$. Second, the continuous decision variable $p_t$ accounts for the production shortages due to missing raw materials in time period $t$ in case demands exceed the available inventory.

Within this notation, the mixed-integer linear programming model for the deterministic problem is

$$\textit{minimize} \qquad \sum_{i \in \mathcal{I}, o \in \mathcal{O}, t \in \mathcal{T}} c^{tp}_{i(t+l_i)} \cdot q_{io} \cdot x_{iot} + \sum_{t \in \mathcal{T}} c^{sh} \cdot p_t + \sum_{t \in \mathcal{T}} c^{iv} \cdot y_t \tag{2.1}$$

*subject to:*

$$y_t \leq \hat{Y} \qquad \forall t \in \mathcal{T} \tag{2.2}$$

$$y_t = y_{(t-1)} + p_t - d_t + \sum_{i \in I} q_{io} \cdot x_{io(t-l_i)} \qquad \forall t \in \mathcal{T} \setminus \{0\} \tag{2.3}$$

$$y_0 = Y_o \tag{2.4}$$

$$x_{iot} \in \{0,1\}, y_t \geq 0, p_t \geq 0 \qquad \forall i \in \mathcal{I}, o \in \mathcal{O}, t \in \mathcal{T} \tag{2.5}$$

The objective function (2.1) minimizes the total costs consisting of the transportation costs, the shortage costs as well as the inventory holding costs. Due to delivery time effects between the ordering from the customer and the delivery of the supplier, the time period of the relevant transportation costs are offset by the respective delivery time $(t + l_i)$. The inventory available in each time period is constrained to a maximum inventory capacity as outlined in constraints (2.2) whereas the inventory balance is ensured in constraints (2.3) and (2.4). The replenishment quantity as defined by the ordering decision $x_{iot}$ and the order quantity $q_{io}$ that is arriving as inventory is offset by the delivery time $l_i$, thus highlighting that in time period $t$ replenishment orders placed in $t - l_i$ will arrive given that $l_i$ can differentiate by supplier $i$.

### 2.4.2 Multi-stage stochastic programming extension

We model the transportation cost uncertainty based on a scenario tree $\tau$ (cf. Ruszczyński and Shapiro 2003, Huang and Ahmed 2009) and assume knowledge of the probabilities of future cost developments at the beginning of each time period $t$. Using this modeling approach, we can capture the transportation cost uncertainty, that a decision maker faces at each order time period $t$, regarding the future transportation costs $c^{tp}_{io(t+l_i)}$, through scenarios and ensure non-anticipativity of the decision maker. Thus, we consider a scenario tree, where a node $n$ in level $t$ of the tree corresponds to a specific realization of the uncertain parameter $c^{tp}_{io(t+l_i)n}$. Each level of the decision tree corresponds to a time period $t$, *i.e.*, there are $|\mathcal{T}|$ levels in the tree. In addition, each node $n$ of the scenario tree, except the root node $(n = 1)$, has a unique parent $a(n)$ while each non-terminal node $n$ itself is the root of a subtree $\tau(n)$. The set $\varphi_t$ refers to all nodes corresponding to a time period $t$, while $t_n$ is the time period corresponding to node $n$. The probability of the realization of node $n$ is denoted by $\pi_n$ with $\sum_{n\in\varphi_t} \pi_n = 1$ whereas the sum of probability of all child nodes of a parent nodes equal the probability of the parent node, *i.e.*, $\sum_{m\in\tau(n)} \delta_{a(m),n} \cdot \pi_m = \pi_n$ for all $n \in \tau$ with $\delta_{a(m),n}$ being the Kronecker delta. The path from the root node $(n = 1)$ to a node $n$ is denoted by $\wp_n$. If $n$ is a terminal node $(n \in \varphi_T)$, then $\wp_n$ corresponds to a *scenario*, and represents a realization of the transportation costs over all time periods $\mathcal{T}$. Let $\mathcal{S}$ be the number of corresponding scenarios (lead nodes) and $\mathcal{N}_\mathcal{T}$ the number of nodes in the whole tree. We summarized some of the notation associated with a scenario tree in Figure 2.2.

Assuming that the complete scenario tree describing all possible realizations and probabilities is available, we can formulate the multi-stage stochastic program as

$$\textit{minimize} \qquad z = \sum_{n\in\tau} \pi_n \cdot \Big( \sum_{i\in\mathcal{I},o\in\mathcal{O},t\in\mathcal{T}} c^{tp}_{i(t+l_i)n} \cdot q_{io} \cdot x_{iotn} + \sum_{t\in\mathcal{T}} c^{sh} \cdot p_{tn} + \sum_{t\in\mathcal{T}} c^{iv} \cdot y_{tn} \Big) \tag{2.6}$$

*subject to:*

$$y_{tn} \leq \hat{Y} \qquad \forall t \in \mathcal{T}, n \in \mathcal{N} \tag{2.7}$$

$$y_{tn} = y_{(t-1)a(n)} + p_{tn} - d_t + \sum_{i\in I} q_{io} \cdot x_{io(t-l_i)n} \qquad \forall t \in \mathcal{T} \setminus \{0\}, n \in \varphi_t \tag{2.8}$$

$$y_{0n} = Y_0 \qquad \forall n \in \varphi_0 \tag{2.9}$$

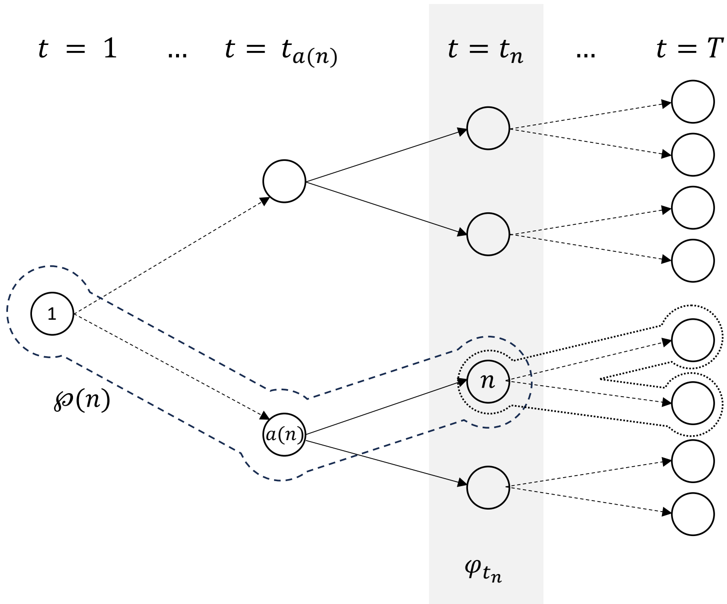


Figure 2.2: Scenario tree notation, see Huang and Ahmed (2009).

$$x_{iotn} \in \{0,1\}, y_{tn} \geq 0, p_{tn} \geq 0 \quad \forall i \in \mathcal{I}, o \in \mathcal{O}, t \in \mathcal{T}, n \in \mathcal{N} \tag{2.10}$$

The above multi-stage model involves a replenishment decision $x_{iotn}$ with the resulting inventory levels $y_{tn}$ and product shortages $p_{tn}$ corresponding to each node $n$ of the scenario tree.

## 2.5 CDDT framework

The goal of the replenishment problem is to determine the cost-optimal replenishment order decision, $a, f_{iot}(\mathcal{V}) \in \{0,1\}$, for each supplier $i$ and each order size $o$ at each order period $t$ after having observed all features, $\mathcal{V}$. Unlike traditional learning frameworks, which maximize the ability to predict historical optimal replenishment decisions $x^*$, our CDDT framework incorporates the objective function $z(x)$ of decision $x$ as defined in (2.6) into the hyperparameter tuning of the learning framework itself. The core idea is that deviations from the binary labels should be evaluated in terms of their cost impact and not just a pure comparison so that, *e.g.*, a replenishment order taken one day earlier or later might only have limited influence on total costs, and thus is less penalized in comparison. While the idea of deriving loss functions from the optimization problem directly has been discovered recently (Elmachtoub and Grigas 2022), we propose a new way of handling the resulting computational challenges of training machine learning models without the need of approximating a tractable surrogate loss function.

The overall CDDT framework is summarized in Figure 2.3. Let $\mathcal{K}$ be the index set of all training data points with $\mathcal{V}_k$ the corresponding feature vector. To obtain the mapping function $f(\cdot)$ that predicts the order decisions based on given features, we train the model with the labels. These labels are obtained from historical data and need to be generated first. The details of the so-called "labeling" step are described in Section 2.5.1. After labels are created, we train the supervised learning algorithm with the following training objective:

$$\min_{f} \sum_{k \in \mathcal{K}} z(f(\mathcal{V}_k)) \tag{2.11}$$

Thus, we do not aim to minimize the absolute difference $|f(V_k) - x_k^*|$ between the predicted and optimal binary decision. We describe the details on the mapping function $f$ as well as the hyperparameter tuning using a genetic algorithm in Section 2.5.2. Through the chosen learning function, the decision rules of the trained model can easily be extracted and visualized in the form of a replenishment policy (see Section 2.6.4.2).

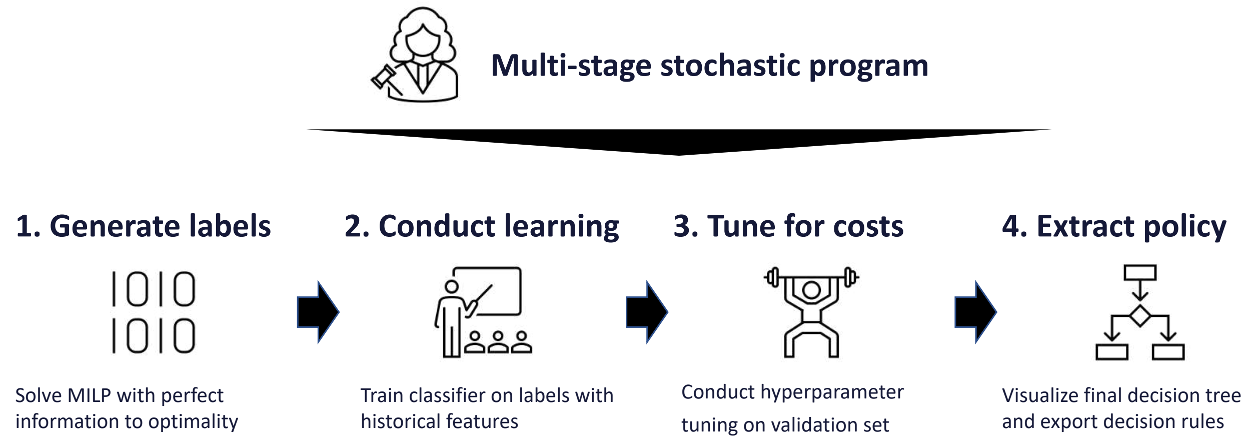


Figure 2.3: Overview of CDDT framework.

### 2.5.1 Labeling the optimal replenishment policy

For a multiperiod inventory problem with multiple suppliers, lead time differences, and transportation cost uncertainty, the optimal replenishment policy cannot be defined in a straightforward way. Instead, we learn from historical data in a supervised way to derive such a replenishment policy that solves the SIRPDD assuming full information. As a result, such a policy needs to define when to order from which supplier in which available order quantity.

In order to do so, we generate labels, *i.e.*, order decisions, that over time represent an optimal replenishment policy under the assumption of full knowledge of future transportation cost increases. These labels cover various different disruption and decision situations so that a significant degree of the uncertainty space is covered. Thus, we derive scenarios $S$ with different planning horizons $\tilde{T}$ for the replenishment problem that describes this uncertainty. Still, it is sufficient to solve each scenario separately assuming perfect information and merge all generated labels afterwards for the training. This reduces the computational complexity and avoids the need of determining the full scenario tree. After solving each scenario, each replenishment order decision in each time period of the planning horizon serves as one label.

We obtain the different scenarios with limited historical data by adjusting both the starting inventory level $Y_0$ as well the planning horizon as a subset of the available historical data while remaining the time-series itself. As a result, scenarios include different decision situations so that even with perfect information, labels are generated for excess and shortage inventory situations. Thus, the different scenarios, must cover a variety of the situations that a decision maker would face in the uncertain future.

Beyond the labels, a supervised learning approach requires features to conduct the training upon. These features contain the available inputs at the time of decision, thus imperfect information. We refer to Section 2.6.2 for an overview of the available case-specific features that link to the replenishment reorder decision in each scenario $s$ and time period $t$.

### 2.5.2 CDDT learning structure

After the associated labels for training data are obtained, we train a supervised learning model and tune its hyperparameters in a separate validation step. For training and tuning, the time-series of all historical labels is split at a certain time period into two time-series; a training set $T^1$ and a validation set $T^2$. This is done by choosing a time period $t^*$ with all observations in $T^1$ prior and all observations in $T^2$ after $t^*$. For each supplier $i$ and order size $o$, we train a classifier with a distinct hyperparameter set. Thus, the number of classifiers to train equals the sum of all order sizes $O$ across all suppliers $I$.

For each classifier, we use the Classification and Regression Tree (CART) (Breiman 1984) to train the decision tree as this algorithm generally performs well in uni-variate split settings with small data sets (*e.g.* Lim et al. 2000, Patel and Prajapati 2018). While other supervised learning algorithms could be used as well, using a decision tree ensures that results are interpretable and replenishment policies can directly be extracted from the trained classifiers. In the CART algorithm, at each node, rules that split the sample based on the feature values provided are chosen to minimize a pre-defined criterion. Several hyperparameters are studied that greatly influence the predictive performance of the CART algorithm (see Section 2.6.2). These hyperparameters need to be provided within the configuration of the CART algorithm. Hyperparameter tuning means identifying a set of hyperparameters that optimizes the performance of the CART algorithm with respect to a pre-defined criteria. In the case of our CDDT framework, we choose hyperparameters that minimize the total costs of the resulting inventory replenishment policy (equation ((2.11))) on the validation set $T^2$.

In order to evaluate all possible combinations of values for the different hyperparameters, a large number of training and evaluation steps is required. Using the minimization of total costs as hyperparameter tuning objective, the total number of possible combinations rises dramatically compared to the hyperparameter tuning for traditional learning objectives as all hyperparameter combinations of all classifiers can only be evaluated together (see line 13 in Algorithm 2). Using the case and hyperparameter ranges as example, 1260 hyperparameter combinations need to be evaluated per classifier when conducting traditional hyperparameter tuning for predictive performance. As each classifier can be evaluated separetely, this results in about 3,000 combinations for three classifiers. In comparison, the hyperparameter tuning in the CDDT results in $2 \cdot 10^9$ combinations as all combinations across the three classifiers need to be evaluated together (thus $1260^3$). In addition, the cost evaluation (see equation (2.11)) is computationally more costly than comparing test labels against test predictions. In the case example, using full grid search results in intractable calculation time for hyperparameter tuning within the CDDT due to the large state space.

To overcome this rise in computational complexity, genetic algorithms have already been successfully applied in hyperparameter tuning with the objective of minimizing an evaluation metric that quantifies the difference between predicted and test labels as part of a validation step (Alibrahim and Ludwig 2021). Unlike these traditional approaches of hyperparameter tuning, we develop a genetic algorithm with the total costs (see equation (2.6)) of the replenishment decision predictions as fitness function to find a well-performing hyperparameter set for the CDDT. Thus, we do not aim to minimize the difference between predicted and test labels as part of hyperparameter tuning but the overall costs of applying the trained classifiers on a validation set. The pseudocode is outlined in Algorithm 2. We refer to Katoch et al. (2020) for a detailed overview on the genetic algorithm operators.

**Algorithm 2** Genetic algorithm for hyperparameter tuning within CDDT framework.

**Input** generations $n^G$, population size $n^P$, mutation rate $\gamma$, sample size $\eta$, timeseries $T^1, T^2$
$P_1 \leftarrow$ Initialize population with $n^P$ random hyperparameter combinations
**for** g=1 **to** $n^G$ **do**
  $P_{g+1} = \{\}$
  **while** $|P_{g+1}| \leq n^P$ **do**
    **for** j = 1 **to** 2 **do** ▷ Generate parents
      $z^* = \infty$
      **for** n = 1 **to** $\eta$ **do**
        $p \leftarrow$ Select randomly from $P_g$
        **for each** $o \in \mathcal{O}$ and $i \in \mathcal{I}$ **do** ▷ Evaluate fitness of $p$
          $f_{io} \leftarrow$ Train with $T^1, p$ ▷ Train
          $\dot{x}_{iot} \leftarrow f_{io}(\mathcal{V}(t))\ \forall t \in T^2$ ▷ Predict
        **end for**
        $z \leftarrow$ solve IRPDD **for** $x_{iot} = \dot{x}_{iot} \quad \forall t \in T^2, o \in O, i \in I$ ▷ Evaluate
        $p_j \leftarrow p$ **if** $z \leq z^*$
      **end for**
      $P_{g+1} \leftarrow P_{g+1} \cup \{p_j\}$
    **end for**
    child $\leftarrow$ Uniform Crossover($p_1$, $p_2$)
    child $\leftarrow$ Mutate(child)
    $P_{g+1} \leftarrow P_{g+1} \cup \{child\}$
  **end while**
**end for**

In a first step, we initialize a new population $P_1$ of size $n^P$ by random selection of hyperparameters for each classifier trained for each order size $o$ and supplier $i$. Thus, each individual in each population refers to a complete set of hyperparameters for all classifiers used. The main objective of this initialization step is to cover a diverse subset of all possible hyperparameter combinations. Then, for each new generation $g+1$, the fittest individuals of previous populations are selected to inherit their genes to the next generation with the objective of increasing the overall fitness across the population. To achieve this, a new and empty population $P_{g+1}$ is initialized in a first step. Then, while the number of individuals $|P_{g+1}|$ has not reached the population size $n^P$, two parents need to be generated in the second step. Each parent is determined out of a random sample of $\eta$ individuals drawn from the previous population $P_g$. We use the tournament selection in which only the fittest individual of the sample is chosen as parent (Miller and Goldberg 1996). In order to assess the fitness of each individual $p$ (see lines $9-13$), we first train each machine learning classifier for each supplier $i$ and order size $o$ with the hyperparameters from $p$ on $T^1$ to obtain the mapping function $f_{io}$. Then, using this mapping function and the observations from $T^2$, order predictions $\dot{x}_{iot}$ are obtained. In the last step of the fitness evaluation, these order predictions for each order size $o$ and each supplier $i$ are evaluated together by solving the corresponding IRPDD on $T^2$ to obtain the total costs $z$. The best individual, *i.e.*, with the lowest $z$, of the random sample is then a parent and saved to the next generation $P_{g+1}$. In addition, the characteristics of both parents $(p_1, p_2)$ are inherited to children through a cross-over. We use the uniform cross-over in which each parent has a random and equal probability of inheriting one of their genes, *i.e.*, hyperparameter choices (Syswerda 1989). Then, each new children is prone to a random mutation to any of the hyperparameters at a probability of $\gamma$. Once the number of individuals in $P_{g+1}$ reaches the population size $n^P$, a new generation is initialized and all steps repeat until the total number of generations $n^G$ is reached. The algorithm terminates by selecting the best-fit individual $p$ of the final population $P_{n^G}$ with the lowest cost $z$ on $T^2$.

## 2.6 Case study

We test our approach using a case study with real disruption data. Section 2.6.1 describes the case, while Section 2.6.2 outlines the numerical setup, labels, and case-specific features. In Section 2.6.3, we introduce replenishment policy benchmarks. Section 2.6.4 presents numerical results. Finally, in Section 2.6.5, managerial insights are drawn.

### 2.6.1 Case introduction

This case is based on a chemical company situated near the river Rhine, Germany. For the case company, more than 40% of all inbound materials are transported through the river Rhine, of which a large share is globally sourced. For these global shipments, only full-truck loads are considered due to the high share of transportation costs compared to inventory holding costs. Strategic network design decisions are given and form the basis for operational replenishment and transport decisions, (e.g., Müllerklein and Fontaine 2024).

Two suppliers are available to deliver the product. The main supplier ($i = 1$) transports a regular order size ($o = 1$) that equals four days of average demand by vessel via the river Rhine and thus is prone to uncertain cost surcharges, which depend on the water level on the day of arrival. The alternative supplier ($i = 2$) uses a different transportation mode (*i.e.*, rail) and is thus not subject to surcharges that depend on the water level. However, the overall transportation costs $c^{tp}_{2t}$ are 110% higher compared to the main supplier's disruption-free costs (thus $c^{tp}_{2t} = 2.1 \cdot c^{tp}_{1t}$). In addition, a larger order can be placed with the main supplier ($o = 2$), which equals 10 days of average demand to build up inventory and avoid potential surcharges. Thus, we differentiate between three types of replenishment orders in each time period $t$: The large order decision with the main supplier

($x_{11t}$), the regular order with the main supplier ($x_{12t}$), and the order with the alternative supplier ($x_{21t}$). Inventory storage capacity is limited to a storage capacity of five weeks of average demand. If the projected inventory exceeds the inventory capacity, the corresponding replenishment order is canceled.

Following industry standards, contractual agreements are in place between the shipment carriers that operate on the river Rhine and their customers that define the surcharges to be paid based on the water levels upon arrival. Due to the high lead times with the main supplier of $l_0 = 21$ days, the case company faces a high level of uncertainty concerning the surcharges to be paid based as they depend on the future water level in 21 days after ordering. To highlight the overall water level fluctuations, Figure 2.4 shows the water level history for the last eight years including the first threshold where surcharges occur in orange and where generally no transport is guaranteed anymore in red. For example, transportation stops occurred in 2015, 2017, 2018, 2020, and 2022, while high tides caused transportation stops in 2018 and 2021. In addition, occurrences where low water levels result in surcharges occur regularly. While some degree of seasonality seems visible, *i.e.*, high tides happen exclusively in winter, while low water levels are typically seen in late summer or autumn, the overall fluctuations on a year-to-year level are significant.

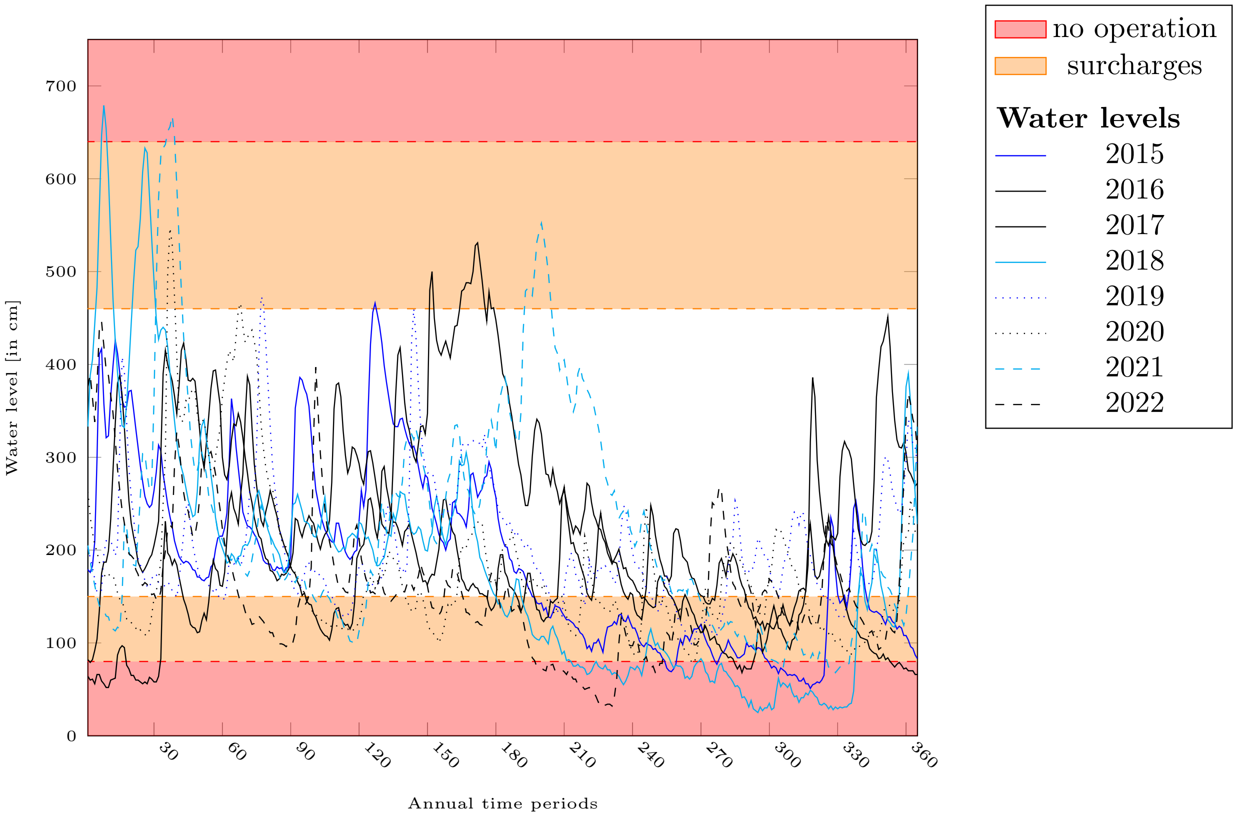


Figure 2.4: Historical water levels at shipment critical point for Rhine River that define surcharges for main supplier ($i = 1$).

If the water level falls below or is higher than the contractually defined thresholds, the resulting surcharges are significant. These surcharges range from 90 EUR to 300 EUR per TEU or even a shipment cancellation for water levels below 80cm and higher than 640cm. The significance of these surcharges also depends on the overall transportation costs of the container as well as the value of the goods transported when considering the trade-off between holding additional inventory at the benefit of avoiding these surcharges. The resulting total costs per TEU, including the surcharges between carriers and customers motivated by the case example, are summarized in Table 2.1.

Table 2.1: Transportation costs per TEU transported including water level based surcharge.

| Water level [cm] | $< 80$ | $[80, 90)$ | $[90, 100)$ | $[100, 110)$ | $[110, 130)$ | $[130, 150)$ | $[150, 460)$ | $[460, 640)$ | $\geq 640$ |
|---|---|---|---|---|---|---|---|---|---|
| Costs TEU [EUR] | - | 415 | 340 | 295 | 250 | 205 | 115 | 205 | - |

### 2.6.2 Numerical setup, features and labels

All numerical experiments were run on an Apple M1 Pro 8-Core processor with 16 GB of RAM. The algorithm is implemented in Python 3.8. For label generation, we solved the IRPDD using Gurobi 9.5 for each scenario to optimality within minutes. All machine learning models were implemented with Scikit-learn (Géron 2022).

Historical data for all features, *e.g.*, water levels, including trends, is available from May 2017 to September 2023. To evaluate our approach, we split available data into a training (2017-2019), a validation (2020-2021), and an evaluation set (2022-2023). In doing so, we simulate an application of the machine learning model in practice. Besides the water levels on the main transportation mode during the time period $t$, several additional features are needed and available. These are summarized in Table 2.2.

Table 2.2: Labels and features used for machine learning approach.

| Labels | |
|---|---|
| $x_{iot}$ | replenishment order of order size $o$ from supplier $i$ in time period $t$ |
| Features | |
| $y_t$ | inventory level at customer location in time period $t$ |
| $IP_t$ | inventory position at customer location in time period $t$ |
| $WL_t$ | water level at time period $t$ |
| $WL_t^{tr3}$ | historical trend of water level development between $t$ and $t-3$ |
| $WL_t^{tr7}$ | historical trend of water level development between $t$ and $t-7$ |
| $PWL_t^{7}$ | prediction of water level at $t+7$ |
| $PWL_t^{14}$ | prediction of water level at $t+14$ |
| $PWL_t^{tr7}$ | trend of change in prediction of water level at $t+7$ for the last three days |
| $PWL_t^{tr14}$ | trend of change in prediction of water level at $t+14$ for the last three days |
| $W_t$ | Calendar week of decision period |
| $M_t$ | Calendar month of decision period |

In a pre-processing step, we calculate the inventory position $IP_t$ based on the inventory level $y_t$, large orders placed with the main supplier ($x_{11t}$), regular orders placed with the main supplier ($x_{12t}$), orders placed with the alternative supplier ($x_{21t}$) as well as prospective shortages $p_t$. Using the inventory position instead of the inventory level as a reorder trigger is standard in most continuous-review stochastic inventory problems (Parlar 1997). In addition to the current water level at the decision time period $t$, we calculate the last three and seven-day trends that indicate whether the water level has been rising or falling just before the decision time period $t$. Historical predictions of future water levels are available with a lag of seven ($PWL^{tr7}$) and 14 days ($PWL^{tr14}$). However, no predictions are available within the relevant lead time of 21 days. This lack of longer prediction horizons is typical as, generally, weather forecasts are available with a 14-day outlook. This setting appeals to general problem settings in which transport decision need to be made before detailed disruption forecasts become available, such as sourcing decisions in e-commerce (Niu et al. 2021). In addition, we create the trend of the water level predictions as a corresponding feature, thus the change of the 7-and 14-day forecast over the last three days ($PWL_t^{tr7}$ and $PWL_t^{tr14}$). Lastly, the calendar week $W_t$ and the calendar months $M_t$ of the decision time period is added.

Due to the label generation process of varying starting inventory levels and shifts in the planning horizon, training and testing data contain many dependent samples, such as multiple samples for the same date. Thus, even though starting inventories and horizons are varied, multiple labels with identical features (same week, months, water level, inventory position, etc.) exist. Given these multiple samples of identical labels as well as the connection between labels in a time-series, applying a random train test-split could result in dependent samples that exist in training and testing, and thus, result in overoptimistic prediction accuracies on testing as information is leaked. To handle the challenge of dependent samples, we build groups of labels through equal week-year combinations and ensure that each group is either present in training or testing but no label of a group in both. The year itself is dropped as a feature as it would not be helpful in making predictions for upcoming years. In addition, we use cross-validation to estimate the performance of the CDDT on unseen data with limited samples. We conduct five folds of training and testing on the training data (years 2017-2019). We assess the costs for the fitness function as average across the trained predictors for each of the five folds when applied on the validation set (year 2020).

A further challenge is posed by the fact that the training data is highly imbalanced: The large main order labels contain 292 order and 19172 no order labels. Generally, this significant imbalance poses a challenge to any machine learning approach. To overcome this, we conduct a random under-sampling of the majority class (Japkowicz 2000). However, instead of forcing a fully balanced distribution of the classes, we conduct the under-sampling to match the disruption-free replenishment order cycle. For the case example, without disruption occurrence and due to the necessity of shipping full-truck loads, an order would be placed every five days. This balance is represented in each of the three different replenishment decisions.

The ranges for all relevant hyperparameters for tuning the decision tree predictors are summarized in Table 2.3. The criterion measures how the quality of a split in a decision tree is evaluated using either the gini criterion for homogeneity of the nodes or entropy for the information gain (James et al. 2021). The maximum depth of the tree sets the maximum number a of nodes a tree can have, i.e. how much the tree can expand, until all leaf nodes are pure or untill all leaf nodes contain less than the minimum number of samples per split. These minimum samples per split describes the threshold for an internal node to become a leaf node. Thus, a node can only become an internal node if the number of samples are higher than the minimum samples per split. In addition, a split will only be considered if the resulting left and right branch of the split each contain at least the minimum number of samples per leaf. Finally, the maximum number of features to be considered each time to make a split decision can be limited up to the total number of features available. In case the maximum number of features is lower than the number of available features, a random selection of features is chosen at each split and evaluated concerning the best feature to use for the split. The number of features in the selection matches the max feature. This mechanism is often used to control overfitting.

Table 2.3: Decision tree classifier hyperparameter ranges for tuning.

| Hyperparameter | Possible values |
|---|---|
| Criterion | Gini, Entropy |
| Maximum depth | None, 3, 4, 5, 8, 12 |
| Min samples split | 2, 6, 10, 20, 50 |
| Min samples leaf | 1, 4, 6, 10, 15, 20, 30,40 |
| Max features | 2, 4, 6, 11 |

Within the CDDT, we run the genetic algorithm with $\delta = 10$ generations, a population size of $\alpha = 100$, a mutation rate of $\gamma = 0.1$, two parents $\beta = 2$, and a random sample size of $\eta = 6$. The genetic algorithm terminates within less than three hours.

### 2.6.3 Comparison with standard policies and traditional machine learning frameworks

To demonstrate the performance of our CDDT framework, we compare the obtained replenishment policy against inventory replenishment policies obtained from the literature and alternative machine learning frameworks. Generally, the inventory replenishment problem under disruption uncertainty with multiple suppliers that differ in their lead time would require a multiple dimensional state space (Chen et al. 2012). Thus, literature dealing with stochastic transportation or purchasing costs is sparse (Darwish 2008). As a result, we consider a general purpose replenishment policy.

The *reorder point - reorder quantity* policy, often referred to as (s,Q) is widely used in practice and extensively studied in literature. They are standard in inventory systems with uncertain demand and delivery times. However, as demands are stable and delivery times are known, the policy can be simplified to triggering an order whenever the inventory level reaches the reorder point that marks the demand during the delivery time of the supplier.

The *risk averse (RA)* policy only orders with the reliable alternative supplier and thus represents the risk-averse idea of not placing orders with the main supplier as there might be the risk of paying surcharges upon arrival of the orders. As a result, transportation costs are not prone to disruptions and are known upfront. However, a cost premium is paid compared to the surcharge-free costs of ordering with the main supplier.

In addition, we benchmark our CDDT framework against machine learning frameworks that maximize each classifier's individual ability to predict the training set's order decisions. Notably, we consider a neural network (ML-NN), a logistic regression (ML-LR), and a decision tree (ML-DT). All machine learning models are tuned using the f1-score as the objective for selecting the best-fit hyperparameters during cross-validation. The f1-score is the harmonic mean of the precision (i.e. positive predictive value) and recall (i.e. sensitivity) with 1.0 being the highest possible value. Even though we use undersampling (see Section 2.6.2), the positive class still contains fewer samples than the negative class. The f1-score can help to balance the metric across positive and negative samples and thus, is a better fit than a simple accuracy metric that would already achieve a high accuracy by solely predicting the negative class. Besides this diverging learning objective in hyperparameter tuning, they are trained with the exact same undersampled labels as the CDDT as well as the same grouping in k-fold cross validation.

### 2.6.4 Results

In this section, we apply the decision rules obtained through the CDDT and other benchmark policies to the unseen evaluation set to compare the cost performance and analyze differences in the order patterns. Then, to understand the cost differences between the CDDT and the ML-DT that use identical hyperparameter ranges and learning algorithms, we compare the prediction performances on the test set and analyze how optimal hyperparameter settings differentiate. In addition, we visualize the results of the tuned ML-DT classifier and discuss challenges of traditional learning frameworks for this problem setting.

#### 2.6.4.1 Cost performance out-of-sample

All replenishment policies are benchmarked against the *perfect information (PI) scenario* that assumes full knowledge of the future transportation cost development. Even though unrealistic as it ignores the problem characteristic of uncertain transportation costs in the future, it gives the lowest bound on the costs of the SIRPDD. Table 2.4 summarizes the results on the out-of-sample evaluation set. This evaluation set contains surcharges on the main transportation mode based on the water levels from 2022-2023 while all machine learning models are trained using labels from 2017-2021.

Table 2.4: Comparison of different replenishment policies on the total planning horizon.

| | | PI | CDDT | ML-DT | ML-NN | ML-LR | (s,Q) | RA |
|---|---|---|---|---|---|---|---|---|
| Obj | Costs | 323.79 | 466.43 | 569.96 | 764.11 | 634.75 | 582.18 | 599.58 |
| | Increase | 0% | 44% | 76% | 136% | 96% | 80% | 85% |
| Orders | Large main | 14 | 20 | 39 | 0 | 35 | 0 | 0 |
| | Regular main | 97 | 90 | 48 | 153 | 60 | 147 | 0 |
| | Alternative | 12 | 5 | 0 | 0 | 6 | 0 | 147 |

Starting with the CDDT, our new learning framework significantly outperforms all other policies.

It represents a cost reduction of roughly 20% compared to the (s,Q) policy, which reflects the current industry standard, and 18% compared to classical machine learning frameworks. Compared to the PI solution, the CDDT represents a cost increase of 44%. Though this indicates further improvement potential, it is in line with recent work of Qi et al. (2023) who determined optimal replenishment quantities for a single supplier in fixed replenishment cycles, thus a more narrow problem setting, and report a gap of 25% to their PI setting.

In addition, the split of the order predictions of the CDDT approximates the ideal split of the PI solution though there remain differences particularly in the number of alternative order decisions. Notably, the split of the order predictions of the CDDT approximates the ideal split of the PI solution. Still, differences in the pure quantities can be observed, while the exact timing of replenishment orders explains the remaining gap. This remaining 44% gap to the perfect information solution highlights the high problem complexity and degree of transportation cost uncertainty that is characteristic for the problem setting of determining the optimal supplier, at the optimal quantity, in the optimal time.

Compared to the traditional machine learning frameworks that are tuned for prediction performance using a neural network (ML-NN) and a logistic regression (ML-LR), we can see that both frameworks result in replenishment order predictions that perform significantly worse than the RA or (s,Q) policy and thus, do not seem a good fit for this specific problem setting. Specifically, the neural network seems to suffer from a severe overfitting reaction as nearly whenever inventory capacity allows, a regular main order is triggered (153 main regular orders). While the logistic regression performs slightly better regarding total costs (634.75), it is also not a good fit for this specific problem setting. In comparison, the ML-DT and the CDDT that use a decision tree as a classifier perform better than the remaining benchmarks. The ML-DT, which uses a decision tree, performs slightly better than the fixed replenishment rules (s,Q) and RA; however, it represents a 22% cost increase compared to the CDDT and highlights the need for the revised learning objective highlighted in equation (2.11). In the ML-DT, no alternative order is released during the evaluation period, and compared to the PI solution, significantly more large main orders are triggered.

Lastly, we compare all results against two fixed replenishment rules. The risk-averse policy of ordering only with the alternative supplier leads to the highest total costs and a cost increase of 85% compared to the replenishment with perfect information. Instead, triggering regular order sizes with the main supplier through an (s,Q) policy reduces the costs by 3% even though significant surcharges need to be paid. Without surcharges, the alternative supplier marks a cost increase of 110% compared to the main supplier. However, even though significant surcharges are paid, the (s,Q) policy still performs slightly better than the pure RA policy. Overall, both fixed replenishment rules do not seem a good fit for this problem setting and highlight the potential of extracting problem-specific rules using the CDDT learning framework.

#### 2.6.4.2 Prediction performance

To recap, the CDDT and the ML-DT are trained on the identical and undersampled data set using group k-fold cross-validation. Still, as seen in Section 2.6.4.1, the CDDT significantly outperforms the ML-DT. Thus, the key differentiation is the diverging hyperparameter tuning objective, which is the f1-score (average across all folds) for ML-DT and the resulting policy's effectiveness on the validation set for CDDT. In the first step, we compare the average prediction performance across the different folds for all three decisions separately. Key prediction scores are summarized in Table 2.5, and the confusion matrix results for a testing fold are shown in Table 2.6.

Table 2.5: Performance scores on testing split.

| | Accuracy | | f1-score | |
|---|---|---|---|---|
| | CDDT | ML-DT | CDDT | ML-DT |
| Large main order | 69.52% | 62.58% | 2.73% | 57.01% |
| Regular main order | 96.55% | 96.56% | 92.79% | 92.98% |
| Alternative order | 92.24% | 99.79% | 88.71% | 99.26% |

As one could expect given that the ML-DT is tuned for f1-score maximization, the ML-DT outperforms the CDDT regarding the observed f1-score across all three decision classifiers. However, three interesting observations can be made. First, even though the f1-score is significantly higher for the large main order decision, the CDDT outperforms the ML-DT in terms of prediction accuracy. This can be explained as due to the undersampling three times more negative than positive labels remain in the dataset. Thus, as can be seen in greater detail in the confusion matrix in Table 2.6, the ML-DT aims at a balanced prediction of positive and negative labels while the CDDT seems to favor an accurate prediction of negative labels. Second, there is no significant difference in prediction scores for the regular order decision with the main supplier between the CDDT and the ML-DT. This observation fits the characteristic of the main regular decision as it represents the replenishment of a decision maker without the transportation cost uncertainty. As a result, both tuning approaches result in similar predictions. Lastly, the trained classifier for the alternative order outperforms the CDDT classifier in terms of f1-score and prediction accuracy. Overall, it is possible to accurately predict optimal regular main order and alternative order decisions using decision trees, while the large main order decision seems inherently more challenging to predict. In addition, based on the prediction scores, one would expect the ML-DT to outperform the CDDT as the higher prediction scores should be reflected in an overall cost-optimal replenishment policy.

Comparing the confusion matrix results (see Table 2.6), it is clear that the lower prediction scores for the large main order decision are due to the tendency of the CDDT classifier for a negative decision. On the testing split, less than 15% of the predictions are positive, while interestingly, the opposite can be seen with the ML-DT. Here, all positive labels in the testing split are predicted accurately and another 87 labels are predicted as false-positive. Likely, this results in predictors that favor the alternative order decision over the inventory build-up decision for the CDDT. In contrast, the opposite seems to hold true for the ML-DT. Overall, the hyperparameter sets themselves seem to play a major role in the classifier performance.

Thus, besides the diverging predictive performance, it is interesting to understand how the optimal hyperparameter sets differentiate for the three decisions. The corresponding optimal hyperparameters for the CDDT and the ML-DT are shown in Table 2.7. Following the overall similar

Table 2.6: Confusion matrix on testing split.

| | Confusion Matrix - CDDT | | | | | | Confusion Matrix - ML-DT | | | | | |
|---|---|---|---|---|---|---|---|---|---|---|---|---|
| | Large main | | Regular main | | Alternative | | Large main | | Regular main | | Alternative | |
| Pred. | 0 | 1 | 0 | 1 | 0 | 1 | 0 | 1 | 0 | 1 | 0 | 1 |
| 0 | 151 | 28 | 2044 | 20 | 303 | 53 | 95 | 87 | 2028 | 26 | 349 | 2 |
| 1 | 48 | 6 | 71 | 638 | 0 | 123 | 0 | 52 | 52 | 646 | 0 | 129 |

prediction score performance for the regular main order, the optimal hyperparameter set for the regular main order decision also nearly matches between the CDDT and the ML-DT. Specifically, the main depth, maximum number of features to be considered per split, and the minimum samples per split match exactly. The key difference can be observed in the large main order decision. For this decision, the CDDT selects each hyperparameter differently than the ML-DT. Important to note is that the CDDT favors a combination of a tree that is not limited in depth (max depth=none) and considers many features at each split while only considering splits that contain a high number of 50 minimum samples. The hyperparameter set of the ML-DT, on the other end, highlights the difficulty of accurately balancing the positive and negative predictions as the optimal set only considers two random features at each split (max features 2) and is of limited depth (max depth = 5).

Table 2.7: Results hyperparameter tuning.

| Order | Model | Criterion | Max depth | Min samples split | Min samples leaf | Max features |
|---|---|---|---|---|---|---|
| Large main | CDDT | Gini | None | 50 | 6 | 6 |
| | ML-DT | Entropy | 5 | 30 | 10 | 2 |
| Regular main | CDDT | Entropy | 3 | 50 | 1 | 6 |
| | ML-DT | Entropy | 3 | 40 | 20 | 6 |
| Alternative | CDDT | Entropy | None | 50 | 40 | 11 |
| | ML-DT | Entropy | None | 20 | 6 | 11 |

The fundamental difference between the CDDT and the ML-DT seems to be in the different hyperparameters and thus decision trees obtained for the large main order decision. One of the key advantages of decision trees for practical application is that the outcome can relatively easily be visualized. This applies to both the CDDT and the ML-DT. Exemplary, we will use this advantage to understand the resulting tree of the ML-DT for the large main order decision in greater detail. The final decision tree for the large main order decision of the ML-DT approach is visualized in Figure 2.5. Positive predictions (class = y[1]) are highlighted in blue while negative predictions are highlighted in orange. Each split to the left equals a true statement, *i.e.*, that the condition is fulfilled, while the opposite statement is false. Thus, each positive or negative prediction can be obtained by combining each condition. For example, looking at the bottom left positive prediction, the decision maker should place a large main order if the calendar week is higher than 12, the current inventory position is higher than 75, the current water level is below or equal to 306cm, it is earlier than June (calendar months $\leq$ 5.5), and the current calendar week is 13 or less. To summarize, we would place an order if we are in calendar week 13, the inventory position is higher than 75 units, and the current water level is below 306cm. While this represents a decision rule that performs well in cross-validation, it would be counter-intuitive for a human decision maker. Suppose the observed current water level is below the surcharge threshold and the 14-day prediction even forecasts lower water levels. This situation indicates a high likelihood of low water levels for the next 21 days, thus a high chance of surcharges to be paid with the main supplier. Still, the final policy obtained by the decision tree would result in an order placement with the objective of increasing inventory, which might not be cost-optimal. However, this ability to sense-check and even adapt such a rule in practice represents one of the significant advantages of decision trees for their application in practice. Interestingly, the ML-DT decision tree considers neither the forecast nor a water level trend feature.

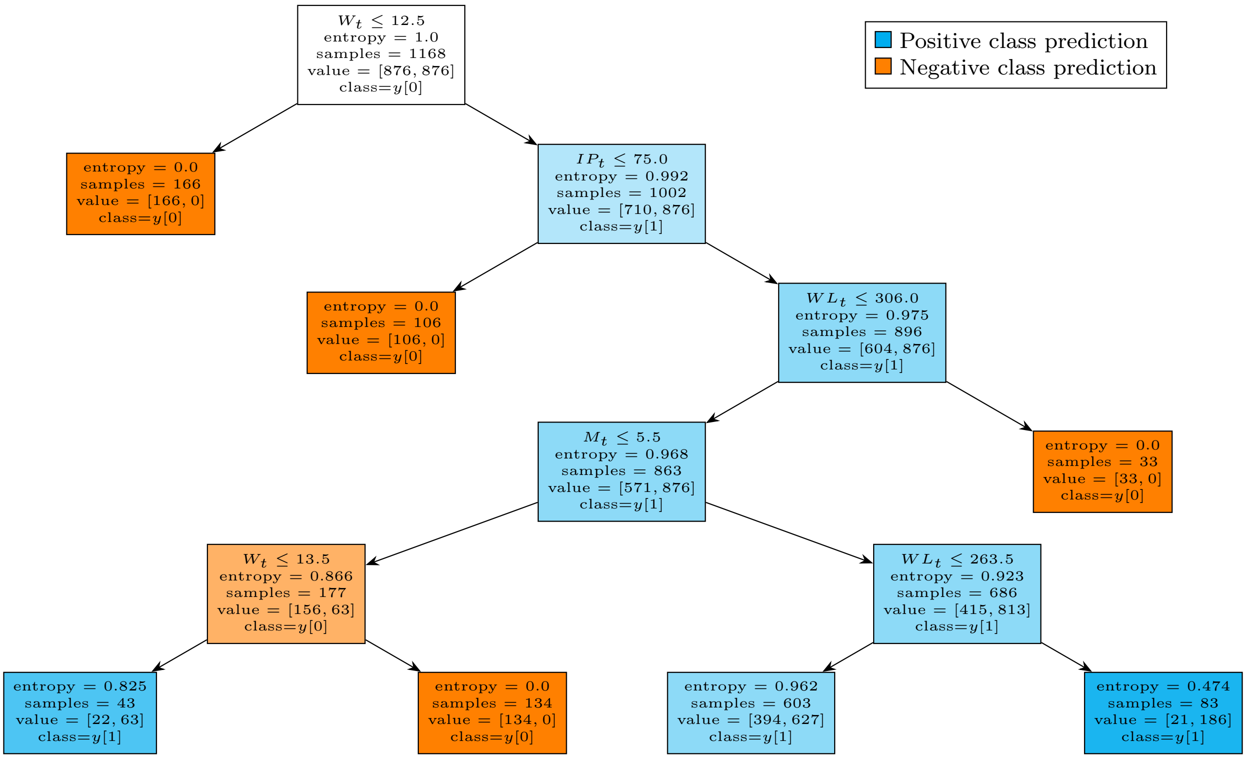


Figure 2.5: Resulting decision tree large main order tuned for prediction accuracy.

### 2.6.5 Managerial insights

To summarize, the following managerial insights are drawn:

1. Through a combination of mathematical optimization with machine learning, replenishment policies for the multi-supplier inventory replenishment problem with transportation cost uncertainty and lead time differences can be obtained that outperform benchmark policies. This data-driven approach requires no knowledge of the underlying stochastic uncertainty but only historical disruption data. Publicly available databases, such as historical water level forecasts, can easily be incorporated as features by linking them to the respective la-

bels to evaluate their value and contribution to future replenishment decisions within the supervised learning procedure.

2. Due to the complexity and inter-dependency of decisions in a multi-supplier replenishment problem with delivery time differences, multiple replenishment quantities, and transportation cost uncertainty, the traditional hyperparameter tuning approach for supervised learning that maximizes individual decision prediction performance leads to improper replenishment policies. In the case example, the resulting policy even results in a cost increase compared to the risk-averse decision of only ordering from the resilient alternative supplier. Thus, problem-specific approaches, such as the CDDT, must be explored further.

3. In this problem setting, the best-performing machine learning framework "only" uses decision trees as supervised machine learning model, which is easy to visualize and interpret in its output. When comparing the ML-DT with ML-NN, the neural network performs significantly worse than the decision tree, indicating that a more complex machine learning model is not helpful for this problem setting. Instead, a well-performing classifier can be trained using decision trees, allowing a human planner to directly understand the proposed decision rules and interact with the replenishment proposals as they can be visualized in a tree structure. As highlighted in Figure 2.5, this also helps to identify results that suffer from overfitting and allows an expert evaluation of the trained classifiers. Thus, potential data issues and flaws can be identified before the CDDT application in practice. Not only are the rules transparent to planners, but if needed, they can be easily adjusted by manipulating the values of the if-else splits.

## 2.7 Conclusion

We have introduced a new problem setting for the inventory replenishment problem with multiple suppliers, lead time differences, and transportation cost uncertainty to decide when to source, which quantity, from which supplier. To obtain the required decision rules, we have developed a new machine learning framework, CDDT, that directly optimizes the total costs of the different replenishment decisions within the hyperparameter tuning. We have tested our CDDT in a case using real-life disruption data and shown that it significantly outperforms standard replenishment policies and traditional machine learning frameworks for inventory replenishment. Particularly, we have shown that the traditional hyperparameter tuning approach of optimizing prediction performance for each replenishment decision leads to inefficient policies. Furthermore, due to the use of decision trees as the supervised machine learning approach, the resulting policy is transparent and, if needed, can easily be adjusted by subject matter experts. Finally, we have highlighted managerial implications on the data-driven inventory replenishment with multiple suppliers and cost uncertainty, leveraging public databases for waterway transport disruption uncertainty.

Our study highlighted the enormous potential for data-driven solutions in the complex field of inventory replenishment with multiple suppliers and supply uncertainty; however, it is not without limitations. We have highlighted the benefits of our CDDT for a single product and presented a solution procedure that develops these rules within a couple of hours on a personal computer. As each decision tree may depend on product characteristics, deploying the proposed approach at scale might include the necessity of handling thousands of stock-keeping-units and thus become computationally challenging. Thus, applying a clustering logic based on product characteristics to determine replenishment policies per cluster will be an exciting research area to allow an application in practice. Another interesting research area would be the planner acceptance and collaboration between planners and experts with a replenishment policy obtained in a purely data-driven way. Lastly, the approach could be applied to alternative cases with highly similar problem settings in which a number of disruption-related information are known to the decision-maker, such as the procurement of commodities at spot versus future prices or cross-border e-commerce operations.

# On product characteristics in a two-echelon resilient network design

# 3 On product characteristics in a two-echelon resilient network design

Daniel Müllerklein, Pirmin Fontaine

**Abstract** Ocean shipping is integral to today's global and interconnected supply chain networks. To supply products to the hinterland, inland waterway transport is vital due to its economic advantages wherever possible. However, major inland waterways are prone to recurring disruptions driven by water level changes that result in surcharges enforced by the shipment carriers. These disruptions can seriously affect a firm's performance. To counteract these disruptions, different resilience strategies, which potentially influence each other, need to be evaluated for each product within the product portfolio.

In this paper, we decide on the resilience strategies and transportation flows for a two-echelon inbound supply chain with multiple products that are needed to produce a single finished good under transportation cost uncertainty to minimize total expected costs. The problem is formulated as a two-stage stochastic mixed-integer linear program. To solve large instances, we propose problem-specific valid inequalities, lower-bound-lifting constraints, and a warm-start procedure that significantly improve the performance.

We present a case study based on a chemical company at the border of the Rhine River. Considering disruptions, the cost-efficient mix of resilience strategies significantly depends on the specific characteristics of each product. Mainly, the need for a multi-product consideration depends on the differences in characteristics of the products sourced. Depending on the product characteristics and cost-ratio specifics, solving the integrated problem can reduce the resilience costs up to 79%. Furthermore, disruption probability and impacts have changed in the last 42 years requiring a shift in the resilience mix.

---

## 3.1 Introduction

All supply chain (SC) networks are exposed to disruptions that can seriously affect a firm's performance and result in stockouts, financial losses, higher costs, and the loss of market share. In today's increasingly global and interconnected SC networks, maritime shipments already deliver approximately 80% of the global trade volume, which is expected to increase even further (ITF 2020). To deliver these goods from global seaports to the mainlands, inland waterway transports play an essential role and will increase in importance due to their advantages in terms of energy consumption per km/ton transported compared to road and rail transport. Due to the increase in extreme weather events, particularly global inland waterway transport disruptions gained growing attention as low- and high-water-level situations affect the shipment carrier's transport capacities and abilities on a recurring level. As a result, carriers enforce contractual surcharges on top of their standard prices or even stop their service completely, which results in stockouts or cost increases for the overall SC network. These surcharges, however, are only determined by the actual water level on the day of shipment and thus are not known in advance. For example, in 2018, the Rhine River's low water levels forced a stop of all waterway transportation for 132 days, resulting in production stops due to material shortages for many companies (Ademmer et al. 2020). In 2022, the Mississippi River experienced a historic drought between September and December, with the lowest water levels observed in October. Despite a significant rise of transportation costs up to 400%, Steinbach and Zhuang (2023) estimated that the drought resulted in a 3.9% reduction in agricultural exports and an agricultural trade loss of 563.9mn USD. Recently, low water levels on the Panama Canal forced vessels to lighten their loads. As a result, Hapag Lloyd announced a 500 USD surcharge per TEU on all cargo between Asia and the US East Coast shipped through the canal. Due to climate change, many experts expect an increased frequency of these high and low water events on major waterways in the future (Koetse and Rietveld 2009).

To a certain extent, these negative consequences can be mitigated by building a resilient SCND combining different resilience strategies to reduce the adverse effects of a disruption. For a decision maker who manages the SC, this means ensuring that the corresponding actions are taken across the product portfolio. The efficiency of the resilience strategies, however, depends on the product's characteristics within the portfolio. For example, keeping extra inventory is cost-competitive for a low price product, while for a highly complex product, a competitive backup-supplier might not be available. Thus, the complexity and characteristics of a product portfolio play an essential role in the resilient SCND.

Regarding the general SCND problem, the influence of specific product characteristics on overall design and SC strategy has been identified early and refined over time (Fisher 1997). The complexity of managing a product portfolio within general SCND has also been addressed in decision models even though a large share of literature still assumes single-product settings (Govindan et al. 2017). While the general toolkit for achieving SC resilience is well understood in research and academia, there is a lack of quantitative work that addresses the impact on product characteristics of resilient SCND (Hosseini et al. 2019a). To ensure that resilience strategies are applied in practice, however, the cost-effectiveness of the individual strategies needs to be assessed (Cohen and Kouvelis 2020).

While existing resilient SCND models have discussed the cost-competitiveness for a single product or a SC in general, there is a lack of research that optimizes the mix of resilience strategies across many products with different characteristics (Ergun et al. 2023).

As a result, decision makers still lack a decision model that incorporates product characteristics into resilient SCND. They need to understand which product characteristics drive the cost-effectiveness of the different resilience strategies and how to assess these characteristics within their portfolio. To manage the resulting complexity, they require a segmentation of products into categories that behave similarly to their ideal set of resilience strategies.

Motivated by the recurring disruptions of major inland waterway transportation worldwide, we model the problem as two-echelon resilient SCND with multiple products. We study an inbound supply chain composed of multiple suppliers at regional and global levels that ship different raw materials (i.e., products) using different transportation modes to a production facility with centralized decision-making. Shipments from global suppliers are gathered at the first inventory echelon (i.e., a warehouse at the seaport). In contrast, regional suppliers directly ship to the second echelon at the production facility. The transportation mode (i.e., river) between the first and second echelon is prone to disruptions that are uncertain concerning their duration, impact, and occurrence along the planning horizon. These disruptions result in surcharges that increase the transportation costs between the first and second echelon. The value of the surcharge depends on the severity of the disruption on the actual day of shipment; thus is uncertain in advance. Depending on the specific product, global and regional suppliers might be available to deliver. In addition, products differ in their characteristics, such as the product value. Thus, a central decision maker decides on the mix of resilience strategies, such as near-shoring, investments in capacity increases, investments in backup suppliers, and additional inventory holding across the product portfolio. The overall objective is to minimize the total expected costs given the transportation cost uncertainty. Notably, we will address the trade-off of proactive investments in resilience strategies and potential surcharges or stockouts on the raw material level.

Our main contributions are as follows:

1. We introduce a two-stage stochastic program for the two-echelon resilient SCND with multiple products and transportation cost uncertainty between the first and second echelon of inventory holding. The SCND problem considers multiple resilience strategies including near-shoring, inventory capacity increase, backup supplier investments, and additional inventory holding.

2. We propose problem-specific valid inequalities, lower-bound-lifting constraints, and a warm-start procedure to improve the solution time and quality of commercial solvers and solve instances with multiple products.

3. We present a case study and discuss the influence of the product characteristics on the optimal mix of resilience strategies.

4. Via the case study, we derive managerial insights on the resilient SCND with multiple products and cost uncertainty. Particularly, we will discuss the effects of shifts in disruption probabilities through external effects, such as climate change.

This paper is structured as follows. Section 3.2 reviews the relevant literature while Section 3.3 describes the problem setting in detail. Then, Section 3.4 presents the mathematical model formulation including its enhancements. Section 3.5 presents the case result. Finally, Section 3.6 concludes by summarizing and detailing open research areas.

## 3.2 Literature review

Section 3.2.1 briefly reviews literature on the influence of product characteristics on general supply chain network design and strategy. Then, in Section 3.2.2 general strategies and levers are discussed to increase SCR. Section 3.2.3 summarizes literature on multi-product SCND with a focus on increasing resilience as objective. Finally, Section 3.2.4 summarizes the research gaps.

### 3.2.1 The influence of product characteristics on SCND

Designing and managing supply chains effectively is a complex and challenging task. Within supply chain management, Fisher (1997) introduced the need to match product characteristics with the ideal supply chain design by distinguishing between functional and innovative products based on their demand characteristics. This original framework has been expanded by Lee (2002), who considered demand and supply uncertainty to distinguish between a need for efficient, responsive, risk-hedging, and agile supply chains based on product characteristics. Huang et al. (2002) differentiate between innovative, hybrid, and standard products and assess their fit to an agile, hybrid, or lean supply chain strategy and design. Based on the proposed frameworks, Wang et al. (2004) developed a decision-support model that decides on the multi-criteria optimal supplier selection for each product based on product characteristics. Kleindorfer and Saad (2005) developed a conceptual framework on managing disruption risks in supply chains. They highlight the need fit the approach taken to the supply chain environment and product characteristics based on empirical results from the chemical industry. Qi et al. (2009) found empirical evidence in China that firms who adapt their supply chain's based on product characteristics outperform firm with a traditional strategy. In a similar effort, Eckstein et al. (2014) empirically investigated the effects of supply chain agility and adaptability on cost performance and identified a correlation to product complexity. Zimmermann et al. (2020) analyzed empirical data from 329 companies and identified that product characteristics are essential in adopting the right supply chain strategies. Wiedmer et al. (2021) analyzed the effect of the Tsunami in 2011 on the automotive sector's trade from Japan to the United States and found that alongside other characteristics product complexity influence a firm's ability to withstand and recover from disruptions. Cohen et al. (2022) conducted interviews with 16 supply chain executives to determine process, partnership, and product complexity as dominant drivers for the mix of resilience strategies in supply chain design.

### 3.2.2 Strategies to increase resilience in SCND

SCR has been defined by various authors in the past including crucial design characteristics and capabilities. We recommend the recent overviews by Hosseini et al. (2019a) and Aldrighetti et al.

(2021). Designing resilient supply chains involves understanding the nature of the disruption uncertainty at hand concerning probability and impact of its occurrence. Due to this uncertainty, supply chains require a detailed understanding of hidden interactions across different decision levels. In order to increase SCR, firms can adjust their network design as well as their tactical and operational decisions (Govindan et al. 2017). Different SCR strategies have been identified and discussed in analytical models, such as supplier segregation, multiple sourcing strategy, inventory positioning, multiple transportation channels, backup suppliers, re-routing, and product substitution (Hosseini et al. 2019a). Even though most studies highlight the benefits of multiple sourcing and backup suppliers, the explicit role of lead time is still not well understood as immediate effects of disruptions and SCR strategies are common assumptions (Aldrighetti et al. 2023).

One of the key implementation requirements for the adaptation of resilience strategies in practices is their cost-competitiveness. Thus, quantitative decision models that decide on the cost-optimal mix of resilience strategies for the SCND under disruption risks gained increasing relevance. Overall, SCND problems under disruption uncertainty developed from simple facility locations to complex integrated decision problems. Klibi and Martel (2013) proposed a new methodology to establish robust solutions to the SCND problem without the need to determine disruption probabilities. Snoeck et al. (2019) combined strategic mitigation with operational decisions by incorporating the inbound supply chain planning with production planning and setup for the chemical industry and proposing a solution scheme based on linear approximation. As an extension of previous supplier selection problems, Hosseini et al. (2019b) incorporated decisions on additional manufacturing capacities and geographical separation of suppliers, considering regional disruption scenarios. Azad and Hassini (2019) developed an optimization model with partial failure of facilities and multi-mitigation strategies and proposed an enhanced BD to solve the problem. Rodríguez-Espíndola (2023) proposed a two-stage bi-objective stochastic model to propose an integrated approach for handling multiple simultaneous disasters. Studying recurring hurricane and tropical storm disruptions, they focused on the year 2013 where three simultaneous disasters caused economic and social implications simultaneously. Alikhani et al. (2023) used a multi-methodological approach to select the best resilience strategies for varying supply chain disruptions. They considered facility fortification, direct shipping, inventory increase, facility dispersation, multiple set covering, and cybersecurity in a single product flow and single time period environment. Aldrighetti et al. (2023) studied a resilient SCND in a multi-echelon, multi-period, and single-product setting with equal disruption probabilities for all locations. Through numerical experiments and a case study focusing on the COVID-19 pandemic, they identified a good trade-off between resilience and investment costs with minimal investments focusing on agile and reconfigurable supply chains. Particularly, backup suppliers outside the main supply chain footprint are most efficient for disruptions on the supply side, while re-routing of material flows was a key SCR strategy for disruptions at own facilities. However, they assumed all disruption and recovery events with immediate impacts, ignoring the potential impact of lead times.

### 3.2.3 Decision models for resilient SCND with multiple products

Schmitt and Singh (2012) developed a simulation model to capture a multi-product, multi-echelon network to reduce supply chain risks. Based on their analysis, the whole system must be considered to find the optimal mix of resilience actions. Baghalian et al. (2013) considered demand and supply uncertainty in a multi-product supply chain to determine the ideal facility location in a robust supply chain network design. Particularly, they argue that the risk acceptance in the supply chain depends on the nature of the product. Sabouhi et al. (2018) considered partial and complete disruptions for the multi-product SCND inbound SCND problem considering quantitative discount levels for the sourcing decision from multiple suppliers. In addition, they presented a pharmaceutical case highlighting the impact of holding cost on the optimal resilience mix. Bottani et al. (2019) developed a bi-objective mixed-integer programming formulation for the resilient SCND specific for the food supply chain. They identified the optimal resilience mix for each product based on the sourcing costs, lead time, capacity consumption, and supply disruption probability. Within their approach, they focused on the efficient redesign of a supply chain network when facing a disruption and proposed a metaheuristic based on an adapted ant colony optimization to solve the problem of redesigning when facing a disruption. Recently, Ghanei et al. (2023) studied an intertwined supply network under a fair collaboration with multiple products that incorporates different resilience strategies when facing transportation cost and facility capacity uncertainty. Using a Monte-Carlo simulation based on the sample average approximation scheme they estimate the expected value function to then solve the resulting network design problem by solving the deterministic optimization problem.

### 3.2.4 Summary of research opportunities

The effect of product characteristics on general supply chain design as well as their influence in building resilient supply chains has been extensively proven empirically. Still, there is a lack of decision models that deal with the real-life need for multi-product problems in resilient SCND (Govindan et al. 2017) to understand how product characteristics influence the cost-competitiveness of resilience strategies. Till date, many papers assume single product flows in resilient SCND to reduce model complexity. However, this neglects both the role of different product characteristics in the cost-optimal mix of resilience strategies as well as a potential interdependence between the products in SCND. Bridging the gap between the individual analysis of certain products as well as the influence of product characteristics on the optimal resilience strategy is seen as one of the key research gaps in SCR literature (Ergun et al. 2023).

## 3.3 Problem setting

We introduce the resilient multi-echelon SCND problem with multiple products. Section 3.3.1 introduces the process and network structure while Section 3.3.2 outlines the relevant product characteristics within the product portfolio. We discuss the effect of uncertain transportation disruptions in Section 3.3.3. Finally, the different resilience strategies available to the decision maker are summarized in Section 3.3.4.

### 3.3.1 Network and process structure

We consider a SCND problem with multiple products needed to produce a single finished good in a discrete-time horizon where the transportation network consists of multiple suppliers (*as sources*), multiple transportation modes (*as arcs*), two-echelon inventory holding locations (*as nodes*), and a single production facility (*as sink*). Two different types of suppliers are relevant: Global suppliers, on the one hand, deliver to the inventory storage location at the first echelon, which is typically located close to a seaport. Here, all products are received, bundled, and then shipped to the second echelon through a distinct transportation mode, which is typically either inland shipping, rail, or truck depending on the availability. Regional suppliers, on the other hand, deliver directly to the inventory storage location at the second echelon. Generally, each product is offered by both global and regional suppliers. Each supplier offers the product at a specific product price and transports the products through a specific transportation mode to the inventory storage of echelon 1 (global suppliers) or the inventory of echelon 2 (regional suppliers). Each of these transportation modes can differ in transportation costs and lead times. For the transport between the first and second echelon, all products share the same transportation mode, and thus time and costs. In addition, global suppliers offer an express delivery at higher transportation costs that are directly shipped to the second echelon. We focus on problem settings where the important transportation link between the first and second echelon of inventory holding is prone to disruptions (see Section 3.3.3). The overall network structure is visualized in Figure 3.1.

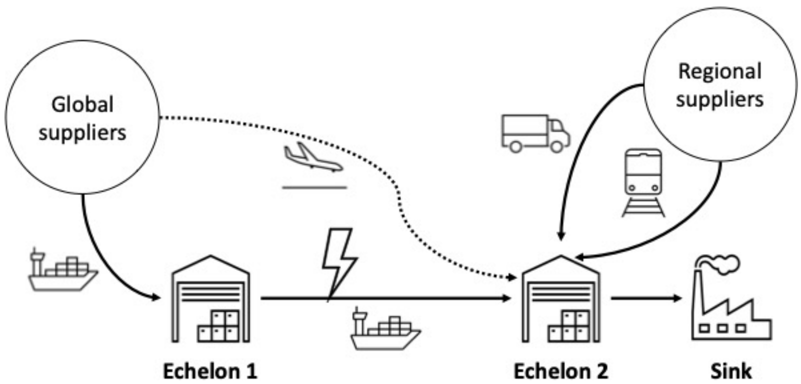


Figure 3.1: Structure of the two-echelon resilient SCND problem with multiple products.

At the beginning of each period, outstanding shipments at each of the inventory echelons that were triggered lead time periods in the past arrive. At the first echelon, shipments to the second echelon can be triggered from the resulting available inventory quantity. At the second echelon, the demand is fulfilled from the available inventory. The final inventory at the end of each period becomes the starting inventory for the next period at each echelon. In case available inventory of echelon 2 of any of the products is not sufficient to fulfill the finished good demands, shortages are considered. As all products are needed to produce a finished good, the product with the highest shortage in each time period determines the overall shortage of the finished good relevant for the total costs.

### 3.3.2 Product characteristics and the variety of product portfolios

We are interested in the influence of product characteristics on the cost-competitiveness of resilience strategies (see Section 3.3.4). We distinguish products based on the following characteristics:

- *Product value.* The product value is a direct driver of inventory holding cost as this is assumed to correlate. Therefore, we distinguish between low and high priced products in terms of their holding costs per unit.
- *Volumetric weight.* The combination of weight and volume is an important driver for air freight cost. As we assume express operational reorders via air freight, the higher the volumetric weight, the higher the express reorder costs.
- *Space requirement.* When multiple products are stored in a single warehouse, there are significant differences concerning the space requirements and thus the capacity consumption of the respective warehouse. Thus, we differ in the capacity consumption of inventory storage capacity per unit stored.
- *Product complexity.* The qualification efforts for suppliers correlate to the overall product complexity. The more complex a product, the higher the efforts in testing and maintaining the specifics. A commodity on the other hand, can be obtained at lower qualification costs as specifications are rather standard and qualification requires mainly administrative efforts.
- *Availability of suppliers for near-shoring.* Some products are generally available to be sourced either regionally or globally while others might only be available globally. This includes, for example, raw materials that might not be available in the specific region such as rare-earth needs as highlighted in the "Critical Raw Materials Act" of the European Union (Cohen et al. 2022, Hool et al. 2023).

Table 3.1 summarizes these product characteristics and defines 16 archetypical product types relevant to resilient transportation network design. Regarding the availability of suppliers for near-shoring, we consider case situations with and without regional supplier availability. In addition, the cost ratio between the transportation costs, the total sourcing costs, and the shortage costs play a significant role in the cost-competitiveness of resilience strategies. While for products and industries with a low share of transportation costs, disruptions that result in pure transportation cost increases might not play a relevant role, the same disruptions might be of major importance for the overall cost-competitiveness in other industries as surcharges account for a much higher share on overall costs.

Using the Rhine River as an example, we outline the typical variety of product characteristics but also the subsets of products where decision-makers are relying on waterway transport. Thus, we highlight the differences in planning challenges for decision makers within and across industries, such as chemicals, commodities (including agricultural products), and automotive.

Companies within the chemical industry source and produce a wide variety of products and, as an industry, are often dependent on waterway transport. Within the chemical industry, some major product groups include commodity chemicals, specialty chemicals, and petrochemicals. Commodity

| Product | Product value | Volumetric weight | Space requirement | Complexity |
|---|---|---|---|---|
| P1 | Low | Low | Low | No |
| P2 | High | Low | Low | No |
| P3 | Low | High | Low | No |
| P4 | High | High | Low | No |
| P5 | Low | Low | High | No |
| P6 | High | Low | High | No |
| P7 | Low | High | High | No |
| P8 | High | High | High | No |
| P9 | Low | Low | Low | Yes |
| P10 | High | Low | Low | Yes |
| P11 | Low | High | Low | Yes |
| P12 | High | High | Low | Yes |
| P13 | Low | Low | High | Yes |
| P14 | High | Low | High | Yes |
| P15 | Low | High | High | Yes |
| P16 | High | High | High | Yes |

Table 3.1: Overview of product portfolio characteristics.

chemicals are typically produced continuously and traded on a large scale in global markets with no differentiation between different suppliers and sourcing options (e.g., $\mathcal{P}1$). Similarly, petrochemicals are also produced on a large scale. However, they differ in a way that during petrochemical production, a number of related products often need to be produced, which can differ greatly in value and storage requirements (e.g., $\mathcal{P}5$). Specialty chemicals, on the other hand, are products made in discrete batch processes, often following specific and unique customer requirements of high value (e.g., $\mathcal{P}10$). Since a typical chemical production site produces a variety of commodity, petrochemical, and specialty chemical products (not exhaustive), decision makers need to balance various different products that could be affected through identical transportation disruptions (e.g., $\mathcal{P}1, \mathcal{P}5, \mathcal{P}10$).

In addition, a large share of the transport volumes is driven by agricultural products and commodities, such as coal, oil, and steel. In contrast to the chemical products involved, many of these commodity products cannot be switched to other modes due to the pure quantities involved that cannot be covered in the short or mid-term elsewhere (e.g., $\mathcal{P}7$). Thus, despite cost implications, the primary threat for decision makers is the non-availability of alternative transportation modes in the short term, requiring potentially different resilience strategies. Generally, however, these products are widely available and can be sourced from many different modes if the respective capacities are ensured.

Lastly, to significantly reduce environmental emissions, the automotive industry has increasingly relied on waterway transport for the transport of its finished vehicles (e.g., $\mathcal{P}16$). While road and rail transport has generally been used within the industry, where available, waterway transport offers significant environmental benefits that are becoming increasingly important to decision-makers due to regulatory changes and challenges.

Overall, various products are affected by the disruption incurred water level changes that result in surcharges or transportation stops. Depending on the specifics of the products to be transported, however, differences in alternative transportation modes, environmental effects, and cost implications need to be considered differently and balanced against the overall objectives and focus of a decision maker.

### 3.3.3 Disruption uncertainty

We define a transportation disruption as an unfortunate event causing a capacity reduction to the critical transportation mode between the first and second echelon of inventory holding. In practice, this is related to a main transportation channel that a vast majority of transport relies on, such as main canals or rivers for inland shipping or railroad infrastructure that connects major seaports with the hinterland. To account for the lost transport capacities, transportation carriers enforce contractually defined surcharges on top of their regular transportation costs based on the actual conditions (e.g., water levels) of the actual day of shipment. These surcharges further balance the transportation demand with the reduced supply based on short-term alternatives. Depending on the disruption impact and mode, the cost effects range from modest increases to full transportation stops, i.e., an unlimited increase in transportation costs.

The resulting uncertainty affects the decision-maker's shipment decisions differently. All direct shipments from the suppliers (tactical level) to either the first or the second echelon must be made under complete uncertainty, i.e., not knowing when, how long, and with which impact a disruption occurs. However, shipments between the two echelons and the express delivery from global suppliers can be made with a significantly lower lead time and thus, with full knowledge on the disruption occurrence.

### 3.3.4 Resilience strategies

A central decision-maker at the production facility sources from various suppliers and is in full responsibility of the inbound logistic flows for all products within the portfolio. The goal is to minimize the expected costs by determining the optimal mix of resilience strategies on the product level. We consider the following strategic, tactical, and operational resilience strategies in a two-stage stochastic decision problem.

*Multi-sourcing (strategic, first-stage).* Qualification of multiple suppliers including multi-sourcing, i.e., purchasing from two or more suppliers in parallel, and the investment in a back-up supplier that is only used in case a disruption occurs at the transportation modes of the primary supplier.

*Near-shoring (strategic, first-stage).* Qualification of a regional supplier that directly transports to the second echelon of inventory holding and thus avoids the transportation uncertainty between the echelons but comes at a cost-premium.

*Inventory capacity adjustment (strategic, first-stage).* Investment decision in additional inventory capacity for the first and second echelon inventory storage that increases the flexibility of decisions on the tactical and operational level.

*Inventory increase (tactical, first-stage).* Decision to increase inventory on the tactical level at the first or second echelon of inventory holding.

*Express re-orders (operational, second-stage).* Decision for express delivery from a qualified supplier at a higher short-term price from a global supplier.

## 3.4 Model development

Sets, decision variables and parameters are introduced in Sections 3.4.1-3.4.3 before we introduce the two-stage stochastic programming formulation in Section 3.4.4.

### 3.4.1 Sets

Multiple products $\mathcal{P}$ need to be supplied to a production facility over a discrete time horizon $\mathcal{T}$. Products are transported from multiple suppliers $I$. Based on the geographical distance between the suppliers and the production facility, we differ between global suppliers $\mathcal{I}^G$ and regional suppliers $\mathcal{I}^R$. The two supplier types deliver to different echelons $\mathcal{N}$ of the supply chain. Regional suppliers directly deliver to the production facility $n = 2$ while global supplier transports are first stored in an external inventory stage at level $n = 1$. In addition, $\mathcal{I}_p$ describes the subset of all suppliers $\mathcal{I}$ that are able to supply product $p$. These can include both global and regional suppliers.

### 3.4.2 Parameters

Scenarios occur with probability $\pi_s$, with $0 \leq \pi_s \leq 1$ and $\sum_{s \in S} \pi_s = 1$ with $\mathcal{S}$ describing the full scenario set during the planning horizon. Scenarios affect the transportation costs ($c^T_{pts}$) between the first and second echelon inventory locations. Based on a base cost of transportation, scenarios reflect the disruption-driven increase of the transportation mode used between the two echelons.

Each product is supplied based on a tactical plan from each supplier at the costs $c^T_{ip}$ which includes transportation costs and the product price. Per time period and product units stored, inventory holding costs $c^H_{np}$ occur that differ between the products and between the echelon of inventory holding. The product with the highest unfulfilled unit of demand $d_{pt}$ in each time period determines the shortage costs $c^P$. The total sum of all demands across the planning horizon is $\hat{d}_p$ for each product $p$. On the operational level, the short-term express delivery from suppliers to the second echelon comes at a cost of $c^E_{ip}$. To qualify a supplier to deliver product $p$, qualification costs $f^I_p$ are needed that depend on the product complexity. For example, while a commodity product can be sourced with minimal qualification steps to be fulfilled, a more specialized and complex product requires more detailed product quality testing and specification sharing. The initial inventory capacity to store inventory on hand is $Y^0_n$. Through an investment decision this capacity can be increased by multiples of $Y^+_n$ at costs $f^Y_n$ per multiple. In the starting period, an initial inventory of $j^0_{np}$ is available. Transportation lead times $l_i$ are considered that depend on the administrative and transportation time from supplier $i$. For global suppliers, the lead time for express reorders is $\hat{l}_i$. For the transport between the first and second inventory echelon, a lead time of $l_0$ is considered. Each product has a specific space requirement $a_p$ that consumes inventory storage capacity.

### 3.4.3 Decision variables

The model decides between different resilience strategies, as introduced in Section 3.3.4, to minimize the total expected costs across all products and inventory storage echelons in a two-stage stochastic program.

The first-stage decisions determine the network structure and capacities for product flows between the suppliers and the echelons of inventory holding. The binary decision $z_{ip}$ determines if supplier $i$ is qualified (= 1) or not (= 0) to deliver product $p$. The starting inventory storage capacity $Y_n^0$ can be increased at each echelon $n$ through integer investments $w_n$ in additional inventory capacity. For each supplier $i$ and each product $p$, transportation quantities $x_{ipt}$ are defined at the first-stage for each time period $t$. These represent the tactical flows from global and regional supplier to the respective inventory echelon $n$. On the second-stage, the operational routing $\bar{x}_{pts}$ between the first and second echelon of inventory holding takes place. Here, the decision maker already knows the disruption in scenario $s$ and can route based on the available tactical shipments and respective inventory holding capacities. In addition, it is possible to decide for operational express re-orders $\hat{x}_{ipts}$ from global suppliers shipped through an alternative transportation mode at shorter lead times.

Additional decision variables are needed to formulate the problem. The on-hand inventory at the beginning of each time period $t$ in each scenario $s$ for each product $p$ and in each echelon of inventory holding $n$ is defined by $y_{npts}$. In case product demand $d_{pt}$ exceeds the available on-hand inventory, shortages $v_{pts}$ occur. For each time period, the overall cost-relevant shortages are determined by the highest shortages $v_{ts}$ that occur across all products.

### 3.4.4 Model formulation

$$
\begin{aligned}
min \quad & \sum_{n\in\mathcal{N}} f_n^Y \cdot w_n + \sum_{i\in\mathcal{I}_p,p\in\mathcal{P}} f_{ip}^I \cdot z_{ip} + \sum_{i\in\mathcal{I}_p,p\in\mathcal{P},t\in\mathcal{T}} c_{ip}^T \cdot x_{ipt} + \\
\sum_{s\in\mathcal{S}} \pi_s \cdot \Bigg( & \sum_{p\in\mathcal{P},t\in\mathcal{T}} c_{pts}^T \cdot \bar{x}_{pts} + \sum_{i\in\mathcal{I}_p^G,p\in\mathcal{P},t\in\mathcal{T}} c_{ip}^E \cdot \hat{x}_{ipts} + \sum_{n\in\mathcal{N},p\in\mathcal{P},t\in\mathcal{T}} c_{np}^H \cdot y_{npts} + \sum_{t\in\mathcal{T}} c^P \cdot v_{ts} \Bigg)
\end{aligned} \tag{3.1}
$$

*subject to:*

$$\sum_{t\in\mathcal{T}} x_{ipt} \le z_{ip} \cdot \hat{d}_p \qquad \forall i \in \mathcal{I}_p, p \in \mathcal{P} \tag{3.2}$$

$$\sum_{t\in\mathcal{T}} \hat{x}_{ipts} \le z_{ip} \cdot \hat{d}_p \qquad \forall i \in \mathcal{I}_p^G, p \in \mathcal{P}, s \in \mathcal{S} \tag{3.3}$$

$$\sum_{p\in\mathcal{P}} a_p \cdot y_{npts} \le Y_n^0 + w_n \cdot Y_n^+ \qquad \forall n \in \mathcal{N}, t \in \mathcal{T}, s \in \mathcal{S} \tag{3.4}$$

$$y_{1pts} = y_{1p(t-1)s} - \bar{x}_{pts} + \sum_{i\in\mathcal{I}_p^G} x_{ip(t-l_i)} \qquad \forall p \in \mathcal{P}, t \in \mathcal{T} \setminus \{1\} | t > l_i, s \in \mathcal{S} \tag{3.5}$$

$$
\begin{aligned}
y_{2pts} = y_{2p(t-1)s} + v_{pts} - d_{pt} + \bar{x}_{p(t-l_0)s} + \sum_{i\in\mathcal{I}_p^R} x_{ip(t-l_i)} + \sum_{i\in\mathcal{I}_p^G} \hat{x}_{ip(t-\hat{l}_i)s} \\
\forall p \in \mathcal{P}, t \in \mathcal{T} \setminus \{1\} | t > l_i, s \in \mathcal{S}
\end{aligned} \tag{3.6}
$$

$$y_{np1s} = j_{pn}^0 \qquad \forall n \in \mathcal{N}, p \in \mathcal{P}, s \in \mathcal{S} \tag{3.7}$$

$$v_{ts} \geq v_{pts} \qquad \forall p \in \mathcal{P}, t \in \mathcal{T}, s \in \mathcal{S} \tag{3.8}$$

$$z_{ip} \in \{0,1\} \qquad \forall i \in \mathcal{I}, p \in \mathcal{P} \tag{3.9}$$

$$w_n \in \mathbb{Z} \qquad \forall n \in \mathcal{N} \tag{3.10}$$

$$x_{ipt}, \bar{x}_{pts}, \hat{x}_{ipts}, y_{npts}, v_{ts}, v_{pts} \geq 0 \qquad \forall n \in \mathcal{N}, i \in \mathcal{I}, p \in \mathcal{P}, t \in \mathcal{T}, s \in \mathcal{S} \tag{3.11}$$

The objective function (3.1) minimizes the total expected costs through first-stage and second-stage decisions across all scenarios. First-stage decisions drive the overall investment costs that occur independent of the respective scenario. They include: Investment decision in additional inventory capacity ($w_n$) at the two echelons of inventory holding at investment costs of $f_n^Y$, the decision to qualify a supplier ($z_{ip}$) to deliver product $p$ at costs $f_{ip}^I$, and the shipment costs ($c_{ip}^T$) for the tactical transportation volumes ($x_{ipt}$) from the qualified suppliers to the inventory storage locations. On the second-stage, the costs per scenario $s$ are determined by the shipments $\bar{x}_{pts}$ from the first to the second echelon, the emergency transports $\hat{x}_{ipts}$ from global suppliers, the inventory holding costs driven by the inventory levels at both echelons ($y_{npts}$), and the shortage costs in each time period driven by the product with the highest individual shortages $v_{ts}$.

Constraints (3.2) and (3.3) ensure that products are only supplied from suppliers qualified. The inventory storage at each echelon $n$ can not exceed the inventory capacity as ensured in constraints (3.4). Constraints (3.5) and (3.6) ensure the inventory balance at each of the echelons while the starting inventory is defined in constraints (3.7). Constraints (3.8) determine the highest shortage across all products as for an inbound SCND problem the highest shortage across all products determines the amount of finished good shortage through production. The remaining constraints (3.9)-(3.11) declare the decision variables.

### 3.4.5 Model enhancements

Particularly with a larger number of products, the model becomes increasingly difficult to solve for commercial solvers. To improve the convergence behavior and provide strong initial solutions, lower-bound-lifting and valid inequalities (Section 3.4.5.1) and a warm start solution (Section 3.4.5.2) are added to improve the standard model formulation.

#### 3.4.5.1 Lower-bound lifting and valid inequalities

Following the idea of lower-bound-lifting inequalities as introduced by Adulyasak et al. (2015), we derive problem-specific lower-bound-lifting inequalities by adding the following constraints.

$$\sum_{i \in \mathcal{I}} z_{ip} \geq 1 \qquad \forall p \in \mathcal{P} \tag{3.12}$$

$$q_p \geq \hat{d}_p - \sum_{i \in \mathcal{I}, t \in \mathcal{T}} x_{ipt} - \sum_{n \in \mathcal{N}} j^0_{pn} \qquad \forall p \in \mathcal{P} \tag{3.13}$$

$$q^{max} \geq g_p \qquad \forall p \in \mathcal{P} \tag{3.14}$$

$$\begin{aligned} \sum_{p \in \mathcal{P}, t \in \mathcal{T}} c^T_{pts} \cdot \bar{x}_{pts} + \sum_{i \in \mathcal{I}^G_p, p \in \mathcal{P}, t \in \mathcal{T}} c^E_{ip} \cdot \hat{x}_{ipts} + \sum_{n \in \mathcal{N}, p \in \mathcal{P}, t \in \mathcal{T}} c^H_{np} \cdot y_{npts} + \sum_{t \in \mathcal{T}} c^P \cdot v_{ts} \\ \geq \sum_{i \in I^G_p, p \in P, t \in T} c^T_{pt_{min}} \cdot x_{ip(t+l_i)} + \min(c^E_{ip} \cdot P, c^P) \cdot q^{max} \qquad \forall s \in \mathcal{S} \end{aligned} \tag{3.15}$$

Constraints (3.12) ensure that at least one supplier is qualified for each product. Constraints (3.13) set lower bound on the total shortage quantity as defined by the difference between the total demand, tactical shipments, and the starting inventories. Constraints (3.14) define the relevant shortage quantity overall through the highest shortage across all products $\mathcal{P}$. Lastly, constraints (3.15) define the lower bound on all scenario-dependent costs in the objective function (3.1) as the sum of the shipment costs between the echelons determined by the shipments from global suppliers $i \in \mathcal{I}^G$ assuming they can be executed disruption-free ($c^T_{pt_{min}}$), and the shortage costs as determined through the minimum between the express delivery costs $c^E_{ip}$ multiplied with the number of products that need to be sourced $P$ and the shortage costs $c^P$.

#### 3.4.5.2 Warm start

Wo obtain a starting solution by using the expected cost scenario and solving the deterministic version of the multi-product problem. We then obtain the solution for each product $p \in \mathcal{P}$ and insert this solution into the mixed-integer linear program (MILP).

## 3.5 Case study

We test our approach using a case study motivated by a real-life example with real disruption data. Section 3.5.1 introduces the case in detail and describes the numerical setup. We compare the algorithmic performance of the standard and enhanced model formulation in Section 3.5.2. Section 3.5.3 presents the numerical results. Finally, in Section 3.5.4, managerial insights are drawn. The algorithm is implemented in Python 3.8 using Gurobi 10.0.3. A desktop PC with an AMD Ryzen 9 5950X 16-Core processor with 3.4 GHz and 128 GB of RAM is used for model execution.

### 3.5.1 Case introduction

Our case study is based on a real-life example from a chemical company with a production facility on the border of the Rhine River, Germany. For the case company, a large share ($\geq$ 40%) of all products required for the production of a typical finished good are sourced from global suppliers and shipped through the Rhine River. Each of these products can be sourced regionally as well at a cost-premium. Within our analysis, we focus on one exemplary finished good in a continuous production with different products needed that form the bill of materials (see Section 3.3.2). Any product missing leads to shortage costs as this forces production to a standstill. In the chemical industry, material shortage costs typically exceed the sum of finished good lost margins and customer penalty costs as complex production systems need to be shut down and re-started. After a restart, it can take hours to days to produce again a quality sufficient for customer requirements.

For each product, one global and one regional supplier is available. Inventory holding costs $c^H_{np}$ are 20% of the product value which is three times higher in the case of a high-value product. Thus, annual inventory holding costs are as well three times higher. Given a low volumetric weight, the express shipment is four times more costly than the steady state transportation from the global supplier. For high volumetric weights, air freight costs rise even more significantly to a multiple of 12 times compared to the disruption-free costs of regular global transport. Compared to a low space requirement, products with a high space requirement require three times more inventory space units. Lastly, a complex product has three times higher supplier qualification costs as more samples are needed and suppliers need to conduct specific investments on their own.

Without disruptions, most global sourced products are transported cost-optimal through ocean freight to one of the major European ports combined with the hinterland transport through inland shipping via the Rhine River. At all major ports worldwide, inventory storage areas can be rented to hold inventory prior to the hinterland transport (first echelon of inventory holding). The inland shipping mode, however, is prone to recurring disruptions due to water level changes that lead to surcharges depending on daily water levels as part of long-term contractual agreements between the transportation carriers and the case company. Due to the high volumes typically transported through inland shipping, there is no alternative transportation mode available in the short-term to ship from the port to the inventory holding at the production facility (second echelon). Instead, products can be sourced from regional suppliers through alternative transportation modes on the tactical level or through short-term express deliveries from global suppliers at significantly higher costs. Without disruptions, the transportation costs and product price difference are 50% higher than the global sourcing whereas the express deliveries are 400% higher. Lead times differ as well with shipments between the two echelons as the fastest with 3 days, regional sourcing and express delivery arrive after 7 days, and the transport to the first inventory echelon with 14 days of lead time from global suppliers.

Concerning the disruption uncertainty that affects the inland shipping transportation between the first and second echelon of inventory holding, Figure 3.2 visualizes the water level fluctuations on the river Rhine from 2015-2022. As can be seen, transportation stops due to low water levels occurred in 2015, 2017, 2018, 2020, and 2022, while high tides caused transportation stops in 2018 and 2021. In addition, occurrences where low water levels force vessels to carry reduced capacities and thus result in surcharges occur regularly. In addition, Figure 3.2 shows seasonal patterns as well. For example, high tides happen exclusively in winter while low water levels are typically seen in late summer or autumn.

Transportation surcharges for low and high water levels are significant, as highlighted in Table 3.2. Overall, the contractual surcharges range from a 78% to a 261% cost increase compared to water levels between 150 and 460cm, while on water levels less than 80cm and higher than 640cm, no transportation is possible. The orange line in Figure 3.2 highlights water level thresholds for cost increases and the red line indicates transportation stops. We consider the last 42 years of water level history as scenarios that cover the uncertainty space with an equal possibility of occurrence of $\pi_s = \frac{1}{42}$.

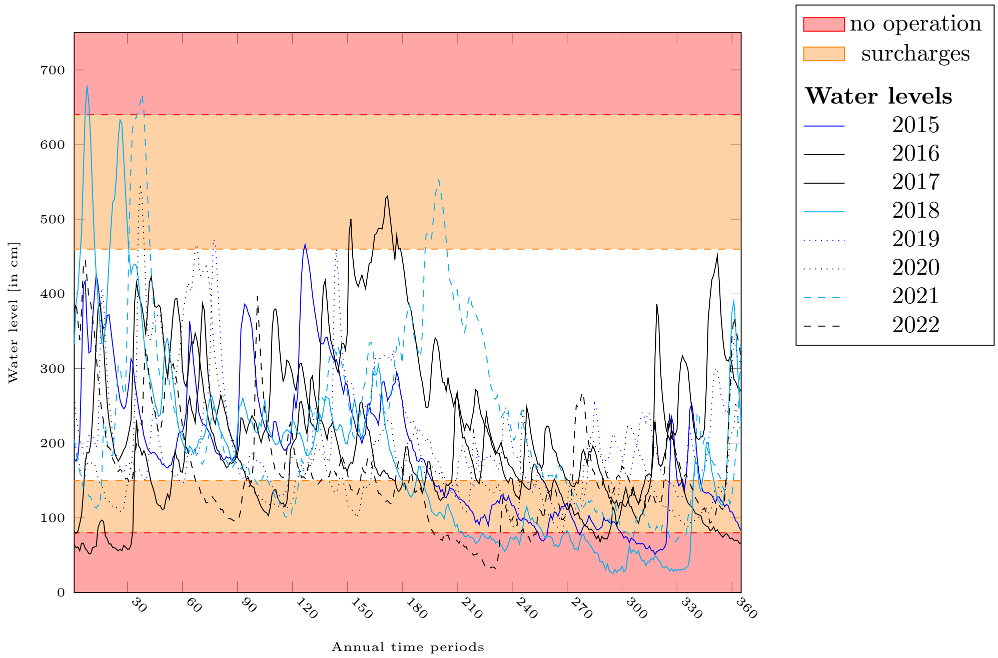


Figure 3.2: Historical water levels at shipment critical point for Rhine River as main transportation mode ($m = 1$).

| Water level [cm] | < 80 | < 90 | < 100 | < 110 | < 130 | < 150 | < 460 | < 640 | >= 640 |
|---|---|---|---|---|---|---|---|---|---|
| Costs [EUR] | - | 415 | 340 | 295 | 250 | 205 | 115 | 205 | - |

Table 3.2: Transportation costs per container transported depending on water level.

### 3.5.2 Algorithm performance

We benchmark our enhanced model formulation against the standard model formulation, solving both algorithms with the commerical solver Gurobi using a branch-and-bound algorithm. The algorithms are terminated after 3,600 seconds or after ensuring an optimality gap of at least 1%. Table 3.3 summarizes the results. We increase the number of products from 1 to 8. As can be seen, the enhanced model formulation outperforms the standard formulation as soon as multiple products of at least two are considered. While the enhanced formulation reduces the computational time by 25% for two products and 14% for three products, it still converges within one hour for four products where the standard model formulation does not find a feasible starting solution. With the enhanced model formulation, the number of products can be increased to seven to still find strong solutions with a proven optimality gap less than 1.57% within one hour. Overall, the higher the number of products, the greater the benefits of identifying strong solutions through the enhanced formulation, while the standard formulation struggles to find feasible solutions.

| | | | GB-LBL | | GB | |
|---|---|---|---|---|---|---|
| $\|\mathcal{P}\|$ | $\|\mathcal{T}\|$ | $\|\mathcal{S}\|$ | CPU [s] | Gap | CPU[s] | Gap |
| 1 | 365 | 42 | 87 | 0.83% | 50 | 0.91% |
| 2 | 365 | 42 | 630 | 0.70% | 841 | 0.85% |
| 3 | 365 | 42 | 2155 | 0.80% | 2509 | 0.91% |
| 4 | 365 | 42 | 2683 | 0.95% | 3600 | 1.56% |
| 5 | 365 | 42 | 3600 | 1.09% | 3600 | - |
| 6 | 365 | 42 | 3600 | 1.29% | 3600 | - |
| 7 | 365 | 42 | 3600 | 1.57% | 3600 | - |
| 8 | 365 | 42 | 3600 | 23.76% | 3600 | - |

Table 3.3: Computational complexity with increasing number of products.

## 3.5.3 Sensitivity analysis

### 3.5.3.1 Product characteristic influence for the single-product problem

We solve the single-product resilient SCND problem for each product independently to compare and evaluate the influences of the different product characteristics in the single product setting. Table 3.4 summarizes the results for products $\mathcal{P}1$-$\mathcal{P}16$ and the average $\overline{\mathcal{P}}$.

| | | | | Capacity investments | | Average inventory | | Share transport volumes | | |
|---|---|---|---|---|---|---|---|---|---|---|
| | Costs | CPU | $\|z\|$ | Echelon 1 | Echelon 2 | Echelon 1 | Echelon 2 | Global | Regional | Express |
| $\mathcal{P}1$ | 187.46 | 69 | 2 | 3 | 3 | 8.27 | 21.43 | 78% | 21% | 1% |
| $\mathcal{P}2$ | 193.85 | 105 | 2 | 1 | 1 | 5.22 | 3.77 | 63% | 35% | 1% |
| $\mathcal{P}3$ | 188.99 | 65 | 2 | 3 | 3 | 9.30 | 21.36 | 78% | 21% | 1% |
| $\mathcal{P}4$ | 195.17 | 89 | 2 | 1 | 1 | 5.50 | 4.23 | 63% | 37% | 0% |
| $\mathcal{P}5$ | 198.04 | 171 | 2 | 2 | 2 | 2.71 | 5.99 | 53% | 46% | 1% |
| $\mathcal{P}6$ | 199.68 | 198 | 2 | 0 | 0 | 1.29 | 0.62 | 45% | 54% | 1% |
| $\mathcal{P}7$ | 198.68 | 134 | 2 | 1 | 1 | 2.60 | 4.81 | 50% | 50% | 0% |
| $\mathcal{P}8$ | 200.28 | 137 | 2 | 0 | 0 | 1.35 | 0.92 | 44% | 56% | 0% |
| $\mathcal{P}9$ | 204.84 | 70 | 1 | 9 | 9 | 15.15 | 46.33 | 96% | 0% | 4% |
| $\mathcal{P}10$ | 211.85 | 135 | 2 | 1 | 1 | 5.22 | 3.77 | 63% | 35% | 1% |
| $\mathcal{P}11$ | 206.98 | 68 | 1 | 9 | 10 | 16.86 | 56.73 | 99% | 0% | 1% |
| $\mathcal{P}12$ | 213.17 | 98 | 2 | 1 | 1 | 5.50 | 4.23 | 63% | 37% | 0% |
| $\mathcal{P}13$ | 216.04 | 195 | 2 | 2 | 2 | 2.71 | 5.99 | 53% | 46% | 1% |
| $\mathcal{P}14$ | 217.68 | 190 | 2 | 0 | 0 | 1.29 | 0.62 | 45% | 54% | 1% |
| $\mathcal{P}15$ | 216.68 | 142 | 2 | 1 | 1 | 2.60 | 4.81 | 50% | 50% | 0% |
| $\mathcal{P}16$ | 218.28 | 149 | 2 | 0 | 0 | 1.35 | 0.92 | 44% | 56% | 0% |
| $\overline{\mathcal{P}}$ | 204.23 | 126 | 1.9 | 2.13 | 2.19 | 5.43 | 11.66 | 62% | 37% | 1% |

Table 3.4: Single product optimal resilience mix.

Overall, we see that the optimal resilience mix differs significantly across the products including the optimal mix of global and regional transportation on the tactical level. Whereas for all low-complexity products (i.e., low supplier qualification costs) a multi-sourcing strategy is cost-optimal, specific products with a high complexity are supplied through single sourcing ($|z| = 1$) in the cost-optimal way. This, however, comes at significant investments in additional inventory capacity for $\mathcal{P}9$ and $\mathcal{P}11$. Thus, for highly complex products with low value and space requirements, carrying additional inventory outperforms a multi-sourcing strategy. Specifically the inventory capacity investments vary across the products. Still, we see that capacities are increased equally across both echelons of inventory holding instead of purely on a single echelon. This allows that not only sufficient inventory can be buffered at the first echelon of inventory holding but then as well shipped in large batches once a disruption-free time period occurs. Lastly, the model split between global, regional, and express transports varies significantly from pure global transport (e.g., $\mathcal{P}9$) to products with at least an equal split across regional and global suppliers (e.g., $\mathcal{P}6$). The key drivers are high inventory holding costs and a high consumption in inventory capacity for these products. Interestingly, this effect is independent from the product complexity ($\mathcal{P}6, \mathcal{P}8$).

As highlighted, a geographical diversification of its supplier base might be challenging or simply not possible for highly complex products or those that require specific raw materials (Cohen et al. 2022). Especially within the European Union certain products can be unavailable and need to be sourced globally due to a lack of key raw materials (Hool et al. 2023). Thus, we compare the previous optimal resilience mix with the mix when only considering global suppliers. The results can be found in Table 3.5.

The following insights can be drawn. First, a missing opportunity to source regionally can influence the total expected costs. The second column ($\Delta$ costs) quantifies the cost increase on product level up to 37%. However, depending on the product characteristics only considering a single, global supplier strategy leads to no or very significant cost increases. Generally, cost increases are higher for products that are more costly in terms of inventory holding due to their product value or higher inventory storage capacity consumption and specifically for products with a high volumetric weight where express orders are higher in comparison. Second, we observe a significant rise in express shipments through alternative transportation modes from global suppliers. Thus, the non-availability of alternative short-term mitigation measures forces an increase in costly air shipments while it is not cost-efficient to fully capture the disruption uncertainty through inventory alone. Lastly, we see a significant increase in inventory capacity investments on strategic level as well as an increase in average inventory average. However, whereas inventory capacity investments increase by a factor of seven on average, average inventory increases only by a factor of three, which indicates a shift in the optimal policies of inventory holding instead of a sole linear increase in average inventory.

#### 3.5.3.2 Benefit of multi-product integration

We now compare the optimal solution on single-product level against the integrated multi-product problem. We focus our analysis on incorporating incrementally products from $\mathcal{P}1 - \mathcal{P}8$ that are required for the production of a single finished good and showing the improvements in resilience costs compared against the optimal solutions of the single-product separated problems. While we accept an optimality gap of 1% as termination criteria for the integrated model, we force true optimality for the separeted problems. The results are summarized Table 3.6.

We define the resilience costs as delta between the theoretical minimum costs that occur without disruptions and the total expected costs with disruption uncertainty. Overall, for eight products, the resilience costs decrease by 4.2% in the integrated model compared to the sum of all single-product expected resilience costs. The most important driver for this change are constraints (3.8),

| | Costs | Δ costs | $\lvert z \rvert$ | Capacity investments | | Average inventory | | Share transport volumes | | |
|---|---|---|---|---|---|---|---|---|---|---|
| | | | | Echelon 1 | Echelon 2 | Echelon 1 | Echelon 2 | Global | Regional | Express |
| $\mathcal{P}1$ | 195.84 | 4% | 1 | 9 | 9 | 15.15 | 46.33 | 96% | 0% | 4% |
| $\mathcal{P}2$ | 209.92 | 8% | 1 | 9 | 5 | 9.38 | 11.70 | 83% | 0% | 17% |
| $\mathcal{P}3$ | 197.98 | 5% | 1 | 9 | 10 | 16.86 | 56.73 | 99% | 0% | 1% |
| $\mathcal{P}4$ | 219.87 | 13% | 1 | 13 | 8 | 14.07 | 28.69 | 98% | 0% | 2% |
| $\mathcal{P}5$ | 228.33 | 15% | 1 | 15 | 10 | 10.97 | 23.12 | 73% | 0% | 27% |
| $\mathcal{P}6$ | 236.09 | 18% | 1 | 13 | 8 | 6.66 | 6.80 | 67% | 0% | 33% |
| $\mathcal{P}7$ | 246.54 | 24% | 1 | 20 | 30 | 21.23 | 79.26 | 98% | 0% | 2% |
| $\mathcal{P}8$ | 274.92 | 37% | 1 | 26 | 31 | 14.66 | 32.26 | 96% | 0% | 4% |
| $\mathcal{P}9$ | 204.84 | 0% | 1 | 9 | 9 | 15.15 | 46.33 | 96% | 0% | 4% |
| $\mathcal{P}10$ | 218.92 | 3% | 1 | 9 | 5 | 9.38 | 11.70 | 83% | 0% | 17% |
| $\mathcal{P}11$ | 206.98 | 0% | 1 | 9 | 10 | 16.86 | 56.73 | 99% | 0% | 1% |
| $\mathcal{P}12$ | 228.87 | 7% | 1 | 13 | 8 | 14.07 | 28.69 | 98% | 0% | 2% |
| $\mathcal{P}13$ | 237.33 | 10% | 1 | 15 | 10 | 10.97 | 23.12 | 73% | 0% | 27% |
| $\mathcal{P}14$ | 245.09 | 13% | 1 | 13 | 8 | 6.66 | 6.80 | 67% | 0% | 33% |
| $\mathcal{P}15$ | 255.54 | 18% | 1 | 20 | 30 | 21.23 | 79.26 | 98% | 0% | 2% |
| $\mathcal{P}16$ | 283.92 | 30% | 1 | 26 | 31 | 14.66 | 32.26 | 96% | 0% | 4% |
| $\overline{\mathcal{P}}$ | 230.69 | 13% | 1 | 14.25 | 13.88 | 13.62 | 35.61 | 89% | 0% | 11% |

Table 3.5: Single product optimal resilience mix without regional supplier availability.

| Products | Model | Total costs | Resilience costs | Δ Costs | Global | Capacity investments | |
|---|---|---|---|---|---|---|---|
| | | | | | | Echelon 1 | Echelon 2 |
| 2 | Integrated | 380.41 | 83.20 | | 74.38% | 5 | 4 |
| | Seperated | 381.31 | 84.10 | 1.08% | 27.93% | 4 | 4 |
| 4 | Integrated | 762.42 | 168.01 | | 70.90% | 8 | 7 |
| | Seperated | 765.47 | 171.06 | 1.82% | 28.48% | 8 | 8 |
| 6 | Integrated | 1152.51 | 260.89 | | 65.99% | 9 | 8 |
| | Seperated | 1163.19 | 271.58 | 4.10% | 35.77% | 10 | 10 |
| 8 | Integrated | 1547.10 | 358.28 | | 62.55% | 10 | 10 |
| | Seperated | 1562.16 | 373.33 | 4.20% | 40.03% | 11 | 11 |

Table 3.6: Comparison of integrated and single-product results for the resilient SCND.

which sets the shortage costs in each time period to the highest shortage across all products. As a result, in single-product models, the shortage costs might be overestimated and result to inefficient resilience strategies as in cases where multiple products (raw materials) are affected, the shortage costs might be lower than over-investments in resilience strategies. While no major differences in inventory investments are observed, we see significant differences in the share of transport volumes from global suppliers compared to regional ones as in the integrated models these are significantly higher. In addition, the resilience cost improvements increase with the number of products considered in the integrated model. Overall, the single-product resilient SCND models might overestimate the resilience costs needed as effects between products are not included. However, the integrated model comes at a significant increase in computational complexity (see Section 3.5.2). Thus, it might be worthwhile to evaluate the case-specific interdependence between the products in order to evaluate whether a single-product model might be justified or an integrated model is needed.

#### 3.5.3.3 Shortage costs driving the need for integration

As highlighted in Section 3.5.3.2, the need for an integration evaluation of multi-product settings can depend on the specific application context and mainly depends on the existence of constraints (3.8). To understand the relevance of the shortage costs on the need for multi-product integration, we conduct a sensitivity analysis on the case-specific shortage costs to understand further implications for the need of a multi-product integration. Thus, we reduce the ratio of shortage costs against the disruption-free transportation costs from 25 to 10. The results are outlined in Table 3.7.

| | $\lvert\mathcal{P}\rvert$ | | | |
|---|---|---|---|---|
| $cSh$ | 2 | 4 | 6 | 8 |
| 2 | 1.08% | 1.82% | 4.10% | 4.20% |
| 1.2 | 1.08% | 1.82% | 4.20% | 12.72% |
| 0.8 | 1.08% | 2.46% | 6.63% | 78.82% |

Table 3.7: Resilience cost improvements based on number of products and shortage costs.

With decreasing shortage costs ($cSh$), the resilience cost improvements start to increase with only four products considered. In comparison, for eight products the disruption-free transportation costs for all products are 0.64 per unit. Thus, $cSh = 0.8$ represents only a minor increase of 25%, resulting in significantly less required capacity investments and resilience costs. Given the disruption-driven cost surcharges as outlined in Section 3.5.1, the importance solving the integrated multi-product problem increases with the number of products and a decrease in shortage costs considered.

#### 3.5.3.4 Resilience shifts in multi-product sourcing

In Table 3.7, we have analyzed the benefits and reductions in resilience costs for solving the integrated model with multiple products assuming a single combination of product characteristics. We have shown that solving the integrated model with two products (i.e., $p_1 = \mathcal{P}1, p_2 = \mathcal{P}2$) leads to improvements in resilience costs of 1.08% in comparison to the single-product optimal solutions. As highlighted in Section 3.5.3.1, the resilience mix for the single product cases depends on the specific product characteristics. After discussing the general improvement potential of considering the joint integrated problem in Sections 3.5.3.2 and 3.5.3.3, we now analyze the behavior of the optimal solutions for different product portfolio combinations in the multi-product setting. Table 3.8 compares the resilience costs for the integrated two-product problem with different product combinations.

Major differences in the resilience cost deltas can be observed based on the product characteristics. Interestingly, in the two product-problem, solving the integrated problem increases in benefits once the product characteristics vary significantly among the two products. For example, solving the integrated problem where $p_1 = \mathcal{P}1$ and $p_2 = \mathcal{P}1$ are of both of the same product archetype leads to no improvements in resilience costs. Overall, the highest observed benefits for solving the integrated problem with equal product types is 3.80% whereas for very different product archetypes considered the lowest improvement observed is 5.80%. Overall, the average improvement increases from 1.36% for equal product archetypes to 7.87% for highly different product archetypes considered in the

| | $p_1$ | $p_2$ | Single-product: Capacity investments Echelon 1 | Echelon 2 | Costs Total | Integrated multi-product: Capacity investments Echelon 1 | Echelon 2 | Resilience costs Δ Single |
|---|---|---|---|---|---|---|---|---|
| Equal characteristics | $\mathcal{P}1$ | $\mathcal{P}1$ | 6 | 6 | 374.91 | 6 | 6 | 0.00% |
| | $\mathcal{P}2$ | $\mathcal{P}2$ | 2 | 2 | 387.71 | 3 | 1 | 0.09% |
| | $\mathcal{P}3$ | $\mathcal{P}3$ | 6 | 6 | 377.98 | 6 | 6 | 3.80% |
| | $\mathcal{P}4$ | $\mathcal{P}4$ | 2 | 2 | 390.35 | 3 | 1 | 2.92% |
| | $\mathcal{P}5$ | $\mathcal{P}5$ | 4 | 4 | 396.08 | 4 | 4 | 0.00% |
| Different characteristics | $\mathcal{P}1$ | $\mathcal{P}11$ | 12 | 13 | 394.43 | 9 | 8 | 7.44% |
| | $\mathcal{P}2$ | $\mathcal{P}9$ | 10 | 11 | 400.83 | 9 | 9 | 5.80% |
| | $\mathcal{P}3$ | $\mathcal{P}11$ | 12 | 13 | 395.97 | 9 | 8 | 8.87% |
| | $\mathcal{P}4$ | $\mathcal{P}9$ | 10 | 10 | 400.01 | 9 | 9 | 7.00% |
| | $\mathcal{P}5$ | $\mathcal{P}11$ | 12 | 13 | 395.97 | 11 | 8 | 10.27% |

Table 3.8: Influence of product mix on multi-product necessity.

two-problem case. Thus, the more differences in the product portfolio to be sourced, the higher the benefits of solving the integrated problem. In general, the improvements not only depend on the number of products and shortage costs (see Section 3.5.3.3) but as well on the specific mix of product archetypes considered.

#### 3.5.3.5 Historical trends in disruption probability and impact shifts

So far, we have assumed all available 42 years of water levels to account for 42 scenarios that represented the uncertainty space of future disruption probability and impact. However, through global warming, droughts and high-water level events might have increased in likelihood (Middelkoop et al. 2001). To understand potential historical shifts, we split the available historical data along the timeline in four decades, assuming that each decade represents the full uncertainty space. Figure 3.3 visualizes the results for the resilience costs, the share of multi-sourcing, the corresponding investments in additional inventory capacity at both echelons, and the share of sourcing from the global supplier. We obtain all results solving the integrated model for products $\mathcal{P}1 - \mathcal{P}16$.

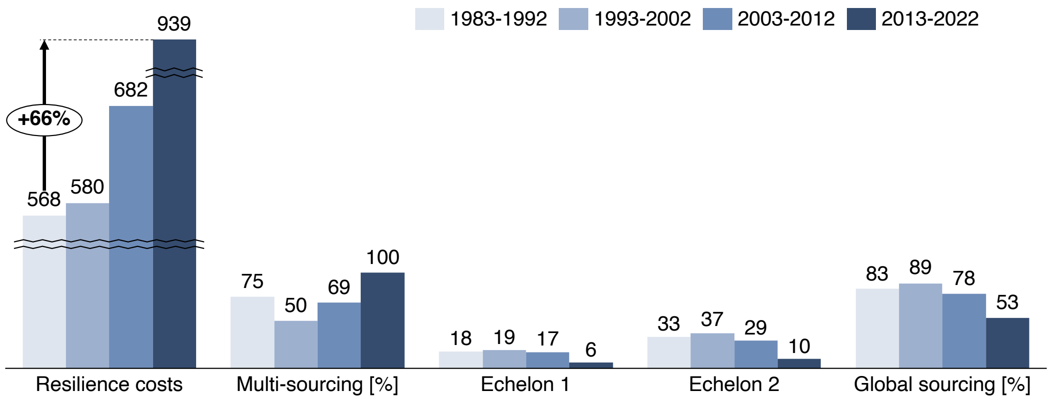


Figure 3.3: The effects of changes in historical disruption probability and impacts.

Overall, the results differ significantly across the different decades. In recent decades, an increase in water-level driven disruption impacts and probability are observed leading to an increase in resilience costs. As shown, the optimal resilience costs for the years 2013-2022 are 66% higher than the resilience costs between 1983-1992. In addition, across all products a multi-sourcing strategy is cost-optimal for the most recent time periods while only for 50% of the products multi-sourcing was cost-efficient from 1993-2002. In comparison, average inventory investments across the first and second echelon of inventory holding are rather stable. For a decision maker, these results highlight one of the distinct challenges in increasing SCR when trends in historical data can be observed. Thus, to increase SCR in the future, assessments of the future probability and impact developments are needed. For inland waterway transport, our results indicate an increased competitiveness of resilience strategies in the future.

### 3.5.4 Managerial insights

To summarize, the following managerial insights are drawn:

- Product characteristics play an important role in the optimal set of resilience strategies. Thus, practitioners need to understand their existing product portfolio as basis for a selection. For highly specific products, even if available, multi-sourcing might not be cost-competitive but rather investments in additional inventory capacity while for other product characteristics holding inventory is not cost-competitive.
- In order to protect against inbound product shortages, obtaining a multi-product view is beneficial and leads to a change in the optimal resilience mix. The need increases with the number of products, a decrease in shortage costs, and high differences in product archetypes within the product mix to be sourced. For homogenous product portfolios or in specific industries with comparably high shortage costs, a single-product view might not lead to substantially different results and be sufficient.
- Our results support that the proclaimed climate change-driven trend in an increase in higher winter-discharge and lower summer-discharge for the Rhine River does not only result in higher resilience costs but as well a shift in strategic resilience strategies. For example, it would have been cost-optimal to multi-source all products independent of their characteristics for the last 10 years while 30 years ago only very specific products would have been multi-sourced. This highlights the need for practitioners to not only think about historical disruption occurrence but as well on drivers that might influence their future occurrence when designing resilient SCND today.

## 3.6 Conclusion and outlook

We have addressed disruption uncertainty in the multi-product two-echelon transportation problem within a two-stage decision process. Through a case study from the chemical industry, we have shown how various product characteristics affect the cost-optimal mix of resilience strategies on strategic and tactical level. Considering multiple products in network design can influence both the total expected cost as well as the cost-optimal mix of resilience strategies. Particularly considering multiple products with high differences in product characteristics increases the observed benefits of multi-product resilient network design compared to single-product solutions. In addition, we have shown that likely through climate change, more resilience investments are needed in the future to protect networks that rely on inland waterway transportation.

Although we have highlighted the benefits of our model, our study is not without limitations. While we have shown that the solution time of a commercial solver can be significantly reduced through the additional use of valid inequalities and a warm-start solution, multi-product resilient network design problems remain computationally challenging to solve. Thus, alternative solution procedures should be elaborated. We studied a supply chain with a single demand destination. While we considered multiple products that are needed for the production of a single finished good, there might be further interrelationships between the different finished goods that might be relevant. Besides, transshipment between a larger number of inventory storage areas could be evaluated as an alternative strategy as well. Thus, the proposed model can set the stage for future multi-product models that more accurately reflect the practical, relevant settings in resilient SCND to increase the adaptability in practice.

## Acknowledgments

We thank the Federal Institute of Hydrology (BfG) for providing the historical data that supported the analysis.

# Contribution 4 - A seven-step supply chain resilience framework for mitigating waterborne disruptions in transportation network design

# 4 A seven-step supply chain resilience framework for mitigating waterborne disruptions in transportation network design

Daniel Müllerklein

**Abstract** Ocean shipping is integral to today's global and interconnected supply chain networks. Due to its economic and environmental advantages, its importance will even increase in the upcoming years. For many ports worldwide, waterway transport forms a crucial part of the connection from the port to the hinterland. However, they are prone to water level-driven disruptions that reduce shipment capacities, which shipment carriers cover through water-level surcharges to be paid by their customers. In extreme water situations, transportation is even forced to a standstill, leading to significant cost increases for shipment customers or even product shortages during transportation stops if no transportation alternative can be identified. Through climate change, both the impact and frequency of waterborne disruptions might increase in the future.

To overcome these challenges in waterway transportation, we propose a seven-step framework enabling decision makers to increase their supply chain resilience. This framework covers all end-to-end planning steps from definition of resilience objective to decision support tools and a performance monitoring. Through various examples and visualization of historical disruption data, we further increase the transparency on planning challenges for resilient transportation network design under waterborne transportation disruptions that have been overlooked in the literature so far.

## 4.1 Introduction

More than 75% of today's worldwide global trade volumes are shipped through ocean freight, and as such, ocean shipping has played a crucial role in the ever-increasing globalization of worldwide supply chains. In order to be imported or exported through maritime transport, products need to be made available at seaports from where products are either shipped to or received from the mainland, often referenced as the hinterland. In general, various transportation modes are available for the transshipment of maritime cargo to or from locations inside the country. For specific industries and seaports, inland shipping plays a critical role in the connection to the mainland. These critical waterways can be found worldwide: 60% of all grain exported from the United States is shipped on the Mississippi River through the Port of New Orleans and the Port of South Louisiana (Steinbach and Zhuang 2023). The Panama canal is of even higher importance for global trade through which more than 70% of all products to and from the United States surpass (LaRocco 2023). In Germany, the Rhine River transports 11% of all chemicals used by the German industry and 30% of coal, crude oil, and natural gas (Ademmer et al. 2020). As these examples show, the availability of cost-efficient waterway transports has enabled the growth and establishment of specific industries within the different regions. Until today, around 20% of all worldwide chemical industries have manufacturing facilities along the Rhine River. In the near future, the importance of waterway transport is even expected to increase due to the environmental and economical benefits compared to rail and road transport (Wiegmans and Konings 2017).

In parallel to this increasing trend of global waterway transports, recent years have also shown how vulnerable worldwide waterways have become to waterborne disruptions triggered by droughts and floods that force transportation carriers to either reduce the shipment load or stop any transportation at all. As water levels fall, the loading capacity of ships needs to be decreased to reduce the ship draft and avoid getting grounded. Thus, the lower the water level falls below critical ratios, the higher the lost capacities, as vessels must reduce their load to reduce the ship draft. With further decreasing water levels, this reaches the point where shipments are economically or practically not feasible anymore as the operating costs (which remain nearly the same) need to be shared among less transportation cargo. In addition, shipment carriers lose revenue as fewer products can be transported. To cover these additional costs, shippers charge contractually agreed low water surcharges depending on the water levels at the reference gauge. For many significant waterways, these contractually defined surcharges mark the industry standard that every shipment customer must adhere to.

Due to their regional importance for the transportation infrastructure, water level disruptions, i.e., significant high or low waters, can significantly affect global trade and regional economies. In recent years, a number of major waterways worldwide have been affected. For example, 2018 an exceptionally dry summer resulted in low water levels at the Rhine River that affected and even stopped cargo transport on the river for multiple weeks and months. While some freight can be re-routed at higher costs, for some heavy and oversized freight, waterway transport marks the only option. To assess the economic implications of the 2018 drought, Ademmer et al. (2020) estimated that a whole month of low water level of the Rhine River reduces industrial production in Germany by about 1%. Specifically, the drought led in parts to production stops for some of the chemical companies along the Rhine River as necessary raw materials could not be received anymore despite a significant rise in transportation costs due to the low water surcharges. As a result, selling costs for the chemical company BASF increased by 99mn EUR. In 2022, the Mississippi River experienced a historic drought between September and December, with the lowest water levels observed in October. Despite a significant rise of transportation costs up to 400%, Steinbach and Zhuang (2023) estimated that the drought resulted in a 3.9% reduction in agricultural exports and an agricultural trade loss of 563.9mn USD. Similarly, droughts in the Panama Canal have resulted in restrictions on the number and type of vessels that can travel the canal. As a result, low water level surcharges of up to 500 USD per TEU have been introduced. Assuming typical disruption-free container rates of 2,000 USD per TEU from Asia to US East Coast per container, this represents a 25% cost increase. However, delays in shipments due to capacity restrictions on the canal might still occur. Due to climate change, waterborne disruptions might even increase in frequency and impact as expected by many experts (van Meijeren and Groen 2010) while they already have significantly affected individual companies, regions, and even global trade flows.

To counteract disruptions in supply chain network design, supply chain resilience frameworks and decision models have been established that focus on proactive and reactive resilience strategies. Still, most research has focused on stylized problem settings that have emerged from typical facility location problems. However, waterborne disruptions differ in their distinct characteristics from most resilient network design problems as they (1) affect transportation modes that connect facilities instead of the facilities themselves, (2) are recurring as they typically occur with seasonal effects on an annual level, and (3) can occur with both high and low impact in terms of transportation surcharges and duration. As inland waterways are expected to increase in importance due to their economic and environmental advantages compared to alternative transportation modes, affected decision makers worldwide need to be made aware of the specific planning challenges and potential solutions to increase their supply chain resilience under waterborne disruptions.

The contribution of this paper is three-fold.

- First, to provide a seven-step framework that guides decision makers facing waterborne disruptions on holistically addressing the planning challenge to increase their supply chain resilience. This framework guides each decision maker from creating an understanding of disruption impacts to measuring the success of resilience strategies and actions.
- Second, to detail the different problem characteristics of waterborne disruptions and highlight specifics that differ from typical problem settings found in resilient supply chain. Improving the understanding of the problem specifics and trade-offs for decision makers forms the basis to promote necessary future research in the area of resilient supply chain design with a focus on waterborne disruptions.
- Third, to provide an overview of recent literature that addresses the typical challenges from various research domains in resilient transportation systems, waterborne shipping, and decision support models in resilient network design.

This paper is structured as follows. Section 4.2 reviews the relevant literature, while Section 4.3 describes the problem setting in detail. Then, Section 4.4 presents the proposed resilience framework for waterborne disruptions. Finally, Section 4.5 summarizes and outlines future research areas.

## 4.2 Literature review

Section 4.2.1 introduces general literature on resilient transportation systems, while Section 4.2.2 focuses on recent research dealing with waterborne shipping disruptions. Then, Section 4.2.3, presents recent decision models to increase supply chain resilience. Finally, Section 4.2.4 summarizes open research questions.

### 4.2.1 Resilient transportation systems

Transportation systems are part of the critical infrastructure that provides essential commodities and services. Similar to supply chains, they have become more and more complex and interdependent, making them prone to disruptions and increasing the time to recover following a disruption. As a result, research on resilient transportation systems is becoming increasingly popular (Mattsson and Jenelius 2015, Zhou et al. 2019). We outline recent work on resilient transportation systems and design in the following with a focus on the transportation modes considered.

For a rail-based container network in the United States, Miller-Hooks et al. (2012) determined the optimal set of mitigation and recovery actions to achieve service constraints of a transportation system given a pre-defined budget through a two-stage stochastic program. While a combination of mitigation and recovery investments has proven optimal, if the budget is increasingly limited, greater benefits were observed when allocating the remaining budget to mitigation actions. Omer et al. (2012) studied the resilience of maritime transportation networks and the impacts of disruptions on port capacities by identifying three different resilience metrics. Azadeh et al. (2013) analyzed a three-echelon supply chain in which disruptions may occur within the transportation links. Using a simulation and different disruption scenarios, they identified the preferred strategy out of the resilience factors of visibility, velocity, redundancy, and flexibility. To increase the overall system understanding, Chen et al. (2017) studied the port-hinterland container transportation network under disruption uncertainty. Due to the specific geographical transportation mode availability of the Port of Gothenburg, which only offers rail and road transport, they focused on the port-rail network and separate resilience actions by the port and rail operators. Motivated by the diverging operator interests, Chen et al. (2018) investigated the strategic resilience investments in a port-hinterland container transportation network. Colon et al. (2020) simulated the impacts of supply and transportation disruptions to assess the criticality of Tanzanian roads, which are vulnerable to floods. Notably, they identified that economic losses increase non-linear with the disruption duration and that different transportation links are more important than others. Karbassi Yazdi et al. (2022) examined critical success factors for the transportation service provider selection in resilient network design using a Delphi approach and multiple-criteria decision analysis. Given uncertain environments and transportation disruptions, they proposed an effective method for determining critical success factors in selecting transportation service providers. Due to its vulnerability and importance to the economy of China, Wang and Yuen (2022) conducted a simulation study on the Yangtze Estuary Deepwater Channel to develop a resilience assessment indicator tested for different accident scenarios. Friedhoff et al. (2023) assessed the resilience of the Rhine-Alpine Corridor, as the central waterway transport artery of continental Europe, and proposed innovative vessel concepts as well as modular mobile terminals to tackle barge congestion and seaports and the effects of extreme low water levels on the Rhine River.

### 4.2.2 Waterborne shipping and port disruptions

We summarize recent work that focused on the uncertainty of disruptions and their impacts on waterway transport through events reducing the port capacity or directly affecting the efficiency of waterway transport worldwide. Folga et al. (2009) presented a systems-level analysis of the economic effects of waterway disruptions, including interdependency considerations between various transportation alternatives and cascading impacts. They applied their methodology to a specific waterway network in the United States. Baroud et al. (2014) quantified the vulnerability and recoverability of inland waterways to a single resilience measure. They applied their proposed measures to the Mississippi River Navigation system to identify which transportation links to focus on in vulnerability reduction policies or recovery actions. Pant et al. (2015) studied the multi-industry economic impact of inland waterway port disruptions using a case study for the Mississippi River transportation system using a multi-regional interdependency model. Oztanriseven and Nachtmann (2016) predicted the economic losses for various waterborne disruption scenarios. They distinguished between short, medium, and long-term disruptions, and found that the disruption duration has a direct effect on the ideal reaction to decision-makers. Jonkeren and Rietveld (2016) identified causes and effects of waterborne disruptions in European infrastructure and assessed the private-public roles in protecting them. Similarly, Darayi et al. (2019) studied the effects of waterborne shipment disruptions on a multi-modal freight transportation network with multiple commodities using a case study from the Mississippi River, highlighting the economic benefits of operational rerouting through alternative transportation modes. To understand and verify appropriate disruption assumptions in existing models, Verschuur et al. (2020) evaluated 141 incidences of storm-lead port disruptions and closures across 27 disasters and found that the disruption duration can vary significantly while in all incidences of storm disruptions, multiple ports are affected in parallel while existing literature predominantly focused on single port disruptions in isolation. Nur et al. (2020) were the first to simultaneously optimize the shallow draft inland waterway port decisions and supply chain network design considering fluctuating water levels. Considering multiple commodities and their characteristics, the number of additional barges and towboats could be increased significantly for a test region in the United States. Monios and Wilmsmeier (2020) discussed the disconnection between the latest climate science along with the actions and visions of actors in the maritime shipping industry. Despite potential further mitigation actions against climate change, they discussed the need for radical changes in supply chains and adaptations to the maritime shipping industry that are needed. Vinke et al. (2022) studied the behaviors during the drought observed in the Rhine River in 2018 and found through a novel method that the overall negative effects can be reduced by incorporating changes to the fleet composition of transportation carriers. As a result of the COVID-19 pandemic and the various pandemic-driven maritime disruptions, Liu et al. (2023) defined customer-oriented maritime supply chain resilience and identified the key enablers to achieve this for freight service providers during a pandemic. Recently, Nayak et al. (2024) studied waterborne disruptions for a hinterland multi-modal transportation and presented a mathematical model formulation, including a case for waterborne disruptions at the Brahmaputra River.

### 4.2.3 Decision support models to increase supply chain resilience

In recent years, research has increasingly focused on quantitative decision models that support the decisions on the optimal mix of resilience strategies for a supply chain network under disruption uncertainty. We distinguish between resilient network design models that aim to improve the network characteristics and design with the anticipation of resulting consequences on an operational level and purely operational decision support models that aim to take the optimal repair actions once a disruption occurs.

Resilient supply chain network design models have developed from primary facility locations to more integrated decision support models. We recommend the recent reviews from Snyder et al. (2016) and Aldrighetti et al. (2021). Beyond pure facility location models, Nooraie and Parast (2016) were the first to propose an end-to-end decision model for resilient supply chain network design from suppliers to customers and multiple time periods. Azad et al. (2016) used a network optimization model to study the cost-effectiveness of installing alternative links in railroad networks under random disruption scenarios, analyzing both - the efficiency of proactive and reactive resilience strategies. For an inbound logistic network model, Namdar et al. (2018) analyzed the benefits of a multiple sourcing strategies under inbound supply disruptions risks. As an extension of previous supplier selection problems, Hosseini et al. (2019b) incorporated decisions on additional manufacturing capacities and geographical separation of suppliers, considering regional disruption scenarios. Goldbeck et al. (2020) presented a multi-stage stochastic programming approach for the joint optimization of investments in capacity and repair capability of production and logistics systems. In addition, they considered both disruptions to transportation links and production facilities in parallel. In order to understand the interactions of different disruption sources, Alikhani et al. (2023) used a multi-methodological approach to quantify the synergistic effects of the resilience strategies in scope and discuss the best-fit of candidate strategies on different disruption characteristics, such as cyberattacks and natural disasters. Recently, Aldrighetti et al. (2023) found that a good trade-off between resilience and investment costs can be achieved with marginal investments focusing on agile and re-configurable supply chains. In addition, they presented a case study focusing on the COVID-19 pandemic.

Besides these end-to-end models that aim to incorporate resilient network design decisions from the strategic to the operational level, a stream of literature further focuses on purely operational decision support following a disruption. For example, Gedik et al. (2014) estimated the consequences of disruptions on a rail transportation network by deciding on the optimal rescheduling after the disruption. Besides the rescheduling, their min-max model can be used to determine the critical elements within the rail network. Ivanov et al. (2016) identified the optimal re-routing of material flows in a multi-stage supply chain after disruptions with different impacts at different times of the planning horizon. In addition, they evaluated the effects of different preparation scenarios on the optimal operational mix of recovery strategies. Birge et al. (2023) studied the systemic implications of shocks to a supply chain network when each firm tries to optimally mitigate potential losses, including re-routing of undelivered orders to alternative buyers. They found that a unique equilibrium exists when buyers and suppliers agree on an efficient strategy of re-routing demands and supplies within the network.

### 4.2.4 Discussion of research opportunities

To date, more research focuses on decision support systems for resilient network design with still fundamental issues in probability estimation (Aldrighetti et al. 2021). Compared to most disruption uncertainty sources, however, historical data on water levels are generally available and, thus, require an increase in data-driven resilient network design approaches to be tested. In addition, while most research has focused on low-probability but high-impact events in resilient network design, more research is needed to understand the effects of disruptions that, as typical waterborne disruptions, share both characteristics: Recurring lower-impact disruptions at a high probability and high-impact but low probability major disruptions, each affecting the same supply chain entities and to be counteracted with the same resilience strategies.

## 4.3 Planning challenges in transportation network design with waterborne disruptions

We want to outline the problem characteristics of such a network in which waterborne disruptions can affect single or multiple arcs in parallel and indicate the type of decision problems and trade-offs a decision maker faces. Section 4.3.1 outlines the typical network characteristics of the problems in scope. Then, Section 4.3.2 characterizes the disruption probabilities and impacts typical for waterborne disruptions. As a topic often overlooked in resilient supply chain design, Section 4.3.3 outlines the possibilities of disruption prediction through an example of the Rhine River. Finally, Section 4.3.4 summarizes the typical trade-offs a decision maker would face depending on the problem specifics.

### 4.3.1 Network considerations based on the importance of waterway transportation arcs

Let us consider a transportation network that sources a variety of products (i.e., raw materials) from sources (suppliers) to transport them through arcs (transportation modes) to a sink (production location). Such a transportation network, as visualized in Figure 4.1, relates to the typical design of an inbound supply chain network with a decision maker who wants to secure raw materials to produce a number of finished products. The different arcs contain five different values of relevance: (1) transportation time, (2) transportation costs, (3) transportation capacity, (4) transportation emissions, (5) and the proneness to disruptions. These characteristics of the transportation arcs are prone to waterborne disruptions, affecting single or multiple transportation arcs in parallel. The uncertain changes of a transportation arc's characteristic values are determining the trade-offs a decision maker faces as transportation arcs that might be cost-optimal in the steady-state might be affected.

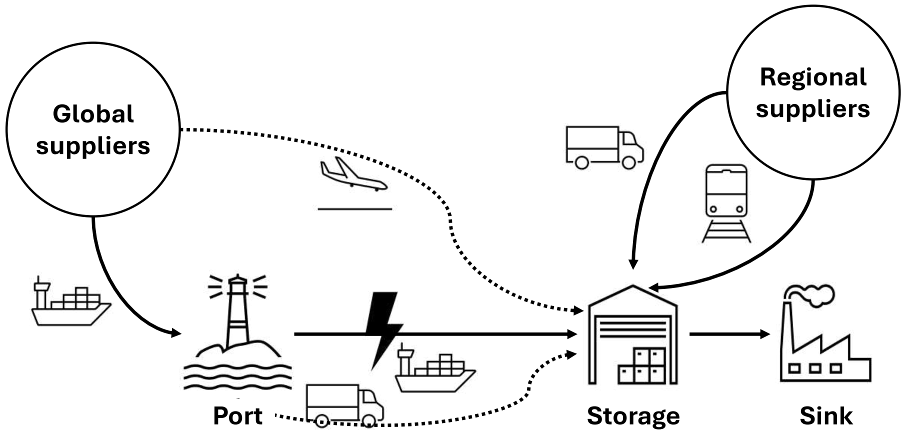


Figure 4.1: Stylized network structure from multiple suppliers to production facility as sink.

First, shifting to an alternative transportation mode might significantly increase the overall transportation time. This structure relates to network design problems where alternative shipping routes are available in case of disturbances to the preferred shipment route but at significantly longer traveling times (and costs). Recent examples include the water level-driven disturbances of the Panama canal, where alternative available routes might require an additional 13 to 25 days of transportation times respectively (Dierker et al. 2024). However, despite higher transportation costs, these lead time increases will, on the tactical level, lead to an increase in inventory safety stock for customers and, in the short-term, lead to stock-outs through an unforeseen longer transportation time. The recent example of re-routing from the Suez Canal due to the armed conflict in the Red Sea resulted in a two-week suspension of the Tesla production in Germany due to a lack of components that were re-routed around the southern tip of Africa (Reuters 2024).

Second, waterborne disruptions can lead to surcharges that decision makers must face. These contractual obligations result in a rise in transportation costs compared to the disruption-free state. Thus, these surcharges directly influence the cost-competitiveness of the transportation mode itself or, ultimately, the sourcing decision taken as the respective transportation arc might be the only relevant link from one of the sources to the sink.

Third, the overall capacity and potential waterborne disruption-driven capacity reduction are relevant. For a major transportation arc with high capacity, no alternative might be available in the short term to cover the lost capacities in case of disruption. In contrast, for a minor arc, sufficient infrastructure might generally be available to cover the lost capacities. Thus, the dependence of the specific network in scope on specific arcs is relevant to evaluating potential proactive and reactive resilience strategies.

Fourth, shifting to alternative transportation modes might significantly affect the environmental impact of the transport network as rail, road, and air transport result in an increase in harmful environmental emissions. With net-zero targets becoming increasingly relevant, decision-makers will be forced to consider this environmental trade-offs in case alternative transportation modes result in a significant increase in travel distance (for the same transportation mode) or transportation mode shifts.

Fifth, the disruption proneness, i.e, probability and impact of disruptions, is in addition a relevant value and characteristic of each arc. The proneness will be discussed in Section 4.3.2 in greater detail.

### 4.3.2 Impact and probability of waterborne disruptions

Though waterborne disruptions are (of course) distinct for the specific transportation situation, there are still common characteristics that differentiate them from traditional planning problems in existing resilient network design problems. While most research has focused on low-probability and high-impact disruption events (or vice-versa), waterborne disruptions typically occur throughout a planning horizon with varying duration and impact. Figure 4.2 highlights the situation at the Rhine River for 2015-2022.

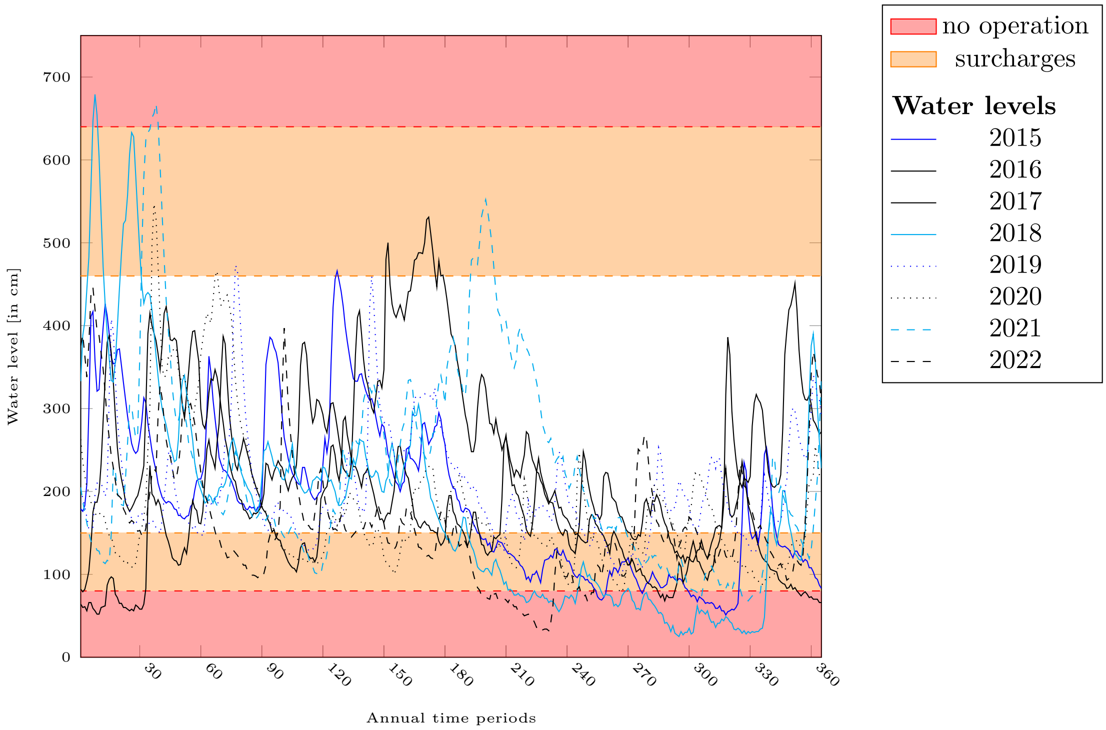


Figure 4.2: Water levels including surcharge levels for Rhine River.

In Figure 4.2, the red area highlights historical water levels that led to full transportation stops along the river. In contrast, orange areas mark water levels that result in surcharges to be paid at increasing levels. Across the eight years, transportation stops of significant length occurred in four out of the eight years; thus, considering an annual planning horizon, a waterborne disruption with high impact can be expected in roughly every second year for an annual planning horizon or with a probability of roughly 50%. However, the orange area of waterborne surcharges is nearly reached every year, often even multiple times. Thus, it becomes clear that waterborne disruptions contain typical disruption characteristics of both low-impact disruptions at high-probability and high-impact disruptions at low-probability.

To highlight the cost implications despite the worst-case of transportation stops, Table 4.1 quantifies the typical dependence between water levels and transportation costs per container for a specific bottleneck of the Rhine River, including surcharges depending on the water level. Once water levels fall below 150cm or rise above 640cm, overall transportation costs rise by approximately 80%. Starting from water levels below 150cm, transportation costs then rise exponentially to allow economically feasible transportation operations until a water level of 80cm where most commercial shipment transportation service providers discontinue their operations.

| Water level [cm] | $< 80$ | $[80, 90)$ | $[90, 100)$ | $[100, 110)$ | $[110, 130)$ | $[130, 150)$ | $[150, 460)$ | $[460, 640)$ | $\geq 640$ |
|---|---|---|---|---|---|---|---|---|---|
| Costs TEU [EUR] | - | 415 | 340 | 295 | 250 | 205 | 115 | 205 | - |

Table 4.1: Transportation costs per container transported depending on water level.

### 4.3.3 Predicting waterborne disruptions in the short-term

Similar to other weather-related events, the majority of water level-driven disruptions can be predicted in the short-term, posing a significant difference in planning problems to many of the established problems found in the literature. Specifically, forecasts on future water level developments can often be found publicly available or at least made available by third parties at a fee. For example, future water level forecasts are made available with a 14-day horizon for the Rhine River, including a probability estimation and confidence level for water levels falling below critical ratios that drive the contractually aligned surcharges. An exemplary forecast can be found in Figure 4.3 that represents the historical forecast on the 25th of September 2023 for the forward-looking 14 days. The upper 90% line indicates that with 90% certainty, the water level at the corresponding future data will be below the respective water level. Overall, a decision maker is able to identify a current fall in water levels expected to peak on the 6th of October with an indicated potential rise in water levels. As the expected future water level would result in surcharges, the decision-maker could now evaluate potential options to postpone or expedite respective shipments to avoid or at least reduce corresponding surcharges. On the other end, even the low-likelihood scenario (10%) still predicts water levels that at least ensure that transportation can continue at surcharges.

As can be seen, the forecast, obtained by an ensemble method of a number of available additional data such as predicted rain, historical rainfalls, snow levels, etc., is characterized by an increasing spread covering identical probabilities for the future. However, the prediction horizon of 14 days somehow provides a general limitation of water level predictions as this marks the general limit of weather and rainfall prediction reliability. In the context of a network design problem for a global supply chain, however, global shipment decisions need to be made far in advance due to a typical lead time of global suppliers that far exceeds 14 days. Thus, these forecasts are predominantly interesting for re-routing decisions on the operational level.

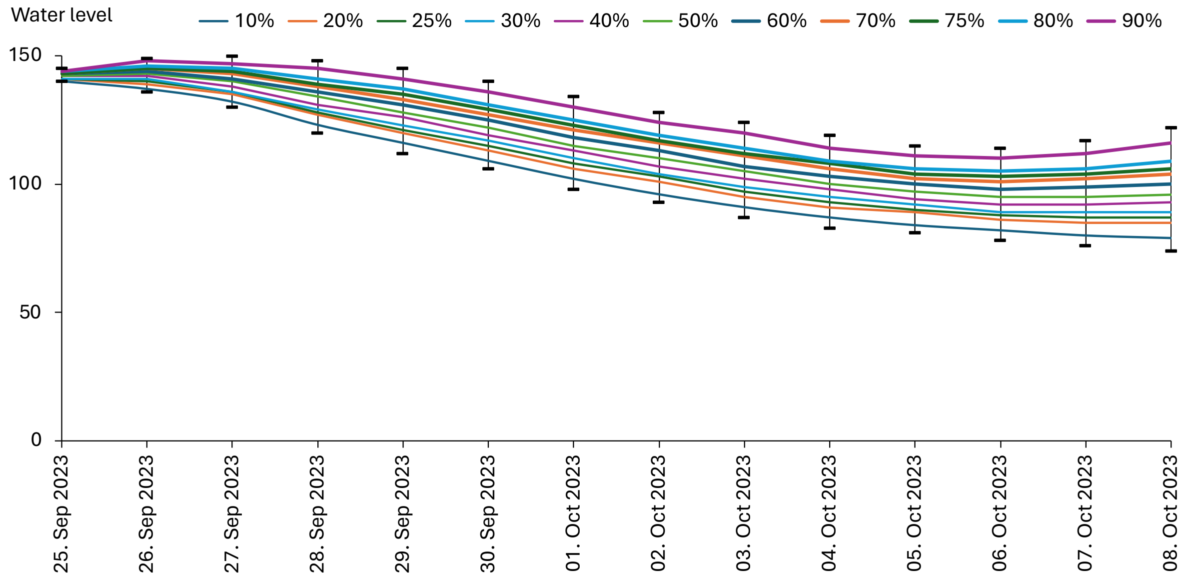


Figure 4.3: 14-day water level probability predictions for Rhine River.

### 4.3.4 Clustering the decision focus based on problem characteristics

Though the characteristics of the waterborne disruptions are (of course) specific to the respective network design, there are distinct planning challenges as network arcs are affected in contrast to the more common node (facility) disruptions in literature. To summarize, based on the arc criticality within the network and the potential impacts of waterborne disruptions, we differentiate three different types of decision focus that ultimately translate to the distinct objectives in resilient network design. The relationship is illustrated in Figure 4.4.

In case the arc is not critical, i.e., a large number of alternative transportation modes are available on the operational level, the tendency of the decision focus is purely an efficient handling of the disruptions that occur on a regular level. Even though disruptions might affect some of the arcs with major impact, e.g., high surcharges to full transportation stops, enough alternative arcs are available so that the decision comes to identifying the best alternative arc for a potentially large amount of products in a short period of time.

With increased arc criticality and the potential impacts of disruptions, the decision focus shifts towards proactive risk management and resilient network design. While some alternatives might be available on the operational level, these are either relatively unfavorable compared to the main transportation arc or lack the spare capacities to cover for the lost transport capacities on the operational level. Thus, decision makers must shift towards proactive resilience strategies such as multi-sourcing or inventory increase.

For one-off and rare black swan events (Taleb 2007) that affect major transportation arcs without real operational alternatives, the decision focus shifts to increasing the robustness of a supply chain. In the supply chain context, black swan events relate to unpredictable events that are of high-impact to a large share of a supply chain and thus have dramatic impacts. Recent examples include the six-day Suez Canal blockage that forced a large share of global transport to a standstill and the

COVID-19 pandemic that forced shutdowns to major ports worldwide.

Within our framework (see Section 4.4), we focus on the proactive risk-management areas as they mark the critical decision area of recurring waterborne disruptions that affect networks on a recurring level. Considering their impact requires a mix of proactive and reactive resilience strategies. However, understanding the potential effects of waterborne disruptions on one's own network designs is an essential first step.

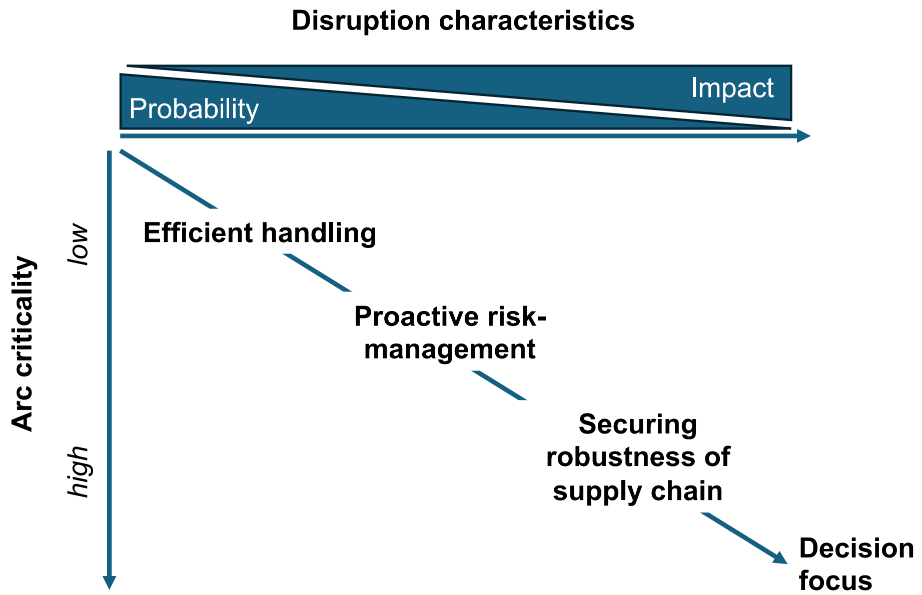


Figure 4.4: Shift of decision focus based on network and disruption characteristics.

## 4.4 Resilience framework for waterborne disruptions

Based on the literature review, a number of practical waterborne disruption examples studied, and discussions with practitioners, we present a supply chain resilience framework for the waterborne disruption management in transportation systems. We illustrate the overall framework in Figure 4.5 representing the seven steps for decision makers to take to increase their supply chain resilience under waterborne disruptions. The focus lies on decision makers that aim at securing their product supply, and thus, source multiple products from various sources whereas a large share of the products is transported through waterway transport. We detail all the steps in the following.

*Step I. Defining the objectives and planning horizon.* At the initial stage, decision makers must first be aware of their detailed objectives and planning horizons that they want to optimize for within the resilient network design. While most resilient network design models assume neutral decision makers and aim at optimizing the expected average total costs, decision makers may tend to be risk averse when facing rare disruptions (Snyder et al. 2016) or rather focus beyond pure economic goals (Aldrighetti et al. 2021). Thus, aligning and understanding the objectives to optimize for marks a first and important step. Beyond being clear on the objective to optimize for, a clear objective further guides the methodologies to be taken later when building decision support

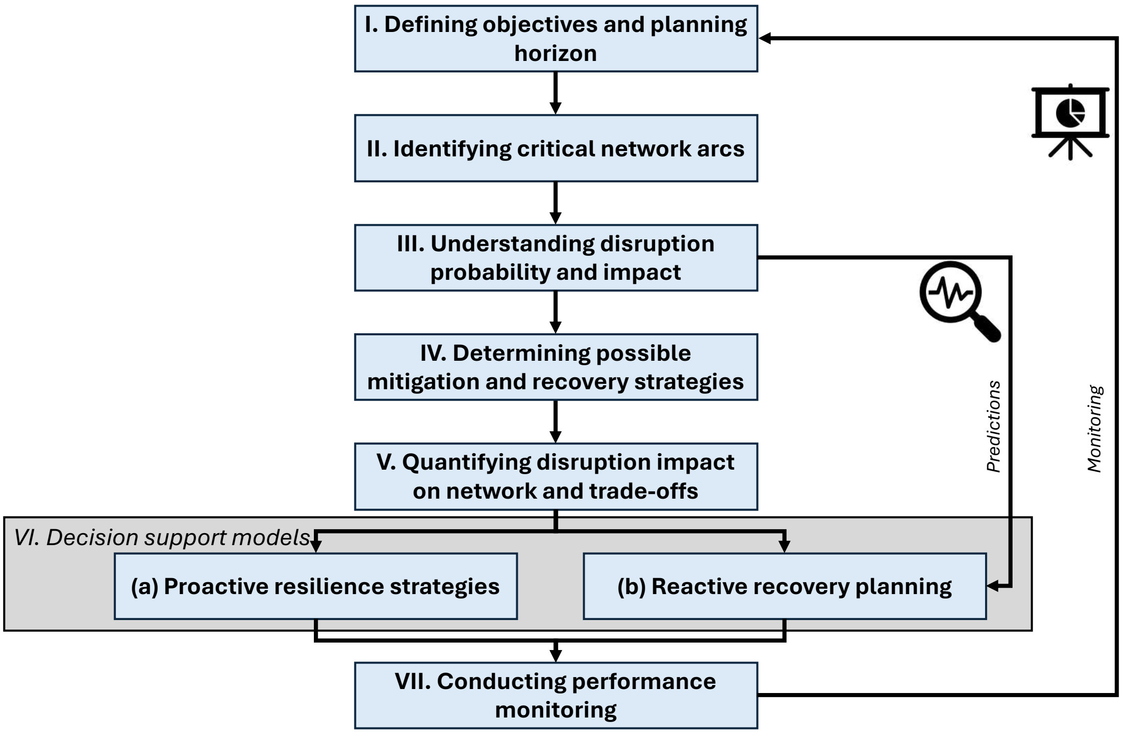


Figure 4.5: Seven-step framework for resilience under waterborne transportation disruptions

models. Typically, the economic objectives range from an expected average cost optimization (neutral decision maker) to a robust optimization in which the costs of a potential worst-case scenario are minimized. Generally, we recommend differentiating economic objectives based on the product's cost structure to be transported depending on the share of transportation cost on total sourcing costs. For example, a low-value commodity at high weight typically has a high share of transportation costs on total sourcing costs. Thus, minor surcharges can already have high economic implications regarding the overall margin of the finished good that can be achieved (for an inbound supply chain). For a high-value, highly complex product, on the other end, even an increase in transportation costs at factor four would not matter that much if transportation costs account for less than 1% of the overall sourcing costs. Thus, it would be far more important to secure the raw material supply in worst-case scenarios of transportation stops rather than total expected costs, given the limited influence of the surcharges themselves. Technically, the objective must be described mathematically to allow its later optimization in decision support models.

*Step II. Identifying critical network arcs.* Next, once the objectives are clear, critical transportation links (arcs within the network) need to be identified to ideally reduce the analysis scope and complexity. The necessary identification can be done by expert judgment through supply chain planners or by modeling the network design and its quantitative analysis. While the latter might be significantly more complex and time-consuming, analyzing the given network structure as a whole helps to uncover so-far unknown disruption risks that might become of relevance in the future (Blackhurst et al. 2018). For a decision maker who needs to secure raw material supply, this often involves creating an understanding of the actual transportation arcs used in the first step. Depending on the Incoterms agreed with suppliers, the transparency on actual transportation modes and arcs, including the shipment origin, needs to be understood first. Only then can critical arcs be identified. Factors that drive the criticality include: The availability of alternative transportation modes, the overall economic relevance of the transportation mode in terms of capacity, the share of products sourced through the arc, and the cost differences to alternative transportation modes. Identifying and focusing on critical arcs further reduces the computational complexity of the necessary decision support tools as then a focus on the specific critical areas is sufficient.

*Step III. Understanding disruption probability and impact.* As highlighted, resilient network design still lacks data-driven approaches but often assumes known distributions (Aldrighetti et al. 2021). In practice, however, an accurate understanding of probability and risks directly influences the evaluated cost-competitiveness of resilience strategies and, thus, is of utmost importance. In contrast to many other disruptive events, such as facility disruption, sufficient historical data on water levels or port disruptions are generally available. Three different factors need to be understood. First, the duration of a disruption needs to be assessed. Regarding potential recovery actions and resulting cost implications, it marks a major difference whether a disruption lasts for a number of days or a number of weeks. Second, the impact needs to be understood, i.e., the potential low or high water situations and the resulting surcharges or transportation stops. In practice, throughout a disruption, different degrees of disruption impacts will be reached as surcharges will vary. For example, within a disruption that lasts a week, different water levels will be reached that may result in different surcharges throughout. Third, the probability is of relevance, i.e., how often did the respective events occurred in the past. Most likely, as waterborne disruptions are influenced by rainfall and other weather-related effects, seasonal characteristics might occur that are of relevance to be understood. Lastly, every historical waterway disruption that occurred is unique in disruption duration, impact, and even the fluctuations of disruption impacts throughout the disruption in itself. To handle this complexity in decision-making, it is recommended to identify stylized waterborne disruption types for each of the relevant waterway transport arc within the network, i.e., a "typical" low-impact versus a high-impact disruption, to assess the respective disruption probability characteristics individually and build richer decision models. This clustering could also be done by differentiating the potential impact a disruption would have on the decision maker or the potential cost-competitive disruption response in terms of mitigation and recovery actions. In addition, they can be enriched and merged with additional data sources, such as weather forecasts or climate prediction models. For the planning and decision support on the operational level, it might be of further relevance to test the historical quality of available historical disruption forecasts or even build and test one's own forecasting models to enrich the reactive and operational resilience decisions.

*Step IV. Determining possible mitigation and recovery strategies.* To increase the resilience of the transportation network against disruptions affecting its arcs, potential resilience strategies taken prior to (mitigation) and following (recovery) a disruption need to be identified. Particularly, they need to be assessed for a wide variety of products sourced as the availability or the consideration of respective strategies might depend on the product characteristics. After corresponding resilience strategies are identified, their costs and benefits are evaluated in the next step. At the same time, the corresponding decision models aim to identify the decisions that maximize the objective given the trade-offs identified. Typical resilience strategies include but are not limited to:

- Mitigation: Investments in inventory capacity, inventory holding, multi-sourcing from different suppliers, near-shoring, product standardization
- Recovery: Operational re-routing between transportation arcs, transshipments, product substitution, and re-scheduling of manufacturing schedules

*Step V. Quantifying disruption impact on network and trade-offs.* Based on appropriate knowledge of disruption probability and impact, it is crucial to understand the impacts of disruptions on the network and their cost parameters, including the potential costs and implications of alternative actions. Thus, it requires a deep understanding of proactive and reactive resilience decisions and their implications. In contrast to existing literature that often assumes green-field approaches in network design, adaptations to existing networks take a long implementation time and are often not in scope. Therefore, it makes sense to break the decision and trade-off discussions down into the evaluation of immediate actions and the evaluation of strategic decisions that are to be implemented on a longer horizon. For the proactive planning on strategic and tactical level, potential capacity adjustments and changes to the facilities within the network need to be assessed in terms of feasibility and their potential investment costs. These assessments require detailed planning and significant efforts, while a resilient network can only be one part of the reasoning and, thus, decision making. On the tactical level, holding additional inventory is the primary proactive resilience strategy. Here, inventory holding costs need to be properly assessed, including typical capital costs, handling costs within the warehouse, and further factors such as relevant depreciation risks. The different factors on the operational level are the most crucial and critical in terms of parameter assessment. Despite the standard transportation cost differences between the disrupted transportation mode and alternatives, it is of further interest to determine the extent of spare capacities available within the larger transportation infrastructure and network. Particularly due to market effects, there might be further increases in transportation costs on alternative transportation modes as spare capacities are not sufficient to cover even though they are not directly affected by disruptions. Lastly, potential lead times are a predominant driver of how fast a decision-maker can react on the operational recovery level and mainly determine whether or not, in the short-term, a stock-out can be prevented or not.

*Step VI. Building decision support models for proactive and reactive resilience strategies.* After obtaining all the data and planning parameters, decision support models can be built to support the decision-making process following the objectives identified in step I to guide decision makers along the trade-offs. The respective decision support models and methodologies will vary with the objective identified. Some of the open questions and trade-offs can only be addressed through a decision maker in combination with representatives from political interests, the transportation carriers, and even potential competitors as investments in the transportation infrastructure itself affects multiple stakeholders in parallel. Some of these questions include joint investment decisions to upgrade the transportation infrastructure and specifically the development of innovative vessels themselves (Friedhoff et al. 2023), which is only possible through economic collaborations across a number of stakeholders and the respective political investments. Through strategic decision support models, respective capacity and investment decisions can be taken while economic benefits are validated. For independent decision makers, decision support tools can guide the investments in inventory or alternative sourcing options (near-shoring) on the strategic and tactical level. On the operational level, building decision support tools is worthwhile that help decision makers react to disruptions in real-time. As a large share of waterborne disruption events forecasts are available, it will be particularly interesting to see how they can be embedded in real-time decision-making. Ideally, decision support tools are developed to guide decision makers towards early warning systems for waterborne disruptions with expected optimal re-routing options. As for a critical transportation mode, multiple products are typically affected in parallel, and decision support tools can further help to handle the short-term complexity that would be overwhelming. On a side note: For the shipment carriers, additional decision support tools could be evaluated on the operational level to more efficiently fulfill customer demands given the disruption-driven shortage in shipping capacities through an improved routing that considers and anticipates the limited load carriage as low water levels affect the various parts of a river differently.

*Step VII. Conducting constant performance monitoring.* The output of the decision support tools and the overall objectives and parameters need to be constantly reviewed to assess whether or not the overall objective is met. Otherwise, decision makers might face the risk of overreacting to either the occurrence or the non-occurrence of disruptions. For example, recent research found empirical evidence that decision makers do react to immediate events, increasing their inventories and operational flexibilities (Durach et al. 2022). Thus, a decision maker that seeks to optimize for total expected average costs might face the risk of increasing inventory further directly after a disruption, while there might be the desire to lower inventories to reduce capital costs in times of no disruptions. To counteract this, the decision maker needs to constantly measure the historical performance on a longer level to make sure that the decisions taken are still in line with the overall objective. In contrast to changing decisions directly after a disruption, on the other hand, the probability and impacts of disruptive events need to be constantly monitored as well. Likely through climate change, shifts in waterborne disruptions probability and impact might occur in the upcoming years, requiring a constant re-assessment of the optimal resilience mix to be taken.

## 4.5 Conclusion

Within this work, we have argued the importance of waterway transport disruptions for global supply chains. We highlighted the need to understand the various problem characteristics for developing supply chains resilient to waterborne disruptions within their network design. These disruptions affect multiple products at once through significant cost increases, longer lead times, and / or structural capacity issues for transportation volumes. Notably, we have highlighted the consequences that recurring disruptions due to low water levels can have, which are further expected to increase in severity due to global warming. To increase the resilience of supply chains facing these planning challenges, we have proposed an end-to-end seven-step resilience framework that helps decision makers guide through the various levels of planning problems and potential solutions that arise.

This work is not without limitations. First, while we proposed an end-to-end decision framework for waterborne disruptions based on numerous discussions with practitioners and a literature review, it still needs to be applied through a case study to highlight the overall benefits. Second, many of the insights are detailed through data analysis of the Rhine River in Europe. Lastly, more research in resilient network design needs to focus on real-world cases in a data-driven way to increase not only the understanding of resilience strategies but also prove their cost-competitiveness in practical applications.

## Acknowledgments

We thank the Federal Institute of Hydrology (BfG) for providing the historical water level data that supported the analysis.

# Bibliography


Ademmer, M., Jannsen, N., Mösle, S., 2020. Extreme weather events and economic activity: The case of low water levels on the rhine river. Kiel Working Paper 2155, Kiel.

Adulyasak, Y., Cordeau, J.-F., Jans, R., 2015. Benders decomposition for production routing under demand uncertainty. Operations Research 63 (4), 851–867.

Aldrighetti, R., Battini, D., Ivanov, D., 2023. Efficient resilience portfolio design in the supply chain with consideration of preparedness and recovery investments. Omega 117, 102841.

Aldrighetti, R., Battini, D., Ivanov, D., Zennaro, I., 2021. Costs of resilience and disruptions in supply chain network design models: A review and future research directions. International Journal of Production Economics 235, 108103.

Alibrahim, H., Ludwig, S. A., 2021. Hyperparameter optimization: Comparing genetic algorithm against grid search and bayesian optimization. In: 2021 IEEE Congress on Evolutionary Computation (CEC).

Alikhani, R., Ranjbar, A., Jamali, A., Torabi, S. A., Zobel, C. W., 2023. Towards increasing synergistic effects of resilience strategies in supply chain network design. Omega 116, 102819.

Alvarez, A., Cordeau, J.-F., Jans, R., Munari, P., Morabito, R., 2021. Inventory routing under stochastic supply and demand. Omega 102, 102304.

Azad, N., Hassini, E., 2019. A Benders decomposition method for designing reliable supply chain networks accounting for multimitigation strategies and demand losses. Transportation Science 53 (5), 1287–1312.

Azad, N., Hassini, E., Verma, M., 2016. Disruption risk management in railroad networks: An optimization-based methodology and a case study. Transportation Research Part B: Methodological 85, 70–88.

Azadeh, A., Atrchin, N., Salehi, V., Shojaei, H., 2013. Modelling and improvement of supply chain with imprecise transportation delays and resilience factors. International Journal of Logistics Research and Applications 17 (4), 269–282.

Baghalian, A., Rezapour, S., Farahani, R. Z., 2013. Robust supply chain network design with service level against disruptions and demand uncertainties: A real-life case. European Journal of Operational Research 227 (1), 199–215.

Ban, G.-Y., Rudin, C., 2019. The big data newsvendor: Practical insights from machine learning. Operations Research 67 (1), 90–108.

Baroud, H., Barker, K., Ramirez-Marquez, J. E., Rocco S., C. M., 2014. Importance measures for inland waterway network resilience. Transportation Research Part E: Logistics and Transportation Review 62, 55–67.

Baryannis, G., Dani, S., Antoniou, G., 2019a. Predicting supply chain risks using machine learning: The trade-off between performance and interpretability. Future Generation Computer Systems 101, 993–1004.

Baryannis, G., Validi, S., Dani, S., Antoniou, G., 2019b. Supply chain risk management and artificial intelligence: state of the art and future research directions. International Journal of Production Research 57 (7), 2179–2202.

Bassiouni, M. M., Chakrabortty, R. K., Hussain, O. K., Rahman, H. F., jan 2023. Advanced deep learning approaches to predict supply chain risks under COVID-19 restrictions. Expert Systems with Applications 211, 118604.

Bazartseren, B., Hildebrandt, G., Holz, K.-P., 2003. Short-term water level prediction using neural networks and neuro-fuzzy approach. Neurocomputing 55 (3), 439–450.

Benders, J. F., 1962. Partitioning procedures for solving mixed-variables programming problems. Numerische Mathematik 4 (1), 238–252.

Berling, P., Sonntag, D. R., 2022. Inventory control in production–inventory systems with random yield and rework: The unit-tracking approach. Production and Operations Management 31 (6), 2628–2645.

Berman, O., Wang, Q., 2006. Inbound logistic planning: Minimizing transportation and inventory cost. Transportation Science 40 (3), 287–299.

Bertsimas, D., Shtern, S., Sturt, B., 2023. A data-driven approach to multistage stochastic linear optimization. Management Science 69 (1), 51–74.

Birge, J. R., Capponi, A., Chen, P.-C., 2023. Disruption and rerouting in supply chain networks. Operations Research 71 (2), 750–767.

Birge, J. R., Louveaux, F. V., 1988. A multicut algorithm for two-stage stochastic linear programs. European Journal of Operational Research 34 (3), 384–392.

Blackhurst, J., Rungtusanatham, M. J., Scheibe, K., Ambulkar, S., 2018. Supply chain vulnerability assessment: A network based visualization and clustering analysis approach. Journal of Purchasing and Supply Management 24 (1), 21–30.

Bollapragada, R., Rao, U. S., 2006. Replenishment planning in discrete-time, capacitated, non-stationary, stochastic inventory systems. IIE Transactions 38 (7), 605–617.

Bottani, E., Murino, T., Schiavo, M., Akkerman, R., 2019. Resilient food supply chain design: Modelling framework and metaheuristic solution approach. Computers & Industrial Engineering 135, 177–198.

Boute, R. N., Disney, S. M., Gijsbrechts, J., Van Mieghem, J. A., 2022. Dual sourcing and smoothing under nonstationary demand time series: Reshoring with speedfactories. Management Science 68 (2), 1039–1057.

Boute, R. N., Van Mieghem, J. A., 2015. Global dual sourcing and order smoothing: The impact of capacity and lead times. Management Science 61 (9), 2080–2099.

Bravo, F., Shaposhnik, Y., 2020. Mining optimal policies: A pattern recognition approach to model analysis. INFORMS Journal on Optimization 2 (3), 145–166.

Breiman, L., 1984. Classification And Regression Trees, 1st Edition. Routledge.

Brintrup, A., Pak, J., Ratiney, D., Pearce, T., Wichmann, P., Woodall, P., McFarlane, D., 2020. Supply chain data analytics for predicting supplier disruptions: a case study in complex asset manufacturing. International Journal of Production Research 58 (11), 3330–3341.

Chang, W.-S., Lin, Y.-T., 2019. The effect of lead-time on supply chain resilience performance. Asia Pacific Management Review 24 (4), 298–309.

Chen, H., Cullinane, K., Liu, N., Jan. 2017. Developing a model for measuring the resilience of a port-hinterland container transportation network. Transportation Research Part E: Logistics and Transportation Review 97, 282–301.

Chen, H., Lam, J. S. L., Liu, N., May 2018. Strategic investment in enhancing port–hinterland container transportation network resilience: A network game theory approach. Transportation Research Part B: Methodological 111, 83–112.

Chen, J., Zhao, X., Zhou, Y., 2012. A periodic-review inventory system with a capacitated backup supplier for mitigating supply disruptions. European Journal of Operational Research 219 (2), 312–323.

Chen, X., Deng, T., Shen, Z.-J. M., Yu, Y., 2023. Mind the gap between research and practice in operations management. IISE Transactions 55 (1), 32–42.

Chopra, S., Reinhardt, G., Dada, M., 2004. The effect of lead time uncertainty on safety stocks. Decision Sciences 35 (1), 1–24.

Codato, G., Fischetti, M., 2006. Combinatorial Benders' cuts for mixed-integer linear programming. Operations Research 54 (4), 756–766.

Coelho, L. C., Cordeau, J.-F., Laporte, G., 2014. Thirty years of inventory routing. Transportation Science 48 (1), 1–19.

Cohen, M., Cui, S., Doetsch, S., Ernst, R., Huchzermeier, A., Kouvelis, P., Lee, H., Matsuo, H., Tsay, A. A., 2022. Bespoke supply-chain resilience: The gap between theory and practice. Journal of Operations Management 68 (5), 515–531.

Cohen, M. A., Kouvelis, P., 2020. Revisit of AAA excellence of global value chains: Robustness, resilience, and realignment. Production and Operations Management 30 (3), 633–643.

Colon, C., Hallegatte, S., Rozenberg, J., 2020. Criticality analysis of a country's transport network via an agent-based supply chain model. Nature Sustainability 4 (3), 209–215.

Contargo, 2023. Water level surcharges for level Kaub. `https://www.contargo.net/de/goodtoknow/lws/kaub/`, acessed: 2023-03-29.

Cordeau, J.-F., Pasin, F., Solomon, M. M., 2006. An integrated model for logistics network design. Annals of Operations Research 144 (1), 59–82.

Crainic, T. G., Hewitt, M., Maggioni, F., Rei, W., 2021. Partial Benders decomposition: General methodology and application to stochastic network design. Transportation Science 55 (2), 414–435.

Darayi, M., Barker, K., Nicholson, C. D., 2019. A multi-industry economic impact perspective on adaptive capacity planning in a freight transportation network. International Journal of Production Economics 208, 356–368.

Darwish, M., 2008. Joint determination of order quantity and reorder point of continuous review model under quantity and freight rate discounts. Computers & Operations Research 35 (12), 3902–3917.

de Treville, S., Bicer, I., Chavez-Demoulin, V., Hagspiel, V., Schürhoff, N., Tasserit, C., Wager, S., Jul. 2014. Valuing lead time. Journal of Operations Management 32 (6), 337–346.

Dierker, D., Lopez, N., Murnane, J., Saxon, S., Szigethi, J., Zampelas, A., Jan. 2024. How could panama canal restrictions affect supply chains? McKinsey & Company.
URL `www.mckinsey.com/industries/travel-logistics-and-infrastructure/our-insights/how-could-panama-canal-restrictions-affect-supply-chains?`

Durach, C. F., Repasky, T., Wiengarten, F., 2022. Patterns in firms' inventories and flexibility levels after a low-probability, high-impact disruption event: Empirical evidence from the great east japan earthquake. Production and Operations Management 32 (6), 1705–1723.

Easwaran, G., Üster, H., 2009. Tabu search and Benders decomposition approaches for a capacitated closed-loop supply chain network design problem. Transportation Science 43 (3), 301–320.

Eckstein, D., Goellner, M., Blome, C., Henke, M., 2014. The performance impact of supply chain agility and supply chain adaptability: the moderating effect of product complexity. International Journal of Production Research 53 (10), 3028–3046.

Elmachtoub, A. N., Grigas, P., 2022. Smart "predict, then optimize". Management Science 68 (1), 9–26.

Ergun, O., Hopp, W. J., Keskinocak, P., 2023. A structured overview of insights and opportunities for enhancing supply chain resilience. IISE Transactions 55 (1), 57–74.

Farahani, R. Z., Rezapour, S., Drezner, T., Fallah, S., 2014. Competitive supply chain network design: An overview of classifications, models, solution techniques and applications. Omega 45, 92–118.

Fisher, M. L., 1997. What is the right supply chain for your product? Harvard business review 75, 105–117.

Folga, S., Allison, T., Seda-Sanabria, Y., Matheu, E., Milam, T., Ryan, R., Peerenboom, J., 2009. A systems-level methodology for the analysis of inland waterway infrastructure disruptions. Journal of Transportation Security 2 (4), 121–136.

Friedhoff, B., Ramne, B., Alias, C., van Hassel, E., Martens, S. E., Felde, J. z., Samuel, L., 2023. Elevating the logistics resilience of the Rhine-Alpine corridor with the help of innovative vessel and cargo handling concepts. Transportation Research Procedia 72, 1998–2005.

Gallego, G., Simchi-Levi, D., 1990. On the effectiveness of direct shipping strategy for the one-warehouse multi-retailer R-systems. Management Science 36 (2), 240–243.

Gedik, R., Medal, H., Rainwater, C., Pohl, E. A., Mason, S. J., 2014. Vulnerability assessment and re-routing of freight trains under disruptions: A coal supply chain network application. Transportation Research Part E: Logistics and Transportation Review 71, 45–57.

Géron, A., 2022. Hands-on machine learning with Scikit-Learn, Keras, and TensorFlow. O'Reilly Media, Inc.

Ghanei, S., Contreras, I., Cordeau, J.-F., Feb. 2023. A two-stage stochastic collaborative intertwined supply network design problem under multiple disruptions. Transportation Research Part E: Logistics and Transportation Review 170, 102944.

Gijsbrechts, J., Boute, R. N., Disney, S. M., Van Mieghem, J. A., 2022. Volume flexibility at responsive suppliers in reshoring decisions: Analysis of a dual sourcing inventory model. Production and Operations Management.

Goldbeck, N., Angeloudis, P., Ochieng, W., 2020. Optimal supply chain resilience with consideration of failure propagation and repair logistics. Transportation Research Part E: Logistics and Transportation Review 133, 101830.

Govindan, K., Fattahi, M., Keyvanshokooh, E., 2017. Supply chain network design under uncertainty: A comprehensive review and future research directions. European Journal of Operational Research 263 (1), 108–141.

Güllü, R., Önol, E., Erkip, N., 1999. Analysis of an inventory system under supply uncertainty. International Journal of Production Economics 59 (1), 377–385.

Hasturk, U., Schrotenboer, A. H., Ursavas, E., Roodbergen, K. J., 2024. Stochastic cyclic inventory routing with supply uncertainty: A case in green-hydrogen logistics. Transportation Science 58 (2), 315–339.

Hool, A., Helbig, C., Wierink, G., 2023. Challenges and opportunities of the european critical raw materials act. Mineral Economics.

Hosseini, S., Ivanov, D., Dolgui, A., 2019a. Review of quantitative methods for supply chain resilience analysis. Transportation Research Part E: Logistics and Transportation Review 125, 285–307.

Hosseini, S., Khaled, A. A., 2019. A hybrid ensemble and ahp approach for resilient supplier selection. Journal of Intelligent Manufacturing 30, 207–228.

Hosseini, S., Morshedlou, N., Ivanov, D., Sarder, M., Barker, K., Khaled, A. A., 2019b. Resilient supplier selection and optimal order allocation under disruption risks. International Journal of Production Economics 213, 124–137.

Hu, B., Kostamis, D., 2014. Managing supply disruptions when sourcing fromreliable and unreliable suppliers. Production and Operations Management 24 (5), 808–820.

Huang, K., Ahmed, S., 2009. The value of multistage stochastic programming in capacity planning under uncertainty. Operations Research 57 (4), 893–904.

Huang, S. H., Uppal, M., Shi, J., 2002. A product driven approach to manufacturing supply chain selection. Supply Chain Management: An International Journal 7 (4), 189–199.

Iakovou, E., Vlachos, D., Xanthopoulos, A., 2010. A stochastic inventory management model for a dual sourcing supply chain with disruptions. International Journal of Systems Science 41 (3), 315–324.

ITF, 2020. Navigating towards cleaner maritime shipping: Lessons from the nordic region. In: International Transport Forum Policy Papers. Vol. 80. OECD Publishing, Paris.

Ivanov, D., Dolgui, A., Sokolov, B., 2019. The impact of digital technology and industry 4.0 on the ripple effect and supply chain risk analytics. International Journal of Production Research 57 (3), 829–846.

Ivanov, D., Pavlov, A., Dolgui, A., Pavlov, D., Sokolov, B., 2016. Disruption-driven supply chain (re)-planning and performance impact assessment with consideration of pro-active and recovery policies. Transportation Research Part E: Logistics and Transportation Review 90, 7–24.

James, G., Witten, D., Hastie, T., Tibshirani, R., 2021. An Introduction to Statistical Learning: with Applications in R. Springer US.

Japkowicz, N., 2000. The class imbalance problem: Significance and strategies. In: Int'l Conf. on Artificial Intelligence. Citeseer, pp. 111–117.

Jonkeren, O., Rietveld, P., 2016. Protection of critical waterborne transport infrastructures: An economic review. Transport Reviews 36 (4), 437–453.

Jonkeren, O., Rietveld, P., van Ommeren, J., 2007. Climate change and inland waterway transport: Welfare effects of low water levels on the river rhine. Journal of Transport Economics and Policy 41 (3), 387–411.

Kalymon, B. A., 1971. Stochastic prices in a single-item inventory purchasing model. Operations Research 19 (6), 1434–1458.

Karbassi Yazdi, A., Mehdiabadi, A., Wanke, P. F., Monajemzadeh, N., Correa, H. L., Tan, Y., 2022. Developing supply chain resilience: a robust multi-criteria decision analysis method for transportation service provider selection under uncertainty. International Journal of Management Science and Engineering Management 18 (1), 51–64.

Karlin, S., 1960. Dynamic inventory policy with varying stochastic demands. Management Science 6 (3), 231–258.

Katoch, S., Chauhan, S. S., Kumar, V., 2020. A review on genetic algorithm: past, present, and future. Multimedia Tools and Applications 80 (5), 8091–8126.

Khalili, S. M., Jolai, F., Torabi, S. A., 2017. Integrated production–distribution planning in two-echelon systems: a resilience view. International Journal of Production Research 55 (4), 1040–1064.

Kleindorfer, P. R., Saad, G. H., 2005. Managing disruption risks in supply chains. Production and Operations Management 14 (1), 53–68.

Klibi, W., Martel, A., 2013. The design of robust value-creating supply chain networks. OR Spectrum 35 (4), 867–903.

Klibi, W., Martel, A., Guitouni, A., 2010. The design of robust value-creating supply chain networks: A critical review. European Journal of Operational Research 203 (2), 283–293.

Koetse, M. J., Rietveld, P., 2009. The impact of climate change and weather on transport: An overview of empirical findings. Transportation Research Part D: Transport and Environment 14 (3), 205–221.

Kosasih, E. E., Brintrup, A., 2021. A machine learning approach for predicting hidden links in supply chain with graph neural networks. International Journal of Production Research 60 (17), 5380–5393.

Kouvelis, P., Li, J., 2008. Flexible backup supply and the management of lead-time uncertainty. Production and Operations Management 17 (2), 184–199.

Lanza, G., Crainic, T. G., Rei, W., Ricciardi, N., 2021. Scheduled service network design with quality targets and stochastic travel times. European Journal of Operational Research 288 (1), 30–46.

LaRocco, L. A., 2023. U.s. trade dominates panama canal traffic. new restrictions due to 'severe' drought are threatening the future of the shipping route. CNBC.

Lee, H. L., 2002. Aligning supply chain strategies with product uncertainties. California Management Review 44 (3), 105–119.

Lim, T.-S., Loh, W.-Y., Shih, Y.-S., 2000. A comparison of prediction accuracy, complexity, and training time of thirty-three old and new classification algorithms. Machine Learning 40 (3), 203–228.

Liu, J., Gu, B., Chen, J., 2023. Enablers for maritime supply chain resilience during pandemic: An integrated mcdm approach. Transportation Research Part A: Policy and Practice 175, 103777.

Mattsson, L.-G., Jenelius, E., Nov. 2015. Vulnerability and resilience of transport systems – a discussion of recent research. Transportation Research Part A: Policy and Practice 81, 16–34.

Mehrotra, M., Schmidt, W., 2021. The value of supply chain disruption duration information. Production and Operations Management 30 (9), 3015–3035.

Mete, H. O., Zabinsky, Z. B., 2010. Stochastic optimization of medical supply location and distribution in disaster management. International Journal of Production Economics 126 (1), 76–84.

Middelkoop, H., Daamen, K., Gellens, D., Grabs, W., Kwadijk, J. C. J., Lang, H., Parmet, B. W. A. H., Schädler, B., Schulla, J., Wilke, K., 2001. Impact of climate change on hydrological regimes and water resources management in the rhine basin. Climatic Change 49 (1/2), 105–128.

Miller, B. L., Goldberg, D. E., jun 1996. Genetic algorithms, selection schemes, and the varying effects of noise. Evolutionary Computation 4 (2), 113–131.

Miller-Hooks, E., Zhang, X., Faturechi, R., 2012. Measuring and maximizing resilience of freight transportation networks. Computers & Operations Research 39 (7), 1633–1643.

Mišić, V. V., Perakis, G., 2020. Data analytics in operations management: A review. Manufacturing & Service Operations Management 22 (1), 158–169.

Monios, J., Wilmsmeier, G., 2020. Deep adaptation to climate change in the maritime transport sector – a new paradigm for maritime economics? Maritime Policy & Management 47 (7), 853–872.

Müllerklein, D., Fontaine, P., 2024. Resilient transportation network design with disruption uncertainty and lead times. European Journal of Operational Research 322 (3), 827–840.

Namdar, J., Li, X., Sawhney, R., Pradhan, N., 2018. Supply chain resilience for single and multiple sourcing in the presence of disruption risks. International Journal of Production Research 56 (6), 2339–2360.

Nayak, N., Sarmah, S. P., Jenamani, M., 2024. A shippers' perspective multimodal freight transportation analysis considering shallow-draft inland waterways. Computers & Industrial Engineering 187, 109793.

Neghab, D. P., Khayyati, S., Karaesmen, F., 2022. An integrated data-driven method using deep learning for a newsvendor problem with unobservable features. European Journal of Operational Research 302 (2), 482–496.

Nikolopoulos, K., Punia, S., Schäfers, A., Tsinopoulos, C., Vasilakis, C., 2021. Forecasting and planning during a pandemic: COVID-19 growth rates, supply chain disruptions, and governmental decisions. European Journal of Operational Research 290 (1), 99–115.

Niu, B., Chen, K., Chen, L., Ding, C., Yue, X., 2021. Strategic waiting for disruption forecasts in cross-border e-commerce operations. Production and Operations Management 30 (9), 2840–2857.

Nooraie, V., Parast, M. M., 2016. Mitigating supply chain disruptions through the assessment of trade-offs among risks, costs and investments in capabilities. International Journal of Production Economics 171, 8–21.

Nur, F., Marufuzzaman, M., Puryear, S. M., 2020. Optimizing inland waterway port management decisions considering water level fluctuations. Computers & Industrial Engineering 140, 106210.

Omer, M., Mostashari, A., Nilchiani, R., Mansouri, M., 2012. A framework for assessing resiliency of maritime transportation systems. Maritime Policy & Management 39 (7), 685–703.

Oztanriseven, F., Nachtmann, H., 2016. Economic impact analysis of inland waterway disruption response. The Engineering Economist 62 (1), 73–89.

Pant, R., Barker, K., Landers, T. L., Nov. 2015. Dynamic impacts of commodity flow disruptions in inland waterway networks. Computers & Industrial Engineering 89, 137–149.

Papadakos, N., 2008. Practical enhancements to the Magnanti–Wong method. Operations Research Letters 36 (4), 444–449.

Parlar, M., 1997. Continuous-review inventory problem with random supply interruptions. European Journal of Operational Research 99 (2), 366–385.

Patel, H. H., Prajapati, P., 2018. Study and analysis of decision tree based classification algorithms. International Journal of Computer Sciences and Engineering 6 (10), 74–78.

Pettit, T., Fiksel, J., Croxton, K., 2010. Ensuring supply chain resilience: development of a conceptual framework. Journal of business logistics 31 (1), 1–21.

Pishvaee, M., Razmi, J., Torabi, S., 2014. An accelerated Benders decomposition algorithm for sustainable supply chain network design under uncertainty: A case study of medical needle and syringe supply chain. Transportation Research Part E: Logistics and Transportation Review 67, 14–38.

Priore, P., Ponte, B., Rosillo, R., de la Fuente, D., 2019. Applying machine learning to the dynamic selection of replenishment policies in fast-changing supply chain environments. International Journal of Production Research 57 (11), 3663–3677.

Qi, L., Shen, Z.-J. M., Snyder, L. V., 2010. The effect of supply disruptions on supply chain design decisions. Transportation Science 44 (2), 151–290.

Qi, M., Shi, Y., Qi, Y., Ma, C., Yuan, R., Wu, D., Shen, Z.-J. M., 2023. A practical end-to-end inventory management model with deep learning. Management Science 69 (2), 759–773.

Qi, Y., Boyer, K. K., Zhao, X., 2009. Supply chain strategy, product characteristics, and performance impact: Evidence from chinese manufacturers*. Decision Sciences 40 (4), 667–695.

Rahmaniani, R., Crainic, T. G., Gendreau, M., Rei, W., 2017. The Benders decomposition algorithm: A literature review. European Journal of Operational Research 259 (3), 801–817.

Rahmaniani, R., Crainic, T. G., Gendreau, M., Rei, W., 2024. An asynchronous parallel Benders decomposition method for stochastic network design problems. Computers & Operations Research 162, 106459.

Reuters, Jan. 2024. Tesla, volvo car pause output as red sea shipping crisis deepens.
URL `https://www.reuters.com/business/autos-transportation/tesla-berlin-suspend-most-production-two-weeks-over-red-sea-supply-gap-2024-01-11/`

Rodríguez-Espíndola, O., 2023. Two-stage stochastic formulation for relief operations with multiple agencies in simultaneous disasters. OR Spectrum 45 (2), 477–523.

Ruszczyński, A., Shapiro, A., 2003. Stochastic programming models. In: Handbooks in Operations Research and Management Science. Elsevier, pp. 1–64.

Sabouhi, F., Pishvaee, M. S., Jabalameli, M. S., 2018. Resilient supply chain design under operational and disruption risks considering quantity discount: A case study of pharmaceutical supply chain. Computers & Industrial Engineering 126, 657–672.

Saghafian, S., Oyen, M. V., 2012. The value of flexible backup suppliers and disruption risk information: Newsvendor analysis with recourse. IIE Transactions 44 (10), 834–867.

Schmitt, A. J., Singh, M., 2012. A quantitative analysis of disruption risk in a multi-echelon supply chain. International Journal of Production Economics 139 (1), 22–32.

Schmitt, T. G., 1984. Resolving uncertainty in manufacturing systems. Journal of Operations Management 4 (4), 331–345.

Silver, E. A., 1981. Operations research in inventory management: A review and critique. Operations Research 29 (4), 628–645.

Silver, E. A., Pyke, D., Peterson, R., 1998. Inventory management and production planning and scheduling. John Wiley & Sons.

Simchi-Levi, D., Schmidt, W., Wei, Y., Zhang, P. Y., Combs, K., Ge, Y., Gusikhin, O., Sanders, M., Zhang, D., Oct. 2015. Identifying risks and mitigating disruptions in the automotive supply chain. Interfaces 45 (5), 375–390.

Snoeck, A., Udenio, M., Fransoo, J. C., 2019. A stochastic program to evaluate disruption mitigation investments in the supply chain. European Journal of Operational Research 274 (2), 516–530.

Snyder, L. V., Atan, Z., Peng, P., Rong, Y., Schmitt, A. J., Sinsoysal, B., 2016. Orms models for supply chain disruptions: a review. IIE Transactions 48 (2), 89–109.

Steinbach, S., Zhuang, X., 2023. Us agricultural exports and the 2022 mississippi river drought. Agribusiness.

Sun, J., Van Mieghem, J. A., 2019. Robust dual sourcing inventory management: Optimality of capped dual index policies and smoothing. Manufacturing & Service Operations Management 21 (4), 912–931.

Svoboda, J., Minner, S., Yao, M., 2021. Typology and literature review on multiple supplier inventory control models. European Journal of Operational Research 293 (1), 1–23.

Syswerda, G., 1989. Uniform crossover in genetic algorithms. In: Proceedings of the Third International Conference on GeneticAlgorithms. Morgan Kaufmann, San Matea, Ca, pp. 2–9.

Taleb, N. N., 2007. Black swans and the domains of statistics. The American Statistician 61 (3), 198–200.

Tang, C. S., 2006. Robust strategies for mitigating supply chain disruptions. International Journal of Logistics Research and Applications 9 (1), 33–45.

Toonen, W., 2015. Flood frequency analysis and discussion of non-stationarity of the lower Rhine flooding regime (ad 1350–2011): Using discharge data, water level measurements, and historical records. Journal of Hydrology 528, 490–502.

van Meijeren, J., Groen, T., 2010. Impact of climate change on the competitive position of inland waterway transport. Tech. rep., Knowledge for Climate.

Van Slyke, R. M., Wets, R., 1969. L-shaped linear programs with applications to optimal control and stochastic programming. SIAM Journal on Applied Mathematics 17 (4), 638–663.

Verschuur, J., Koks, E., Hall, J., 2020. Port disruptions due to natural disasters: Insights into port and logistics resilience. Transportation Research Part D: Transport and Environment 85, 102393.

Vinke, F., van Koningsveld, M., van Dorsser, C., Baart, F., van Gelder, P., Vellinga, T., 2022. Cascading effects of sustained low water on inland shipping. Climate Risk Management 35, 100400.

Wang, G., Huang, S. H., Dismukes, J. P., 2004. Product-driven supply chain selection using integrated multi-criteria decision-making methodology. International Journal of Production Economics 91 (1), 1–15.

Wang, N., Yuen, K. F., 2022. Resilience assessment of waterway transportation systems: Combining system performance and recovery cost. Reliability Engineering & System Safety 226, 108673.

Whybark, D. C., Williams, J. G., 1976. Material requirements planning under uncertainty. Decision Sciences 7 (4), 595–606.

Wiedmer, R., Rogers, Z. S., Polyviou, M., Mena, C., Chae, S., 2021. The dark and bright sides of complexity: A dual perspective on supply network resilience. Journal of Business Logistics 42 (3), 336–359.

Wiegmans, B., Konings, R., 2017. Inland Waterway Transport. Routledge.

Williams, B. D., Tokar, T., 2008. A review of inventory management research in major logistics journals. The International Journal of Logistics Management 19 (2), 212–232.

Xiao, G., Yang, N., Zhang, R., 2015. Dynamic pricing and inventory management under fluctuating procurement costs. Manufacturing and Service Operations Management 17 (3), 321–334.

Xiong, X., Li, Y., Yang, W., Shen, H., 2022. Data-driven robust dual-sourcing inventory management under purchase price and demand uncertainties. Transportation Research Part E: Logistics and Transportation Review 160, 102671.

Zhou, Y., Wang, J., Yang, H., 2019. Resilience of transportation systems: Concepts and comprehensive review. IEEE Transactions on Intelligent Transportation Systems 20 (12), 4262–4276.

Zimmermann, R., Ferreira, L. M. D., Moreira, A. C., 2020. An empirical analysis of the relationship between supply chain strategies, product characteristics, environmental uncertainty and performance. Supply Chain Management: An International Journal 25 (3), 375–391.

# Appendix A

# Appendix for Cost-driven decision tree rules for transportation planning under cost uncertainty

## A.1 Hyperparameter settings for alternative machine learning models

As highlighted in Section 2.6.3, we compare the performance of our CDDT using a decision tree as classifier against traditional learning approaches using a decision tree, a neural network, and a logistic regression. Compared to the CDDT, each machine learning model is tuned with the objective of maximizing the f1-score during the hyperparameter tuning using a full grid search. In contrast to the CDDT, the full grid search takes less than an hour for each classifier trained.

Regarding the hyperparameter ranges, the ML-DT is trained using the same hyperparameter ranges as the CDDT. The respective parameters for the ML-NN are summarized in Table A.1. For the logistic regression, the default hyperparameters of the Scikit-learn environment are used.

| Hyperparameter | Possible values |
|---|---|
| Activation | tanh, relu |
| Solver | sgd, adam |
| Alpha | 0.0001, 0.05 |
| Learning rate | constant, adaptive |

Table A.1: Neural network hyperparameter ranges for tuning.